Dynamic simulation and analysis of a real biomass plant for cogenerative applications in a public building

Auteur : Hick, Christophe
Promoteur(s) : Lemort, Vincent
Faculté : Faculté des Sciences appliquées
Diplôme : Master en ingénieur civil électromécanicien, à finalité approfondie
Année académique : 2015-2016
URI/URL : http://hdl.handle.net/2268.2/2021

University of Liège - Faculty of Applied Science
Thermodynamics Laboratory
&
Fondazione Bruno Kessler
Research center

Dynamic simulation and analysis of a real biomass plant for cogenerative applications in a public building

Christophe Hick

Academic year : 2015 - 2016

Graduation Studies conducted for obtaining the Master's degree in Electro-mechanical Engineering

President of the jury :
Dewallef P.

Composition of the jury :
Lemort V. (Main Adviser)
Quoilin S.
Amicabile S.

Dynamic simulation and analysis of a real biomass plant for cogenerative applications in a public building

by Christophe Hick

Master's Thesis submitted on the 20th of August 2016 to the Faculty of Applied Sciences of the University of Liège for obtaining the Master's degree in Electro-mechanical Engineering

---

Nowadays, biomass power plant are becoming very popular. They are usually combined to an Organic Rankine Cycle (ORC) to generate some electricity. These systems are increasingly installed nearby free or cheap sources of biomass but whereas it is already widespread in buildings with a constant heat demand, applications for variable heat demands are limited. This increasing number of biomass plant is mainly due to incentives from the government and due to a global wish of decreasing the CO_2 emission.

This work investigates a real biomass plant for cogenerative application in a public building. First of all, the dry cooler, the biomass and natural gas boilers, the heat exchangers, the pumps, the pipes, the ORC and the building are modelled individually. The behaviour of each model is compared with the product data to validate the models. Then, the whole power plant is modelled. The model shows that the power plant, with the assumptions and constraints adopted for the study, is not profitable. Two different aspects are studied to improve its profitability. On the one hand, different control logics are tested. Different methods of controlling the power plant are implemented and compared. The results show that a control logic based on variable speed pumps has lower financial losses seeing that the pumps' electrical consumption decreases. On the other hand, different levels of temperature are investigated. The results show that the financial benefits of the power plant are strongly dependent on the temperatures. This last consideration highlights that the heat distribution system should work at a low temperature in order to increase the electricity generated with the ORC and decrease the thermal losses to the ambient. Ideally, the ORC should also have a high electrical efficiency in order to have a more efficient power plant.

Finally, to conclude this work, a parametric study is made about the buying price of the biomass and electricity in order to determine in which situations the profits of the power plant start to be positive. All these studies show that the installed biomass power plant combined to an ORC needs either a higher production of electricity (a higher electrical efficiency and a low temperature of condensation) or cheap biomass to have benefits. And in order to recover the investment cost of the biomass plant studied, the power plant should have both a high production of electricity and a cheap biomass. On the contrary, a smaller biomass providing only thermal power to the ORC is financially more interesting and should have profits even if the biomass is expensive.

Acknowledgements

I would first like to thank Vincent Lemort for giving me the great opportunity to realize my master thesis abroad. I also want to thank him for his precious time and his advice from distance.

I also want to thank Luigi Crema for having hosted me in the ARES unit during my internship in FBK. These last months were an amazing experience and I learned so much in many engineer fields.

I would more particularly like to thank Simone Amicabile for his continuous support, his friendship, his help and also for the opportunity to write a paper with him.

I would like to thank Fabrizio Alberti for his help in the beginning of my master thesis and his motivation in the elaboration of a collaboration between the University of Liège and FBK.

I also want to say I'm really glad that I have met all the people from ARES (FBK). Thanks for your friendship and the help when I had questions. I learned a lot thanks to you.

I want to thank Adriano Desideri, Roberto Ruiz Flores and all other people from the Thermodynamics Laboratory (ULG) for their help, their time and their advice.

Finally, I want to thank all my friends and my family. You were an amazing support even from distance.

Contents

1 Introduction **1**
- 1.1 Preface . . . 1
- 1.2 Objectives . . . 1
- 1.3 Organization of the manuscript . . . 2

2 Context and state of the art **4**
- 2.1 Context . . . 4
- 2.2 The project Bricker . . . 5
- 2.3 Building description . . . 6
- 2.4 Active technologies . . . 7
  - 2.4.1 Power Generator Units . . . 8
    - 2.4.1.1 Biomass . . . 8
    - 2.4.1.2 Gas Boilers . . . 10
  - 2.4.2 Energy Conversion Unit . . . 11
    - 2.4.2.1 Organic Rankine Cycle System . . . 11
  - 2.4.3 Energy Distribution Units . . . 12
    - 2.4.3.1 Dry Cooler . . . 12
    - 2.4.3.2 Heat Exchangers . . . 15
- 2.5 Passive technologies . . . 15
  - 2.5.1 Aerating windows . . . 16
  - 2.5.2 PCM . . . 16

3 Description of simulated power plant **17**
- 3.1 Description of the system . . . 17
- 3.2 Instrumentation of the system . . . 19
- 3.3 Control logic . . . 20
  - 3.3.1 Seasonal main routine . . . 22
  - 3.3.2 Biomass subroutine . . . 23
  - 3.3.3 ORC subroutine . . . 24
  - 3.3.4 Dry cooler subroutine . . . 24
  - 3.3.5 Water-oil heat exchanger subroutine . . . 24
  - 3.3.6 Natural gas boilers subroutine . . . 29
- 3.4 Working schemes . . . 29

4 Modelization and validation of the dynamic model **34**
- 4.1 Components from ThermoCycle . . . 34
- 4.2 Study and validation of the components implemented . . . 37
  - 4.2.1 Heat exchanger . . . 37
    - 4.2.1.1 Oil-Water heat exchanger . . . 38
    - 4.2.1.2 Water-Water heat exchanger . . . 40

4.2.1.3 Water-Glycol heat exchanger . . . 40
4.2.2 Biomass . . . 41
4.2.2.1 Biomass boilers efficiency . . . 43
4.2.2.2 Biomass consumption . . . 44
4.2.3 Organic Rankine Cycle . . . 45
4.2.3.1 Extrapolation of the characteristic curves . . . 47
4.2.4 Building . . . 48
4.2.4.1 Power demand curve . . . 49
4.2.5 Dry cooler . . . 50
4.2.5.1 Working behaviour outside its nominal value . . . 51
4.2.6 Gas Boilers . . . 53
4.2.6.1 Implementation of the old control logic . . . 53
4.2.6.2 Analysis of the old thermal production system . . . 55
4.2.7 Three-way valves . . . 59
4.2.7.1 Sizing of the valves . . . 60
4.2.7.2 Consumption of the pumps . . . 61
4.2.8 Thermal losses . . . 62
4.2.8.1 Oil tank . . . 62
4.2.8.2 Insulated pipes . . . 63
4.2.9 Validation of the main biomass control logic . . . 63

5 Optimisation and analysis of the power plant 66
5.1 First configuration . . . 66
5.1.1 Distinctive features . . . 66
5.1.2 Results obtained and drawbacks . . . 68
5.1.3 Improvement of this configuration . . . 70
5.2 Second configuration . . . 71
5.2.1 Distinctive features . . . 71
5.2.2 Results obtained and drawback . . . 73
5.3 Suggested layout for the implementation on-site . . . 73
5.3.1 Drawback . . . 73
5.4 Improvement of the installed layout . . . 74
5.4.1 Modification of the dry cooler control . . . 74
5.4.1.1 Optimisation of the dry cooler . . . 76
5.4.2 Optimal control strategy . . . 77
5.4.2.1 Economical study . . . 79
5.4.3 Parametric study . . . 80
5.4.3.1 No thermal demand . . . 83
5.4.3.2 Low thermal power demand . . . 84
5.4.3.3 Medium thermal demand . . . 87
5.4.3.4 Nominal thermal demand . . . 88
5.4.3.5 Price sensitivity . . . 89
5.5 Reduction of the size of the biomass boiler . . . 91

6 Conclusion and perspectives 93
6.1 Conclusion . . . 93
6.2 Further developments . . . 94

Bibliography 94

Appendices 98

A Fluid properties **99**

B Dymola Model **101**

List of Figures

2.1 Illustration of the old Belgian power plant. 6
2.2 Subdivision of the Belgian building in different blocks. 7
2.3 Block diagram of the Belgian power plant. 7
2.4 Modulation expected of the biomass boiler. 9
2.5 Illustration of the biomass with its gas exhaust tower and its storage tank. . . 10
2.6 Simple ORC cycle [3]. 11
2.7 ORC cycle with regenerator [3]. 11
2.8 Air flow schemes of the air cooled heat exchanger - (a) Horizontal, forced draft (b) Horizontal, induced draft (c) Vertical (d) A-frame (figure from Kuppan Thulukkanam [6]). 13
2.9 Influence of the wind on the warm air recirculation [7]. 14
2.10 Recirculation of hot air inside the dry cooler to avoid freezing [13] 15

3.1 Layout of the Belgian site. 18
3.2 Flow chart of the main routine. 22
3.3 Flow chart of the biomass subroutine. 23
3.4 Flow chart of the ORC subroutine. 25
3.5 Flow chart of the cooling tower subroutine. 26
3.6 Flow chart of the water-oil heat exchanger subroutine. 27
3.7 Flow chart of the auxiliary boilers subroutine. 28
3.8 Working scheme : ORC generation mode and Dry Cooler. 29
3.9 Working scheme : ORC cogeneration mode, Building and Dry Cooler. 30
3.10 Working scheme : ORC cogeneration mode, W-O HEX and Building. 31
3.11 Working scheme : ORC cogeneration mode, W-O HEX, W-W HEX and Building. 32
3.12 Working scheme : W-O HEX, W-W HEX and Building. 33
3.13 Working scheme : Previous Power Plant. 33

4.1 Fundamental thermodynamic law applied to a discretized cell[16]. 35
4.2 Interface of the Flow1DimInCModel. 35
4.3 Interface of the models CountCurr and MetalWall. 35
4.4 Interface of the pump. 36
4.5 Interface of the OpenTank. 36
4.6 Interface of the temperature sensor. 37
4.7 Interface of the mass flow rate sensor. 37
4.8 Interface of the valve. 37
4.9 Interface of the heat exchanger. 38
4.10 Inside view of the heat exchanger model. 38
4.11 Small Dymola model used to study the heat exchanger. 39
4.13 Dymola interface of the biomass boiler. 41
4.14 Inside view of the biomass model. 41

4.12 Heat transfer and losses during the combustion cycle of a biomass boiler [20]. 42
4.15 Interface of the model CombustionDynamic. 42
4.16 Variation on efficiency in function of partial load ratio($0 \leq f_{cp} \leq 1$) [25]. . . 44
4.17 Dymola interface of the ORC. 46
4.18 ORC electrical power generation for different condensation and evaporation temperatures. 47
4.19 ORC thermal power consumption for different condensation and evaporation temperatures. 47
4.20 ORC thermal power generation for different condensation and evaporation temperatures. 48
4.21 Model of the building. 49
4.22 The interface of the building in Dymola. 49
4.23 Fluctuation of the building power consumption during the year. 50
4.24 Model of the Dry Cooler. 50
4.25 Dry cooler interface. 50
4.26 Fluctuation of the power dissipated with the air flow rate. 52
4.27 Fluctuation of energy efficiency ratio with the power dissipation. 52
4.28 Dymola model for the computation of the time delay. 55
4.29 Illustration of a delayed transition with a condition. 55
4.30 Model implemented for the control logic of the three gas boilers. 56
4.31 Determination of the hot water production set point temperature. 56
4.32 Illustration of the Dymola model used to study the old power plant. 57
4.33 Thermal power production of the old power plant. 57
4.34 Fluctuation of the temperature due to the ON-OFF system. 58
4.35 Dymola model used for the reference case of the 3-way valve study. 59
4.36 Dymola model of the alternative configuration of the 3-way valve. 61
4.37 Interface of the stratified tank. 62
4.38 Interface of the isolated pipe. 62
4.39 Variation of the thermal losses with the temperature for an isolated pipe. . . . 63
4.40 Model of the biomass and its oil tank. 64
4.41 Variation of the power production when the power plant has a fast variation of thermal power consumption. 65
4.42 Variation of temperatures when the power plant has a fast variation of thermal power consumption. 65
4.43 Variation of volume required to compensate the slow Biomass' reaction as a function of the reaction time of the biomass and the variation's speed of the thermal demand. 65

5.1 Illustration of the first layout. 67
5.2 Increase of the temperature $T_{21}(T_{inlet,cd})$ due to wrong control system. 68
5.3 Activation of the dry cooler even if the building power required $Building.Q$ is high. 69
5.4 Activation of the dry cooler even if the building power required $Building.Q$ is high. 70
5.5 Activation of the dry cooler even if the building power required $Building.Q$ is high. 70
5.6 Illustration of the model used for sizing the pump $PumpHxOil\_1$ (named $P2$ in the Figure 5.1). 72
5.7 Mass flow rate profile over time. 72
5.8 Heat exchanged over time. 73

5.9 Illustration of the proposed layout. 74
5.10 Fluctuation of the controlled temperature over time. 75
5.11 Electrical power consumption over time. 76
5.12 Evolution of the electrical consumptions as a function of the thermal demand. 81
5.13 Number of GCs and mass of biomass burned as a function of the thermal demand. 81
5.14 Daily profits as a function of the thermal demand. The daily profits correspond to the profits of the power plant working 24 hours at the specific thermal demand. 82
5.15 Daily quantity of biomass burned and produced net electricity using the generation mode of the ORC. 83
5.16 Daily profits using the Biomass only to produce electricity. 84
5.17 Variation of the water distribution temperature with the temperature of condensation and variation of the daily profits with different set point temperatures. 85
5.18 Daily net electricity generated and biomass consumption (respectively the right and left axis). 85
5.19 Daily profits as a function of the thermal demand. The daily profits correspond to the profits of the power plant working 24 hours at the specific thermal demand. 87
5.20 Variation of the profits with the set point temperature T_{17}. All the results are shown in €/day. 88
5.21 Daily net electricity generated and water distribution temperature. 89
5.22 Evolution of the mix of biomass and natural gas power generation to fulfil the thermal heating demand. 92

A.1 Properties of Glycol-water mix. 99
A.2 Properties of Therminol SP. 100

B.1 Illustration of the power plant in Dymola. 102

List of Tables

3.1 Mass flow rate sensors. 19
3.2 Temperature sensors. 19
3.3 Pressure sensors. 20
3.4 Internal sensors of each component from the system. 21

4.1 Physical characteristics and nominal working point of the heat exchanger Oil-Water 1500 kW. 39
4.2 Physical characteristics and nominal working point of the heat exchanger Water-Water 7500 kW. 40
4.3 Physical characteristic and nominal working point of the Glycol-Water heat exchanger 515 kW. 41
4.4 Value of the k parameter from the equation (4.34). 61

5.1 Total electricity consumption. 76
5.2 Dependence on the electricity consumption with the glycol-air ratio. 77
5.3 Different control strategies considered. 78
5.4 Comparison of the control strategies studied for a simulation of 240 days and one year. The *Heating period* represents the 240 days of heating demand. . . 80
5.5 Parametric study of the power plant working with the ORC and DC set point temperatures equal respectively to 45°C and 40°C. 90
5.6 Parametric study of the power plant working with the set point temperatures T_{17} and T_4 fixed at 45 and 225°C. 90
5.7 Parametric study of the power plant working with the set point temperatures T_{17}, T_4 and T_{16} fixed at 45, 225 and 70°C and a temperature of 58°C in the inlet of the building's heating distribution network. 91
5.8 Comparison of profits of the real and downsized power plant. 92

Nomenclature

Acronyms

COP	Coefficient of performance
DC	Dry Cooler
GWP	Global Warming Potential
HEX	Heat Exchanger
NCV	Net calorific value
ORC	Organic Rankine Cycle
PCM	Phase Change Material
PCUs	Power Conversion Units
PDUS	Power Distribution Units
PGUs	Power Generation Units
PID	Proportional–Integral–Derivative controller
PLR	Partial Load Ratio

Symbols

$\dot{m}$	Mass flow rate	$[kg/s]$
$\dot{Q}$	Heat transfer rate	$[W]$
$\dot{V}$	Volumetric flow rate	$[m^3/s]$
$\dot{W}$	Power	$[W]$
η	Overall surface efficiency	$[-]$
ρ	Density	$[kg/m^3]$
A	Surface area	$[m^2]$
cp	Specific heat capacity	$[J/(kg \cdot K)]$
h	Specific enthalpy	$[J/kg]$
k	Thermal conductivity	$[W/(m \cdot K)]$
m	Mass	$[kg]$

N	Number of discretization	$[-]$
ncv	Net Calorific Value	$[J/kg]$
P	Pressure	$[Pa]$
Q	Thermal energy	$[MWh]$
T	Temperature	$[^{\circ}\mathrm{C}]$
U	Heat transfer coefficient	$[W/(m^2 \cdot K)]$
U	Internal energy	$[J]$
V	Volume	$[m^3]$

Subscripts

b	Building
bm	Biomass
cd	Condenser
dc	Dry cooler
ev	Evaporator
ex	Exhaust
f	Fan
g	Glycol
in	Inlet
is	Isentropic
meas	Measured
ng	Natural Gas
nom	Nominal
o	Oil
out	Outlet
sp	Set point
su	Supply
tot	Total
w	Water
wa	Wall

Chapter 1

Introduction

1.1 Preface

This thesis is related to the study and the implementation of the Belgian layout from a European funded project named *BRICKER*. The thesis is realized in collaboration with the Thermodynamics Laboratory of the University of *Liège* and FBK (*Fondazione Bruno Kessler*, a research center located in *Trento*, *Italy*).

Biomass power plants are increasingly installed in Europe. This is mainly due to a wish to decrease the emission of carbon dioxide CO_2. Furthermore, there are some constrains and goals set by the European commission to reach a bigger share of green energy in the overall energy consumption by 2020. To increase the use of renewable energy, one solution is to use the biomass which is considered as a green energy even if it emits CO_2 due to the capture of CO_2 during its growth. The energy consumption of buildings represents an important share of the total energy consumption in Belgium (about 35% [1]). Seeing that the old buildings are usually not well insulated, energy retrofitting can be considered to make the building energy efficient. New technologies can decrease the thermal demand (e.g. aerating windows or walls containing Phase Change Material *PCM*) and some of them can make the power plant more energy efficient and decrease the CO_2 emission (e.g. Organic Rankine Cycle *ORC* and Biomass boiler). In consequence, replacing old natural gas power plant with biomass power plant can avoid an important emission of CO_2 and might be the solution to reach these goals. In addition, considering that bigger biomass boilers are cheaper per unit of capacity than smaller biomass boilers, it is interesting to see first the potential financial benefits of a biomass power plant for cogenerative applications in a building having huge thermal and electrical demand. This leads to the question: "Is a big biomass power plant for cogenerative applications profitable in public buildings?"

1.2 Objectives

The objectives of this work can be summarized as follows:

- Developing a dynamic model of each component of the whole power plant and validate them separately with product data.
- Testing through dynamically simulated environment the reliability, flexibility and stability of the control logic.

- Investigating other possible control strategies to determine the optimal control strategy. The final goal is to evaluate the variation of the profits with an optimisation of the control strategy and the controlled temperatures, and with a modification of the size of the biomass boiler. Furthermore, these studies enable to answer the question : "Is a big biomass power plant for cogenerative applications profitable in public buildings?".

1.3 Organization of the manuscript

An overview of the present work can be described as follows:

- Chapter 2 : the Bricker project is explained more in detail. It starts with a small explanation of the three demo sites from the project *Bricker*. It is followed with a description of the active and passive technologies used to decrease the energy consumption and reach a trigeneration system. A specific attention will be given to the Belgian site which is studied in detail during this thesis. A state of the art is given for each technology installed in the Belgian site and a small part of this chapter is dedicated to a description of the building studied.

- Chapter 3 : a description of the final layout of the Belgian site is firstly given. The final layout corresponds to the last and most optimised configuration considered in this thesis. After that, a recapitulation of the active and passive measurement point is given with an explanation of their purpose. A distinction is made between sensors used to modulate the power production and the ones used for monitoring the temperatures, pressures, and mass flow rates. This chapter finishes with a discussion and a clarification about the final control logic, the flow chart, and its control strategy. The explanation about the control logic of the power plant is made for different working schemes. Each working scheme corresponds to a different combination of components (like the biomass boiler, the Organic Rankine Cycle *ORC*, dry cooler,...) and different heating demands.

- Chapter 4 : this chapter is focused on the implementation of the system using *Dymola*. A brief description is given for each sub-component used from the external library *Thermocycle* with a list of the equations situated inside them. It is followed by the description of the implemented models necessary to describe all the components from the power plant. Each implemented model is explained with its equations and the assumptions made during the study. Finally, each subsection (one per component of the power plant) ends with comparisons between the results obtained with the models implemented and product data. This whole chapter aims to show that the results can be trusted and that they are close to the reality. Indeed, if all the models are giving accurate results, the model of the whole power plant should give trustful results.

- Chapter 5 : it explains the different configurations and their corresponding results. It starts with the first configuration designed by the partners of the project *Bricker*. This is followed by the issues faced with this first layout configuration. All the problems encountered are exposed and an explication is given at each step of the modification of the layout and its control logic. All the modifications aim to solve the issues to finally have a power plant working as wanted. The second main part of this chapter is about the installed layout. Indeed, the studied power plant has been installed and some modifications are required in the suggested control logic to have the power plant working. Once the modifications are made, different control logics are suggested and compared to see the most interesting economically system. When the optimal control logic is found, a

study about the set point temperature is made to find the optimal working conditions. This study aims to show the behaviour of the system for different heating demands and to optimise some of the working schemes of Chapter 3. Finally, a specific focus is given on the profitability of the power plant. The profits of one typical year will be determined for the optimal case and a comparison with the suggested case is made to show that tuning the control logic can hugely improve the economical benefits.

Chapter 2

Context and state of the art

This chapter starts with a small explanation of the the demo sites from the project Bricker and with the goals of the project. Afterwards, the Belgian site is explained and a description is given about the active and passive technologies used to decrease the energy consumption and reach a trigeneration system. A state of the art is given for each technology installed in the Belgian site. Finally, some links are made between the state of the art and the real components of the installed power plant.

2.1 Context

This thesis is taking place into a European project named *BRICKER* that has received funding from the European Union's Seventh Programme. The whole study is made using Dymola. This program is able to study a system in transient which leads to unexpected behaviours.

Dymola is a modelling and simulation environment suitable for any kind of system like thermodynamic, mechanical (robotics), electrical, control system and so forth. It is really powerful and as it is an object-oriented programming language, we can test faster many configurations which will indirectly improve the quality of the sizing of the components by finding the optimal solution.

Considering the inertia is essential when studying a whole building. Indeed, the building, as well as the production and distribution network, have a huge mass which means an important inertia. For instance, the old buildings mainly use radiators which have a colossal heat capacity while the new ones might use more innovative technologies like radiant ceilings coupled with Thermally Activated Building Systems (TABS). This last technology allows the building decreasing its maximal peak power demand. All other things being equal, the maximal power demand can also be decreased in old building by making renovations like replacing the windows, increasing the insulation of the walls with a second layer of insulation (if possible), increasing the inertia by incorporating a thin layer of Phase-Change Material (PCM) or with one of the many other existing renovations. All these renovations lead to a decrease of the maximal power needed which leads to an undersizing of the components (and so a decrease in the total cost of the new installation) or leads to a better energy efficiency and then in a reduction of fossil fuel consumption.

There are many buildings owned by the government or by privates which are mainly based on massive fuel consumption with huge CO_2 emission. For this last reason, it is really important to consider the incorporation of new technologies with zero emission energy production into the private and public sector. The third sector (non-profit building) might also be consid-

ered if people want to decrease their own fuel consumption.

2.2 The project Bricker

The aim of this project is to develop a replicable, high energy efficient and cost effective system that will be adapted to others non-residential buildings to improve their energy efficiency by at least 50% which will be a drastic reduction of the energy consumption. This project is divided into a few steps to achieve this goal. Its first step is to reduce the energy demand with retrofitting solutions. The second step is to study zero emission energy production technologies. The next step is to incorporate these solutions into old buildings and make simulations of the whole system. The last step is to demonstrate the performance in terms of energy efficiency and in terms of the return on investment in three demo sites (this thesis takes place in the two last steps as it is about dynamic simulation and analysis). This will be followed by spreading a retrofit solution package to consider renovations in other similar buildings.

Talking more specifically about one of the demo site (situated in Liège), there are 370 similar buildings owned by *Province de Liège* which is one of the main partners of the project. Indeed, even if all the buildings are different in terms of needed power, the necessities behind the suggested retrofitting solution and its control logic are almost the same when the weather does not change too much. That is why extrapolation of the results to general solutions (which can be used everywhere) can be made.

The project has threes demo sites situated in Belgium (Liège), Spain (Cácares) and Turkey (Aydin Merkez). They are all characterized by different weathers which mean different needs. The Bricker project aims to decrease the energy consumption by the use of active and passive technologies. These different technologies are mixed together to reach a trigeneration system for Spanish and Turkish demos and a cogeneration (electricity and heat) system for the Belgian site. Moreover, an investigation of the optimal combination of all the available technologies and a control logic well developed is needed to take advantages of all these technologies to achieve a high percentage of renewable energy ratio in the building demand (thermal and electrical load). Many technologies are used to improve the energy efficiency of the system. Here are some of the technologies that can be used to retrofit a building: Biomass, ORC, Aerating windows, Ventilated façade, Dry Cooler, PCM (Abbreviation of "Phase-Change Material"), Wet Cooling Tower, Solar parabolic collectors and Chillers. The technologies which allow a reduction of energy consumption are called active technologies and the ones which reduce the energy losses are called passive technologies. In each of the three demos, both passive and active technologies are used.

This thesis is focused on the demo site situated in Liège. From these technologies, only the first six are implemented in the building of Liège. Indeed, Belgium has a mild summer weather with a low cooling demand and a few uncomfortable periods (overheated periods) are accepted. For this reason, neither the Chiller nor the solar parabolic collectors is investigated in this thesis. The main reasons that drove this choice are the lack of space for the installation and the weather.

In the next subsections, a brief description of the Belgium building is given and it is followed by a state of art of the active and passive technologies integrated for retrofitting the building. A general description is given and discussed in the following pages. Finally, based on this State of the art, links are made between the engineer choices and the real components (implemented in the demo site).

2.3 Building description

The *Institut Supérieur Industriel de Liège* "ISIL" building, in Liège, is characterized by a high yearly natural gas consumption of 183.1 kWh_{th}/m^2y and an electricity consumption of 22.2 kWh_{el}/m^2y over a huge area of 23600 m^2. The equivalent primary energy consumption is 296.5 kWh/m^2y. The building, showed in Figure 2.2, is divided into 7 blocks each having their own different pipes distributing heat from the power plant to the radiators. It hosts more than one thousand students and it was built in 1964. The energy performance is evaluated as a class E on a scale from A++ "the most energy efficient" to G "the less energy efficient" (according to the Belgian legislation). This poor energy performance can be explained by the presence of many windows.

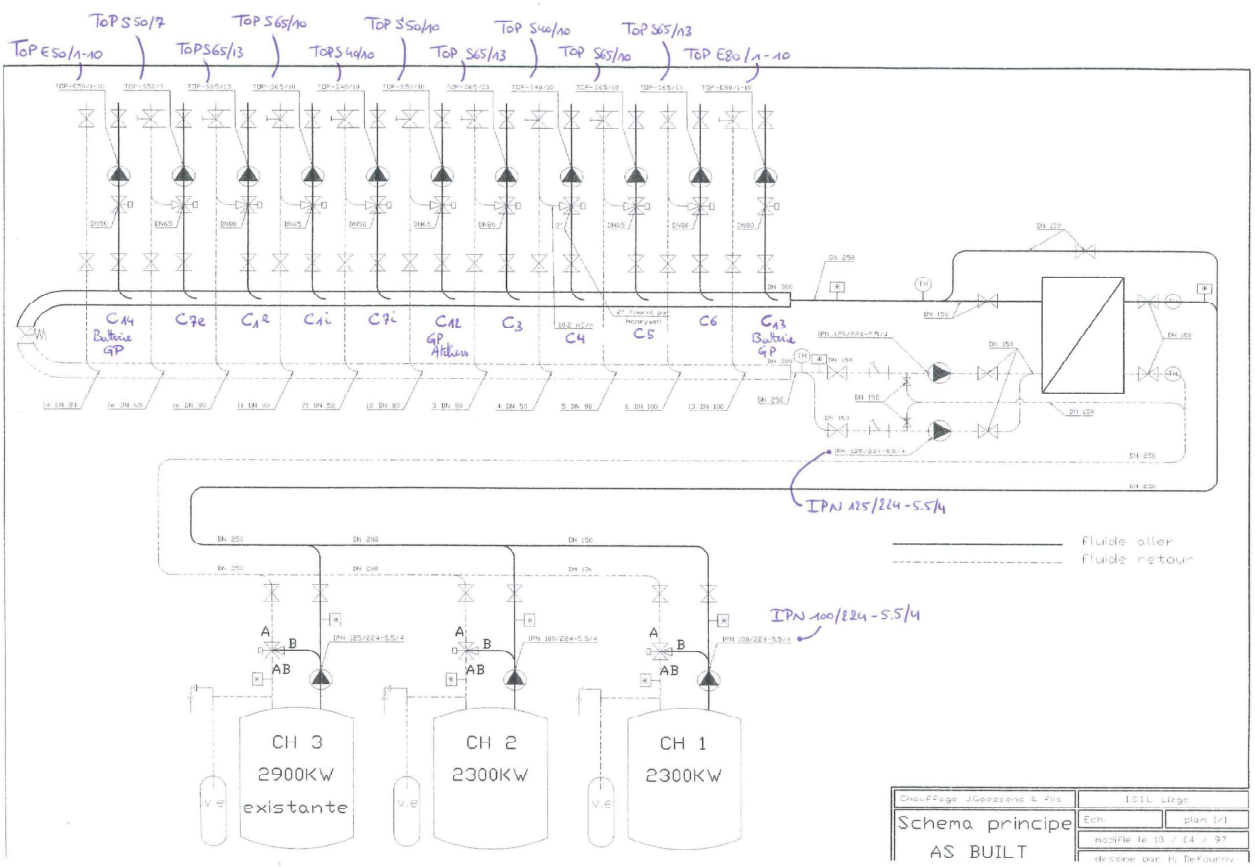

Figure 2.1: Illustration of the old Belgian power plant.

Figure 2.1 shows the old power plant composed of three natural gas boilers, one heat exchanger and 11 water loops (8 hydraulic circuits for indoor heating (radiators) and 3 for ventilation units). Each of the water loops controls their power transmission using a modulation on the aperture of their 3-way valve.

From the whole building (Figure 2.2), only the blocks I and VI are renovated with the passive technologies described in the following sections. After applying the retrofitting solutions, these two blocks are expected to reach an energy performance certificate of class B (primary energy consumption $\in [51-90] kWh/m^2y$). This corresponds to a reduction of about 62.5% on the annual primary energy consumption of these two blocks.

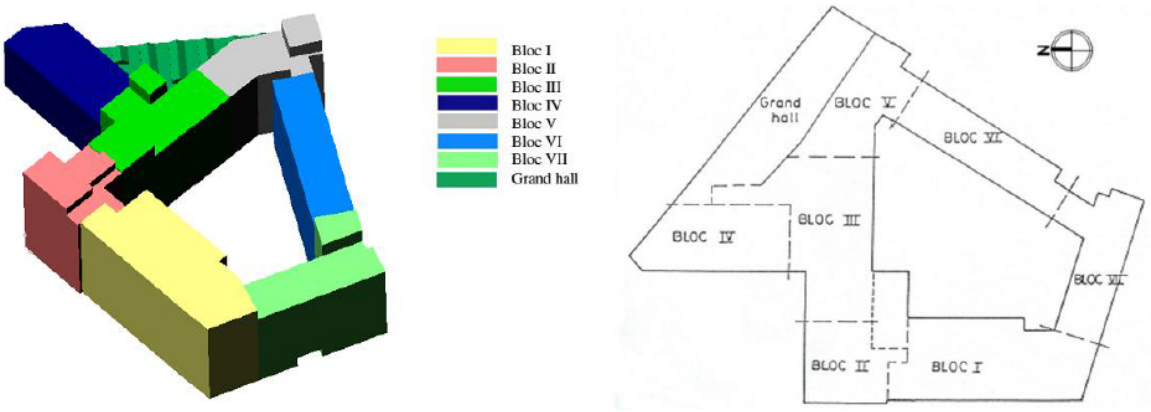

Figure 2.2: Subdivision of the Belgian building in different blocks.

2.4 Active technologies

The active technologies regroup all the technologies producing or transforming the energy. The active technologies from the whole energy system are often showed in a block diagram. This is a specific schematic diagram used to illustrate the role of each subcomponent. The block diagram of the Belgian layout is showed in Figure 2.3.

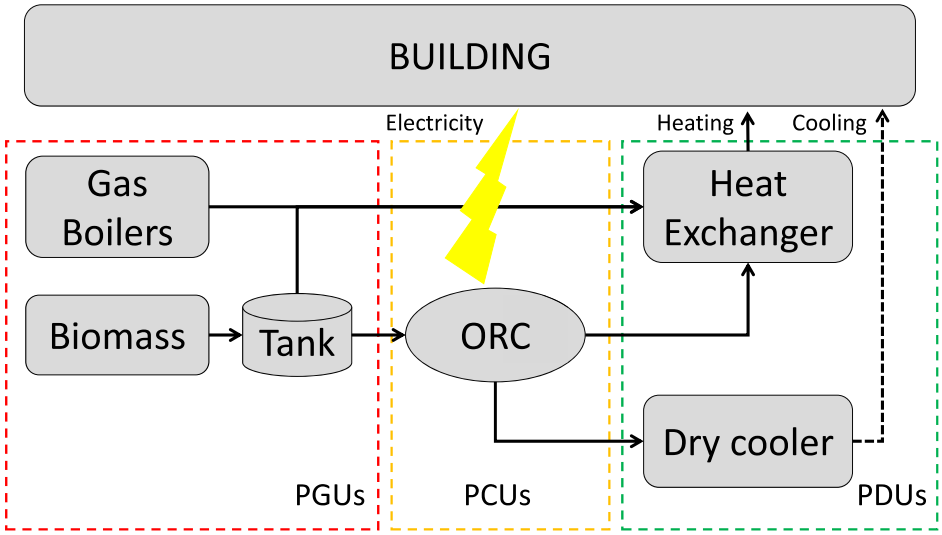

Figure 2.3: Block diagram of the Belgian power plant.

In this latter figure, the power plant is divided into three subcomponents : Power Generation Units (*PGUs*) which transform the primary energy (natural gas, biomass,...) into thermal energy, Power Conversion Units (*PCUs*) which transform one type of energy to an other one and Power Distribution Units (*PDUs*) which are necessary to fulfil the heating and cooling demand of the building.

Power Generation Units These units regroup the Gas boilers using water as process fluid and

the biomass boiler running with thermal oil. *PGUs* have to generate the right amount of power to meet the power required by the building at any time. To meet this demand, both systems have to work together and exchange information to use the biomass as much as possible which leads to a higher reduction of CO_2 emissions. In this system, the biomass has to produce the power consumed by the ORC and keep the temperature constant to reach the designed working conditions of the ORC. Finally, a storage tank can be added in the system to damp the variation of the demand and compensates the slow variation of the biomass power generation.

Power Conversion Units *PCUs* are the units converting the thermal power of the oil to electricity and thermal power transmitted to the water loop. This thermal power can be dissipated using a dissipation unit (like a dry cooler) or can be used to heat the building.

Power Distribution Units *PDUs* regroups the units to distribute the power and meet the thermal demand (pipeline, radiators, heat exchangers) and the units that dissipate the power to the environment (Dry cooler).

2.4.1 Power Generator Units

2.4.1.1 Biomass

The main interest in using biomass instead of natural gas is that biomass is a renewable energy with a zero global emission of pollutants. Some countries, like Belgium, are ready to give money to people producing energy with renewable energy sources. Due to a wish of increasing the renewable percentage share in the overall building consumption and seeing that the ORC requires a constant thermal power, the incorporation of biomass in the new part of the power plant is considered.

In the Belgian demo site, the biomass boiler has the main role, i.e. producing the power consumed at the evaporator of the ORC and limiting the consumption of natural gas as much as possible. The biomass boiler gives the power needed by the ORC which corresponds to 466 kWh (for the designed temperatures). Therefore, the biomass boiler must be sized to generate this power at least. The capacity of the installed biomass boiler is:

- 1500kW. The idea behind this sizing is to produce not only the power needed by the ORC. The main goal is to replace an old gas boiler of the previous generation system and to have a bigger proportion of renewable energy in the energy mix of the building.

The nominal outlet temperature of the biomass boiler is 260°C and the nominal temperature outside the oil tank (after the mix, see Figure 2.5) is the nominal temperature needed for the ORC (225°C). Knowing the working temperature (225°C), studies and engineer choices are made to decide which fluid will carry the power from the biomass to the ORC. The selected fluid is *therminol SP*, an oil fluid type. Indeed, to reach 225°C with liquid water, we need to pressurize it until about 25 bar. The steam is also rejected for the same reason. A high pressure means more expensive equipment, a system more complicated to control, more dangerous and a higher operating cost. Indeed, despite its high buying cost, a non-pressurized oil will not provoke any explosions/issues and the consumption of the pumps is lower with the higher density of the oil which makes the oil the best choice when it's available in the location studied.

The provider of the biomass boiler delivers it with its own internal logic control. That's why the control logic suggested and presented in next chapter works in parallel with the control

logic of all the inner components. The biomass boiler has a constant flow rate of 30 kg/s imposed by its inner control logic and in case there are issues, an alarm is activated when the flow rate goes under the minimal allowed flow rate of 24 kg/s. Another part of the warning system is about the outlet temperature that shouldn't exceed the 300°C to avoid degrading the oil (the evaporation of the chosen oil is 351°C [2]). Finally, following the providers' advice, one start a day should not be exceeded.

Unlike normal gas boilers, the biomass boiler is much less flexible. The biomass boiler is characterized by a huge inertia and its reaction time is longer than the one of a gas boiler. In comparison, a natural gas boiler takes about 2 minutes to reach its maximal power while the biomass boiler needs a few hours to reach its maximal power depending on its maximal power. After the starting process is finished, we can expect a faster variation of power. Figure 2.4 explains how the biomass is expected to work.

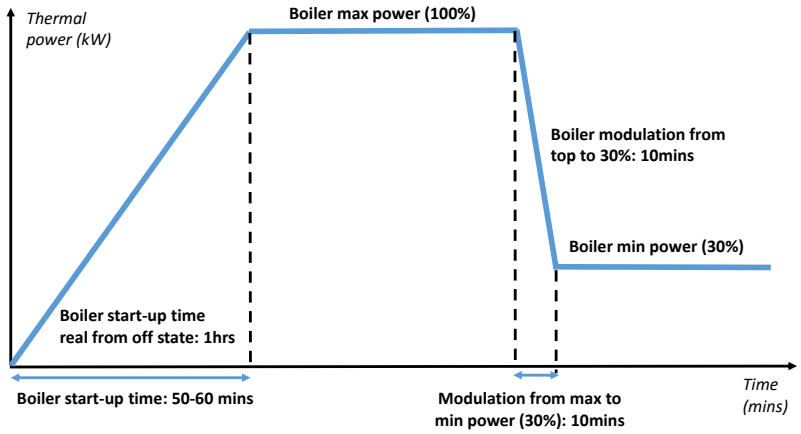

Figure 2.4: Modulation expected of the biomass boiler.

This long reaction time might be problematic with a fast variation of the power needed from the building. As the power needed has to be fulfilled directly all the time, other component from the installation (like the tank,pumps,...) have to compensate this lack of fast variation. In the next paragraphs, the reaction of the biomass boilers is described when it is submitted to different inputs is given.

If the power extracted in the heat exchangers Oil-Water increases, the oil tank inlet temperature falls down and so does the oil tank temperature. To keep constant the temperature of the oil going to the main loop, the 3-way valve (Figure 2.5) decreases its bypassed mass flow. Before any reaction of the system, the internal control of the biomass will read a lower temperature than the set point temperature (T_{out},see Figure 2.5) due to a lower T_{in}. In reaction, it will increase the quantity of biomass burned which increases the outlet temperature (T_{out}) to reach its set point temperature (260°C). With the reaction of the biomass boiler, the temperature of the oil tank increases and the 3-way valve has to adjust its bypassed flow to keep constant the oil temperature going to the main loop.

The other case is a decrease of the demand which implies a temperature increment and an overpass of the set point temperature. The proportional integral derivative controller *pID* reacts this time with the opposite reaction:

- The 3-way valve increases its bypassed flow rate

- The temperature in the oil tank increases which implies an increase of the boiler inlet temperature and then implies a decrease of the biomass burned to keep constant the outlet temperature T_{out}.

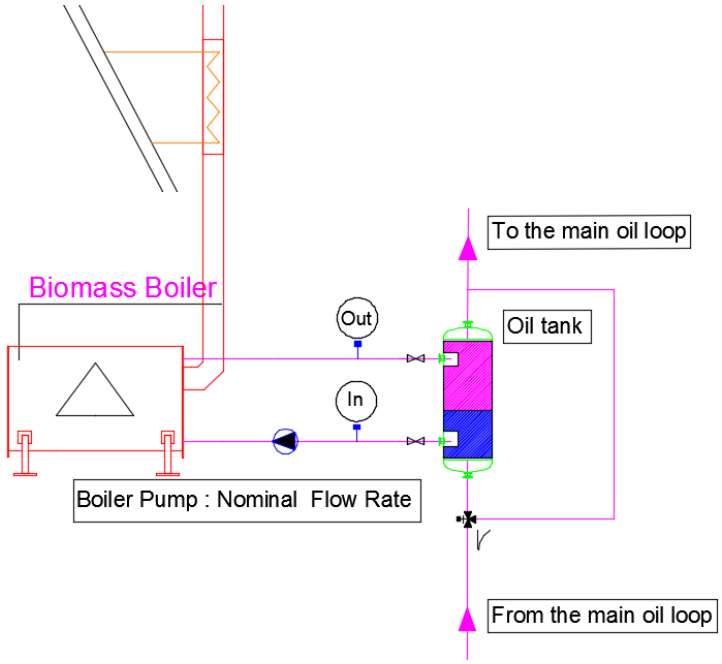

Figure 2.5: Illustration of the biomass with its gas exhaust tower and its storage tank.

Finally, concerning the effectiveness of the biomass boilers process, the biomass installed is expected to have an efficiency up to 90%. This is an important difference with new natural gas boilers which have an efficiency near 98%. Furthermore, the biomass boilers should be turned OFF for a thermal generation lower than 30% due to really efficiency at low partial load ratio *PLR*. Ideally, the thermal power necessary to run the ORC should be higher than this minimal PLR to keep high global efficiency.

2.4.1.2 Gas Boilers

Natural gas boilers are widely used in old buildings due to a really low gas fuel price in the past. The boilers installed in the Belgian Layout are working at low temperatures which allow using non-pressurized water as processing fluid. As they are working with a great energy efficiency combined to low capital investment, they are a good alternative to a biomass boiler when this latter is not an option (difficult/uncertain access to biomass fuel). Thanks to their technical characteristics, natural gas boilers are more flexible than biomass boilers. Their reaction time is much lower than biomass boilers and the range of their thermal power generation are wider than the one from a biomass as they haven't any minimal power production (30% for the biomass installed as previously said). Their regulation system in the retrofitted power plant is the same (based on an old control logic) and it will work in parallel. In general, their regulations are easier as they are more flexible and it's possible to fulfil the demand at every time step due to their fast reaction.

2.4.2 Energy Conversion Unit

2.4.2.1 Organic Rankine Cycle System

The Organic Rankine Cycle *ORC* is the equivalent of the steam cycle for low temperature heating source. At low temperature, the steam cycle has a low efficiency and it is thus necessary to use other fluids to keep a good efficiency. The block diagram of a simple ORC cycle is shown in Figure 2.6. A simple way to increase the efficiency of this ORC cycle is to place a heat recuperative exchanger as showed in Figure 2.7.

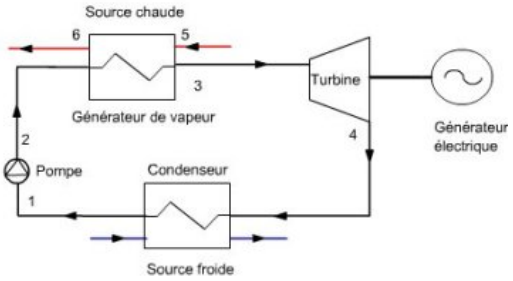

Figure 2.6: Simple ORC cycle [3].

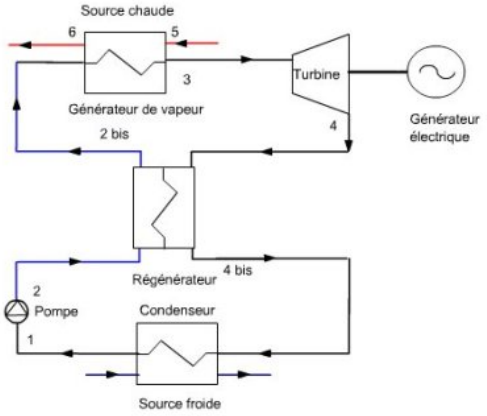

Figure 2.7: ORC cycle with regenerator [3].

As stated by Lemort [4], the selection of the working fluid is one of the key issues when designing an ORC. There are many fluids which can work at the desired temperature. However, during the fluid selection, many aspect can be taken into account to select the most appropriate process fluid. Here is the list of the different aspects/constrains:

- high thermodynamics performances,
- high vapor density to avoid having condensation when the evaporating temperature change really fast with a decrease of oil temperature (it happens when the ORC is working in transient),
- no deep vacuum in condenser,
- low volume ratio on the expander ("Turbine" in Figure 2.6),
- low mass flow rate to have a smaller pump,
- evaporating pressure lower than 30 bar,
- large availability,
- have a low consumption of the pump comparing to the turbine production $\left(\frac{\dot{W}_{pump}}{\dot{W}_{turbine}} \approx 15\%\right)$
- and low environmental impact (GWP) and high-security level.

The ORC, provided by the manufacturer *Rank*, is working with a heat source of 225°C and the working fluid is $R245fa$. The new part of the power plant consists in a biomass boiler directly connected to the ORC which should work without interruption during the whole year except in the summer when the whole power plant is shut down. If the heating demand is

low, the excess power from the condenser side of the ORC is dissipated in a dry cooler. The ORC generates 386 kW_{th} and 65 kW_{el} in cogeneration mode (characterised by a dissipation loop inlet temperature of 60°C). Moreover it can also work in generation mode (production of electricity only) which is characterised by a lower condensation temperature and thus a higher production of electricity (94 kWh_{el} for a dissipation loop inlet temperature of 20°C). Indeed, as the condensation temperature is low, the thermal power is unusable for heating and the only useful power is the electrical power.

2.4.3 Energy Distribution Units

2.4.3.1 Dry Cooler

The dry cooler is also called "Air Cooled Heat Exchanger". Contrary to the wet cooling tower, the dry cooler consists in a closed loop where the process fluid inside the pipes is cooled by an indirect contact with the air. These heat exchangers cool down the circulating fluid with ambient air flow through the heat exchanger fins. The spacing between these fins is really small (only 2,1 mm for one product of *Luvata* [5]) and depending on their diameter, the efficiency can almost reach the efficiency of a heat exchanger water based. Using air instead of water as cooling fluid is economically advantageous. The operating and maintenance costs are much lower than a water cooled exchanger. Indeed, with air, there are less operation issues like corrosion problems, deposition of dirt or leakages between the two fluids. Finally, in some location, the water is less available and/or more expensive (arid region, law controlling the water use, environmental problems like the heating of rivers,...). However, the air heat exchanger requires larger heating surface as the heat transfer coefficient is lower and the capital cost of an air heat exchanger is most of the time more important than one working with water. Though the capital cost is higher, the operating cost of the air heat exchanger and its reduction of possible operating issues make it more advantageous.

The main role of the dry cooler is to dissipate the excess power generated by the power plant or the building. In the Belgian layout, the dry cooler is only needed for dissipating the power generated by the ORC as there isn't any cooling demand from the building. More generally, the dry cooler is also utilised for refrigerant applications, air conditioning or free cooling. For low temperature applications (i.e. if installed outside), the fluid cooled by the air has to be a water-glycol mix to avoid freezing. The proportion of glycol depends on the system location (altitude, temperature,...).

Figure 2.8 shows possible design configurations of the dry cooler each differentiated by a different air flow through the dry cooler. All the schemes can be used for a large range of cooling capacity. The most common one is the horizontal orientation. However, for the lowest power to dissipate, the vertical configuration is preferred for its great reduction of needed area. Despite this main advantage, the performance of this specific air cooled heat exchanger depends on external factors like the wind direction. The A-frame or the equivalent V-frame configurations represents a good choice when great performances are required with a limited floor area. The A-frame and V-frame are more and more used in various domain for their great performance and their high cooling capacity per square meter. The fans can be situated below (forced draft (a) Figure 2.8) or above (induced draft (a) Figure 2.8) the heat exchanger. As the induced draft is located after the heat exchanger, it receives a hotter air than a forced-draft configuration. It means that the induced draft has a higher power consumption for the same mass flow due to higher air density. Although the induced draft required more power, the flow distribution is more uniform which increases the efficiency of the heat exchanger and balances its previous disadvantage. In consequence, both system consumption is more or less the same

for a fixed power dissipation. According to Kuppan Thulukkanam [6], both fans locations have different advantages and disadvantages:

- Forced draft
  - This configuration has a lot of advantages like the location of the fans allowing a simpler access for their maintenance. The incoming air is cooler which reduces the consumption of the fans as previously explained.
  - However, this configuration is subjected to hot air recirculation between the output of the dry cooler and the input of the fans. This issue, depending on the weather, increases the inlet temperature and thus decreases the heat exchange efficiency and reduces the capacity of the heat exchanger. The influence of the wind is showed in Figure 2.9. For a given capacity, a higher air flow rate or a higher heating area is required. This effect can be limited with vertical walls next to the heat exchanger.
- Induced draft
  - The configuration is easier to assemble and install. As already said, the distribution of the air flow through the heat exchanger is more uniform with this fan location. The potential issue of warm air recirculation is reduced due to a higher air rejection height. The hat (confer (b) Figure 2.8) provides some protection from the outside for the fins.
  - The maximal operating temperature is limited due to the effect of hot air on the fans.
  - The maintenance of the heat exchanger is easier with this fans location.

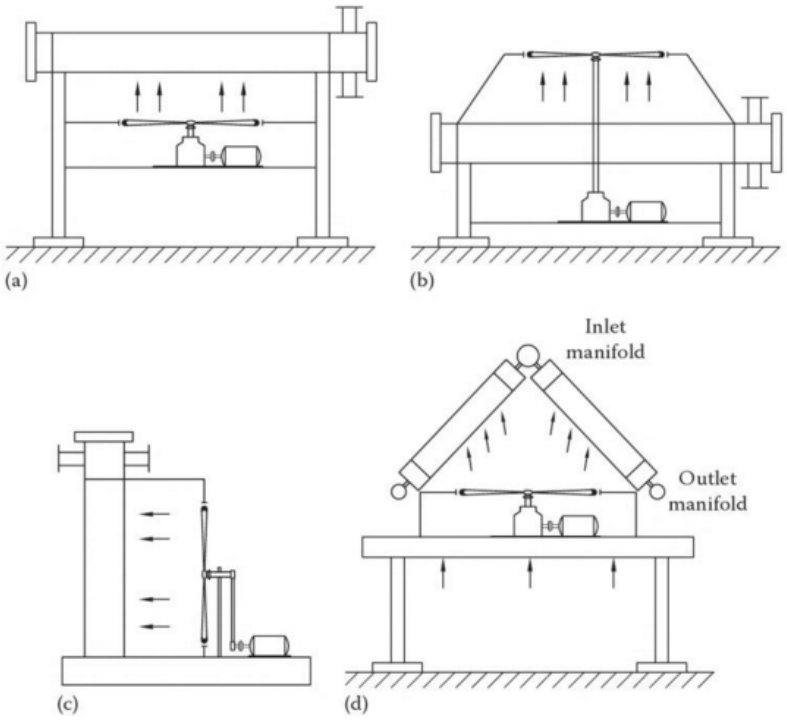

Figure 2.8: Air flow schemes of the air cooled heat exchanger - (a) Horizontal, forced draft (b) Horizontal, induced draft (c) Vertical (d) A-frame (figure from Kuppan Thulukkanam [6]).

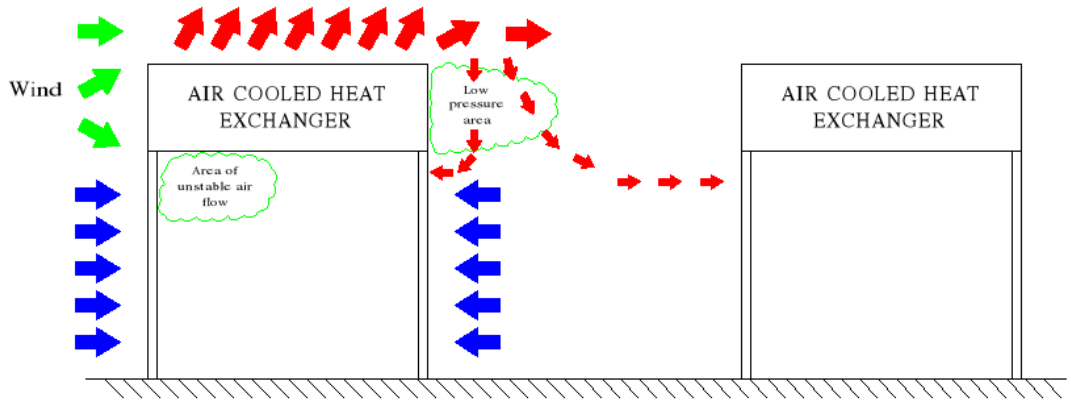

Figure 2.9: Influence of the wind on the warm air recirculation [7].

The dry coolers are differenced with their configurations, the characteristics of the fans and also with the type of their fins. There exist many different fin types like L footed, overlapped 'L', plate fin, extruded, serrated, embedded (G-Fin) or elliptical as stated in the product description of SPX cooling [8]. Each fin types are used for specific applications and the perfect fin has to be chosen depending the environment. The company *Deltathx* [9] gives a description on the fabrication process of the different finned tube types and their common applications. The product descriptions [10](*Deltathx*) and [11](*Sevojno*) explain the working range of the different fin types. All these possible choices make distinctive dry coolers having their own unique efficiency/capacity.

After having decided the orientations, the number of the fans and their diameter are computed depending on the cooling capacity necessary. The cooling capacity also varies with the fan rotational speed and the fluid flow rate through the dry cooler.

That is why a study to find the most efficient cooling system and the most appropriate control strategy can decrease hugely the operating cost. Indeed, a good sizing allows using the system at its nominal point most of the time which means at a higher efficiency. Moreover, the air flow control is primordial when there are large seasonal temperature differences. Concerning the control strategy, there are many possible ways of controlling the dry cooler. The Ref.[6], [12] and [13]) give different modulations of the power dissipation:

- The air inlet temperature can be controlled with a by-pass and/or a recirculation of warm air. The Figure 2.10 shows the recirculation of hot air inside a dry cooler. This voluntary recirculation is only required in some extreme cases to avoid freezing.
- The dissipated power can be controlled with a variation of the air flow. Simply switching on/off some fans can provide a quite good control when there are a lot of fans. Sometimes, multi-speed motors are used to achieve a better control. Finally, fans with variable frequency motor (modulated by a PID to vary the air flow rate) can be used. This last control is the best control we can have while varying only the air flow rate.
- Another way to control the power dissipation is modulating the speed of the pump feeding the dry cooler with the process fluid. A decrease of its mass flow reduces the power exchanged. This control method can only be used when the process fluid flow rate isn't imposed by the system.
- Finally both of the previous control can be used at the same time to reduce the electrical power consumption of the system.

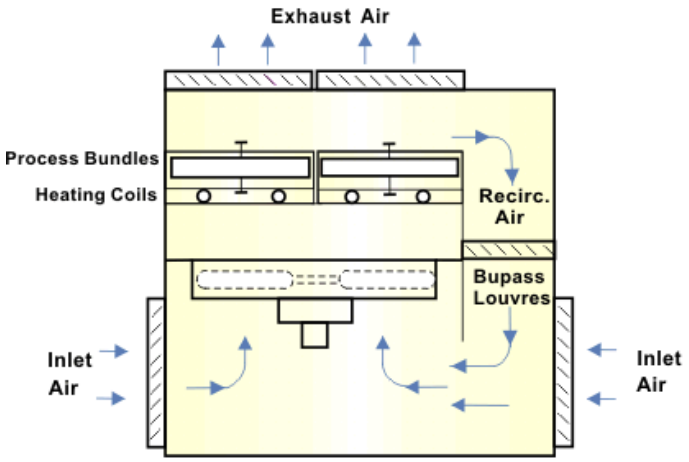

Figure 2.10: Recirculation of hot air inside the dry cooler to avoid freezing [13] .

2.4.3.2 Heat Exchangers

The heat exchangers are the most important elements from the Power Distribution Units. These *PDUs* comprise the heat exchangers between the power generation units *PGUs* and the distribution network and they also comprise the heat exchangers heating the air inside the building. The heat exchangers are mainly used to pass from one level of temperature to an other or the change the process fluid. There exist a lot of different heat exchangers. They can be counter/co-current and they can use fins if necessary (it depends on their applications). A heat exchange between two liquids does not require high area to have a good effectiveness. However, when the power is exchanged from one liquid to a gas, the heat transfer coefficient is much smaller and fins are necessary to keep constant the power flow. Indeed, the power is equal to $A.U.\Delta T$ meaning that a bigger heat exchange surface offsets the decrease of the U factor. The heat exchangers from the Belgian site are three plate heat exchangers. Their role is described below and their physical characteristics are given in Chapter 4:

Water-Water Heat Exchanger This heat exchanger transmits the power from the water circulating in natural gas boilers to water distribution loop. This specific heat exchanger is from the old system and its characteristics are well known.

Oil-Water Heat Exchanger It transmits the power from the thermal oil loop to the water loop distributing the power in the different block of the building. It is part of the components added to renovate generation power plant and contrary to the water-water heat exchanger, it requires a sizing.

Glycol-Water Heat Exchanger It is also a part of the new power plant and a sizing is made with the nominal power extracted from the ORC condenser.

2.5 Passive technologies

Passive technologies are technologies which reduce the energy consumption of a building by enhancing its energetic performance. There exist a lot of different ways to increase the energetic performance. In the following subsections, a brief description is given about the technologies implemented in the Belgian demo site and their predicted improvement of the energy system (in terms of energy saving/consumption reduction).

2.5.1 Aerating windows

They are windows with an integrated ventilation system. With an energy recovery heat exchanger, they aim to reduce the thermal losses during the aeration. This integrated system can be placed into other parts of the building like walls or central HVAC unit (heating, ventilating and air conditioning unit). With this technology, the polluted air is extracted from the building and it's replaced by fresh air which is preheated by indirect contact with the extracted air. The air exchange, required for the indoor air quality, (IAQ) is made with active or passive ventilation technologies (respectively HVAC units and windows opening).

Retrofitting an old building with aerating windows consists in a huge energy saving as the effectiveness can be really high by the use of a counter flow heat recovery exchanger composed of micro-channels (made from synthetic material which allows us to have a high surface density). The energy saving can be a huge fraction of the total losses depending on the fenestration ratio. Furthermore, this system is characterized by low pressure drops and it is also really interesting because it's possible to regulate the flow of air recycled by a control of the IAQ or based on predicted occupancy curves.

2.5.2 PCM

The Phase Change Material, *PCM*, is usually incorporated in the building to increase the inertia of the building and limit the maximal power demand. They have a really low temperature of solidification/liquefaction which makes possible to use their latent and their sensible energy (higher thermal storage per unit of weight and constant temperature). This specific material is often placed inside small sphere incorporated in a shell material that has a higher melting temperature. In the retrofitted building, the shell material is a polysiocyanurate layer (PIR) that offers excellent thermal insulation combined with the high thermal capacity of the PCM microcapsules. As stated by *RGEES* [14], a company specialized in design and manufacture of temperature control and thermal energy storage, the PCM is used to:

- shift the heating and cooling load in time to reduce the peak value and thus reduce the capacity of the equipment (average load instead of the maximal load), the operating and maintenance cost,
- produce thermal energy when the thermal energy source is available (i.e. cheaper to produce) and use it later when needed
- and to reduce the CO_2 footprint with a decrease of the cooling/heating demand.

In the Belgian demo site, only a part of the building, Blocks I and VI (Figure 2.2), is renovated with the passive technologies. The corresponding load of this two blocks accounts for 38% of the total load. The energy saving of only the $PCM + PIR$ layer is 12.5-15% of their total consumption and considering also the aerating windows, the total energy saving should reach up to 65% of their total consumption as previously said [15].

Chapter 3

Description of simulated power plant

This chapter explains the Belgian Bricker layout and its control logic. The first section of this chapter describes the Belgian system implemented by showing and explaining the last configuration studied during this thesis. The second section regroups and explains the role of all the sensors installed. A distinction is made between sensors needed to control the behaviour and the optional sensors. These latter sensors are used for monitoring but they haven't any active participation in the control strategy. It is followed by the last section of this chapter which is a description of the flow chart associated to the last layout and its control logic. The control logic is then applied to different working cases that can be encountered during the year.

3.1 Description of the system

A drawn of the production and distribution network is shown in Figure 3.1. In this diagram, a separation is made between the old production system and the one installed for the Bricker project using a dark line. The new part of the power plant (above the dark line) consists of a thermal oil loop and an extension of the water loop. The old production system consists in a water loop which connects three gas boilers to the distribution network through a heat exchanger. In Figure 3.1, each compound of the power plant has a different color:

Heating loop - Thermal oil The thermal oil loop, which carries the power produced by the biomass boiler to the heat exchanger and the ORC, is illustrated in pink.

Condensing loop The water loop in orange is used to dissipate the heat from the ORC's condenser with the cooling tower is the power required by the building is too low. When the power required by the building is bigger than the power released by the condenser, the power needed is extracted at the Water-Oil heat exchanger.

Heating loop - Water The previous generation system based on hot water flow is shown in red in Figure 3.1.

Control cable The control cables are illustrated with blue lines and they connect the pumps or the 3-way valves to the sensors that are used to modulate them.

Concerning the sensors, illustrated in blue in Figure 3.1, a detailed analysis is made for each of them in the following sections. In the next pages, their position and their main role are explained.

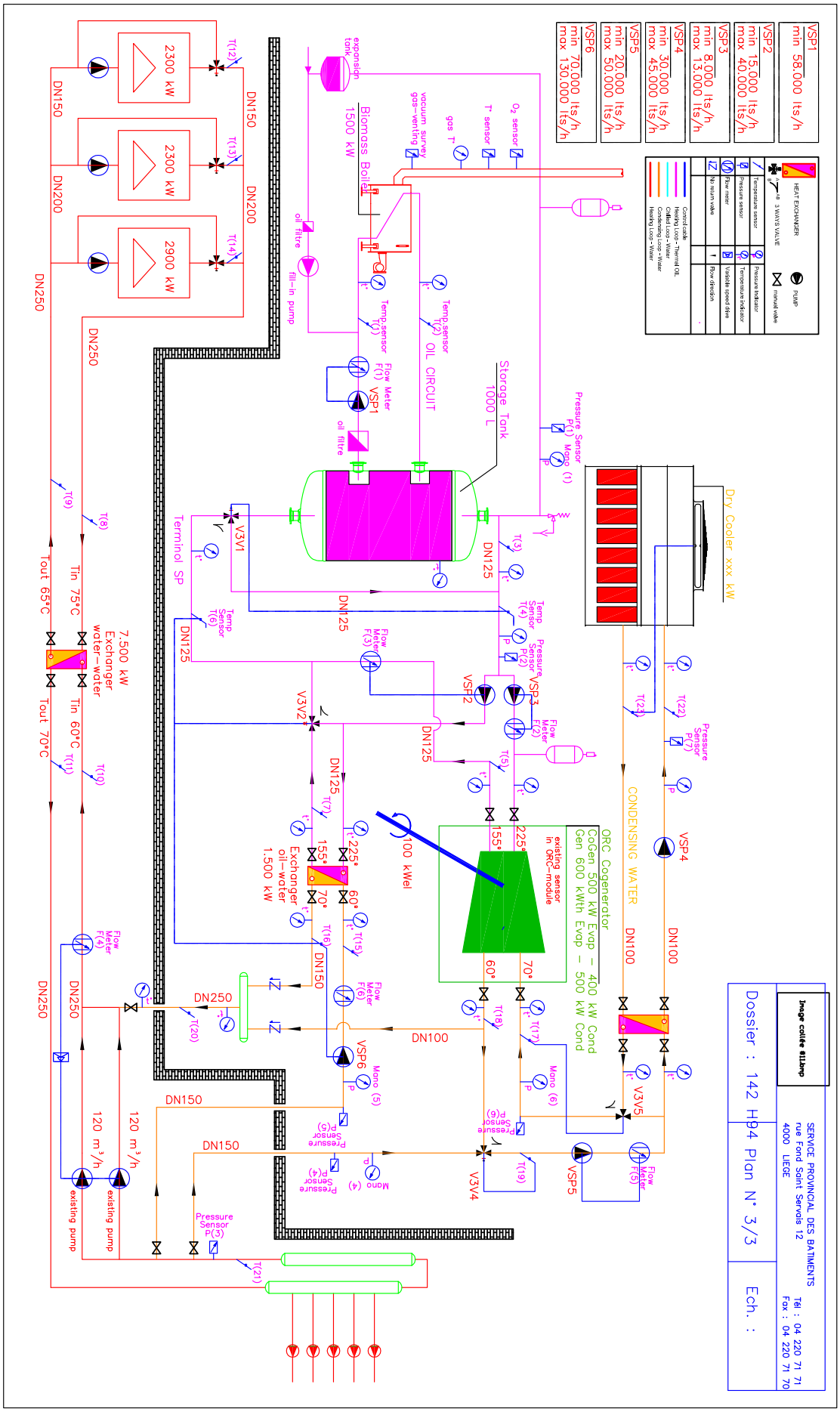

Figure 3.1: Layout of the Belgian site.

3.2 Instrumentation of the system

This part of the chapter describes the sensors from the Belgian layout illustrated in Figure 3.1. This picture shows the position of all the sensors installed in the most interesting points of the system to collect data and to monitory the power plant. There are three different types of sensors to measure the temperature, the pressure and the flow rate. As already said, some of them are necessary as inputs for the control logic and the others are only installed for monitoring and collecting data purposes. With these extra sensors, the behaviour of the system can be verified, the energy flux can be computed everywhere and the first laws of the thermodynamics can be verified. Table 3.1, 3.2 and 3.3 are respectively a list of sensors placed in the Belgian system (respectively the mass flow rate, the temperature and the pressure sensors). The three tables give the position and the role of each sensor.

Table 3.1: Mass flow rate sensors.

Flow Meter	Side	Role
F_1 (Inlet Biomass)	Thermal oil side	Control
F_2 (Inlet ORC)	Thermal oil side	Control
F_3 (Water-Oil HEX inlet)	Thermal oil side	Monitoring
F_4 (Water-Water HEX outlet)	Water side	Monitoring
F_5 (Inlet ORC condenser)	Water side	Control
F_6 (Water-Oil HEX inlet)	Water side	Monitoring

Table 3.2: Temperature sensors.

Temperature sensors	Side	Role
T_1 (Inlet Biomass)	Thermal oil side	Monitoring
T_2 (Outlet Biomass)	Thermal oil side	Monitoring
T_3(Outlet tank)	Thermal oil side	Monitoring
T_4(Inlet ORC)	Thermal oil side	Control
T_5(Outlet ORC)	Thermal oil side	Monitoring
T_6(Intlet Valve V3V1)	Thermal oil side	Monitoring
T_7(Water-Oil HEX outlet)	Thermal oil side	Monitoring
T_8 (Inlet hot side W-W HEX)	Water side	Monitoring
T_9 (Outlet hot side W-W HEX)	Water side	Monitoring
T_{10} (Inlet cold side W-W HEX)	Water side	Monitoring
T_{11} (Outlet cold side W-W HEX)	Water side	Monitoring
T_{12} (Outlet gas boilers 1)	Water side	Monitoring
T_{13} (Outlet gas boilers 2)	Water side	Monitoring
T_{14} (Outlet gas boilers 3)	Water side	Monitoring
T_{15} (Inlet cold side W-O HEX)	Water side	Monitoring
T_{16} (Outlet cold side W-O HEX)	Water side	Monitoring
T_{17} (Inlet condenser ORC)	Water side	Monitoring
T_{18} (Outlet condenser ORC)	Water side	Monitoring
T_{19} (Outlet valve V3V4)	Water side	Monitoring
T_{20} (Outlet Bricker's system)	Water side	Monitoring
T_{21} (Outlet building's distribution)	Water side	Monitoring
T_{22} (Inlet Cooling Tower)	Water side	Monitoring
T_{23} (Outlet Cooling Tower)	Water side	Control if we considered VSP4

Table 3.3: Pressure sensors.

Pressure sensors	Side	Role
P_1 (Inlet biomass boiler)	Thermal oil side	Monitoring
P_2 (Inlet evaporator ORC)	Thermal oil side	Monitoring
P_3 (Outlet distribution)	Water side	Monitoring
P_4 (Inlet ORC condenser)	Water side	Monitoring
P_5 (Inlet cold side W-O HEX)	Water side	Monitoring
P_6 (Inlet pump VSP6)	Water side	Monitoring
P_7 (Inlet Cooling Tower)	Water side	Monitoring

Table 3.1, 3.2 and 3.3 are a list of the sensors used for monitoring and controlling the system behaviour. Additionally to these sensors, there are the sensors installed directly inside some components like the ORC and the biomass boiler which have their own sensors needed for their internal control logic. Some external sensors might thus be redundant with internal sensors. However, some of the internal sensors might not be accessible from the outside and they are thus unusable for the control unit. If they are accessible from the external control unit, some sensors could be avoided.

The main role of the sensors is collecting data and controlling the system. Furthermore, they can also be utilized to send warning messages to the operator. In case of wrong utilisation or simply when issues happen, the temperature can be outside the normal temperature range requiring some reaction like eventually interrupting the biomass boiler (when the outlet temperature of the biomass boiler overpass its limit, an alarm triggers and the operator can thus decide interrupting or not the biomass boiler). The same reasoning can be made for other components like the ORC that has to be interrupted when the temperatures are too high or when the flow rate isn't in the authorized range value.

The expected internals sensors of each component are listed in Table 3.4. In this table, the monitoring variables are listed and a link is made with their corresponding alarms. These alarms and their control system are delivered by the providers of the component. Most of the time, the precision of those sensors from the sellers is relatively low and it is not enough for collecting data, monitoring and controlling the system behaviour. That's why extra sensors are considered even if they are redundant. Furthermore, the temperature sensors are really cheap and they are no reasons not using them for collecting the data that would be necessary for a future tuning of the system.

3.3 Control logic

As the system has many components that have several conditions for safe operation, there is a need for a consistent and well-structured routine. In this subsection, the flow chart corresponding to the last layout considered is shown and explained. The aim of this flow chart is to explain how the system could work and gives an example of a possible software implementation for its control logic. To make easier to understand, the flow chart is divided into the main routine "Seasonal main routine" and subroutines for each component. Each subroutine works in parallel and they eventually include an internal control logic of the component. In the following pages, the operational routine "Seasonal main routine" is explained in detail. After this explanation, a description of the subroutines and of how the power generation system works is given.

Table 3.4: Internal sensors of each component from the system.

Biomass boilers	Role	Other information
T_{in}	Monitoring	Thermal oil temperature at the biomass boiler inlet
P_{in}	Monitoring	Thermal oil pressure at the biomass boiler inlet
$\dot{m}_{bm}$	Monitoring	Quantity of biomass burned
T_{bm}	Monitoring	Temperature of the biomass before combustion
T_{out}	Monitoring and control Internal alarm	Thermal oil temperature at the biomass boiler outlet (sensor connected to the boiler system) Alarm activated if temperature above 300°C
$T_{o,tank}$	Monitoring Internal alarm	Thermal oil temperature in the expansion tank (sensor connected to the boiler system) Alarm activated if temperature above 300°C
T_{fumes}	Monitoring Internal alarm	Temperature of the fume at the exhaust (sensor connected to the boiler system) Alarm activated if temperature under 250°C
$P_{chamber}$	Control Internal alarm	Combustion chamber pressure (negative /De-pressurization) Exhaust fan speed modulation to avoid leakages of combustion gases (sensor connected to the boiler system) Alarm activated if outside the range $[-0.1;-1.5]$ bar
$\dot{m}_o$	Monitoring Internal alarm	Thermal oil flow rate through the biomass boiler (sensor connected to the boiler system) Alarm activated if flow rate $\leqslant 24m^3/h$ (=80% of its nominal value)
Vol_o	Monitoring Internal alarm	Volume of the thermal oil in the expansion tank (sensor connected to the boiler system) Alarm activated if V_{tot} is too low due to leakages
$T_{chamber}$	Monitoring Internal alarm	Combustion chamber temperature) (sensor connected to the boiler system) Alarm activated if temperature outside the range $[450;900]$ °C
ORC	**Role**	**Other information**
$T_{o,in}$	Monitoring Internal alarm	Thermal oil temperature at the ORC inlet (sensor connected to the ORC internal logic) Alarm activated if temperature above 335°C
$\dot{V}_o$	Monitoring Internal alarm	Thermal oil flow rate through the ORC evaporator (sensor connected to the ORC internal logic) Alarm activated if flow rate $\geqslant 14m^3/h$ (its nominal value=$13m^3/h$)
$T_{w,in}$	Monitoring Internal alarm	Water temperature at the ORC condenser inlet (sensor connected to the ORC internal logic) Alarm activated if temperature above 70°C
$\dot{V}_w$	Monitoring Internal alarm	Water flow rate through the ORC evaporator (sensor connected to the ORC internal logic) Alarm activated if flow rate $\leqslant 30m^3/h$ (its nominal value=$37m^3/h$)
$T_{w,out}$	Monitoring	Water temperature at the ORC condenser outlet
$T_{o,out}$	Monitoring	Thermal oil temperature at the ORC evaporator outlet
$P_{gross,el}$	Monitoring	Gross electrical power output from the ORC
Dry cooler	**Role**	**Other information**
$T_{w-g,in}$	Monitoring	Water glycol temperature at the dry cooler inlet
$T_{w-g,out}$	Monitoring	Water glycol temperature at the dry cooler outlet
$\dot{m}_f$	Monitoring	Air mass flow through the fan

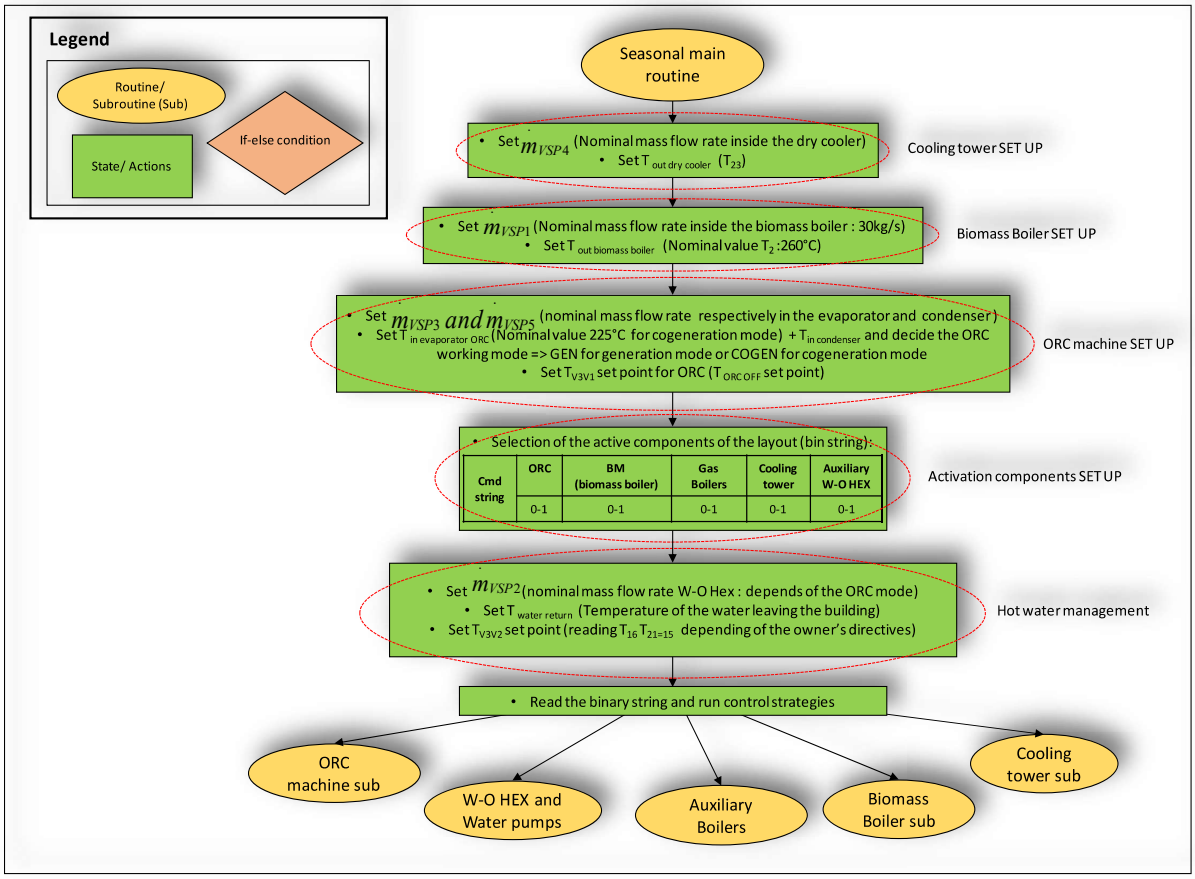

Figure 3.2: Flow chart of the main routine.

The main routine is showed in Figure 3.2. The subroutines of the biomass, ORC, Cooling Tower, Water-Oil heat exchanger and the auxiliary boilers can be seen in Figures 3.3, 3.4, 3.5, 3.6 and 3.7 respectively. This control logic works with the suggested layout which is described in the begin of this chapter. These subroutines were realised based on the most up to date data and on many discussions.

3.3.1 Seasonal main routine

In the main routine (Figure 3.2) which is the higher level of the control logic, all the inputs needed for the control strategy have to be given by the operator. These inputs have to be fulfilled before switching on the system and they are mainly the set point temperatures for the thermo-valves and the nominal mass flow rates for the pumps. These inputs correspond to the optimal working conditions of the components. As already said, these optimal working conditions depend on the period of the year seeing that the optimal temperature is not the same for high and low thermal demand. Using all the data fulfilled, the software creates a binary string (number composed of 0 and 1) saying which components of the system are used or turned off. This number is then read by all the subroutines working independently.

3.3.2 Biomass subroutine

The routine for the biomass boiler, represented in Figure 3.3, is simple as there are almost no free parameters influencing the working conditions. When the signal to switch on is given by the operators ($Cmd(2) = 1$), the software checks that the pump are working well and if so, it imposes the mass flow rate given as input to the main routine. To fix the right mass flow rate, a modulation is made on the frequency of the pumps or the pressure losses with manual valves. After the activation of the pump $VSP1$, the biomass boiler burns the quantity of biomass needed to reach the set point fixed by the operators during the input's filling of the main routine. The quantity of biomass needed to fulfil the power required (and so reaching the set point temperature) is determined by the internal control strategy provided by the biomass supplier.

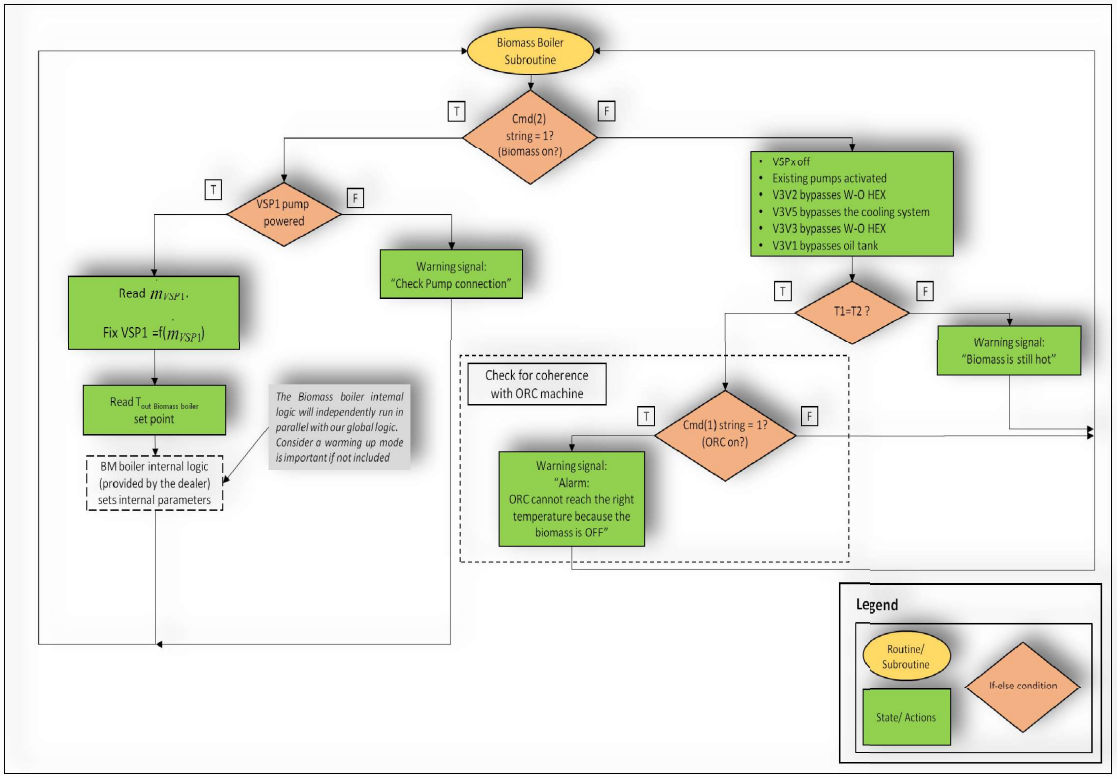

Figure 3.3: Flow chart of the biomass subroutine.

The only action left controlled by the user is the aperture of the 3-way valves situated before the tank. A valve completely opened means a maximal extraction of power from the biomass and a closed valve leads to the shutdown of the biomass. Indeed, the outlet temperature increases until the limitation temperature (chosen by engineers) is reached and a warning signal is send to shut down the biomass.

If the string says that the biomass is OFF (for maintenance or simply because it's not needed), the pumps and the valves are turned off (a question of security concerning the valves). Moreover, the inlet and outlet temperatures of the biomass are compared to verify that the biomass isn't hot any more. Finally, the software checks the consistency of the inputs given by the operators. Indeed, in case the ORC is ON without its source of power (biomass boiler OFF), a warning system is sent to the operator to alert him of this incoherence.

3.3.3 ORC subroutine

Once the ORC subroutine, Figure 3.4, receives the binary number, the software verifies that the pumps VSP3 et VSP4 are powered when the Cmd(1) string is 1 (ON). If there are any issues with the pumps, a warning signal is sent to the operator to check the pumps connection. When everything is working fine, we read the oil inlet temperature of the evaporator to control that the temperature is in the working range temperature. This latest temperature is controlled with the aperture of the valve V3V1.

The valve V3V1 controls the mass flow rate through the oil tank. If the oil temperature going to the main loop is too low, the aperture of the 3-way valve is modified to decrease the bypass of the oil tank.

When the temperature is in the working range of the ORC evaporator and when the evaporator is warmed, the internal control logic from *Rank* activates the ORC and modulates the speed of the pumps VSP3/4/5 depending on the functioning mode of the ORC. Finally, when the ORC is switched OFF, the corresponding pumps are turned OFF. During the warming process of the ORC, the pumps VSP3 and VSP5 are on though the ORC, modulated by its internal logic, is off waiting to reach the range of working temperatures.

3.3.4 Dry cooler subroutine

The subroutine of the cooling tower is illustrated in Figure 3.5. When the cooling tower is OFF, the associated pumps and the fan are switched OFF and an alarm is activated if the ORC is ON. When the cooling tower is ON and if the pumps are powered, the set point temperature is read from the main routine and the PID of the valve V3V5 controls the aperture to get the right temperature in the inlet of the ORC's condenser.

3.3.5 Water-oil heat exchanger subroutine

The water-oil heat exchanger subroutine is illustrated in Figure 3.6. When the water oil heat exchanger isn't operational, the program turns OFF the pumps and the two associated PID. It will also check the consistency of the model by looking if the natural gas boilers are activated to fulfil the power required.

If the heat exchanger is operational, the program checks that the two associated pumps are powered. It fixes the frequency of the pumps to have the desired oil mass flow rate (chosen during the sizing of the system) and it reads the two set point temperature. The two set point temperatures T_{16} and T_{21} are read and if one of them is out of its range, the system modifies one characteristic of the system. If the return temperature of the building T_{21} is out of its range, the frequency of the pump $VSP6$ is modulated to modified the mass flow rate through the heat exchanger. A temperature lower than the set point implies an increase of the mass flow to get back to the right temperature. Indeed, if the mass flow rate in the water loop increases, the pI controller regulating the 3-way valves $V3V2$ increases the oil flow rate in the heat exchanger to reach the water outlet temperature. Those two regulations are made in parallel and the parameters of the pI controller are chosen wisely to have the desired reaction.

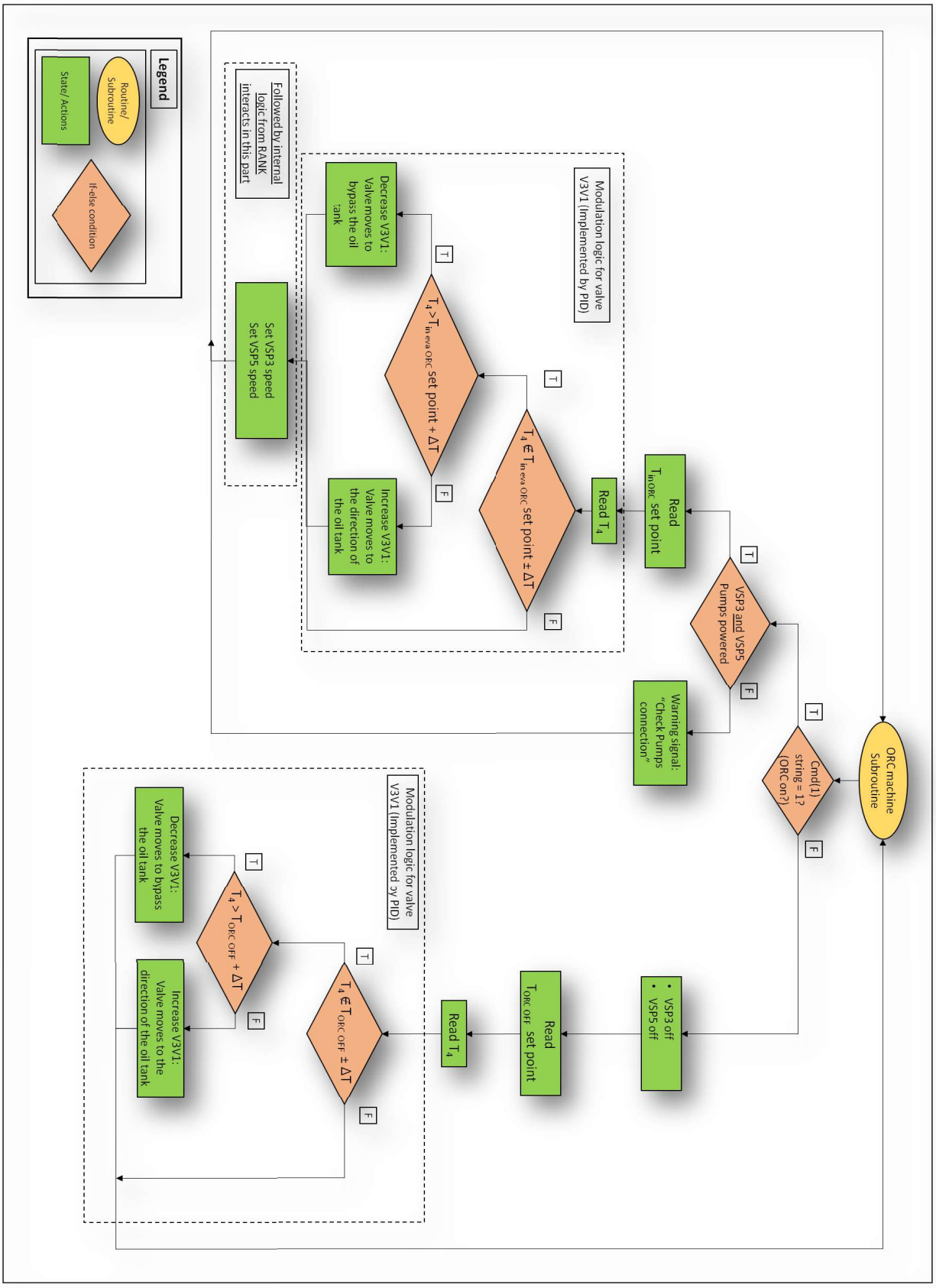

Figure 3.4: Flow chart of the ORC subroutine.

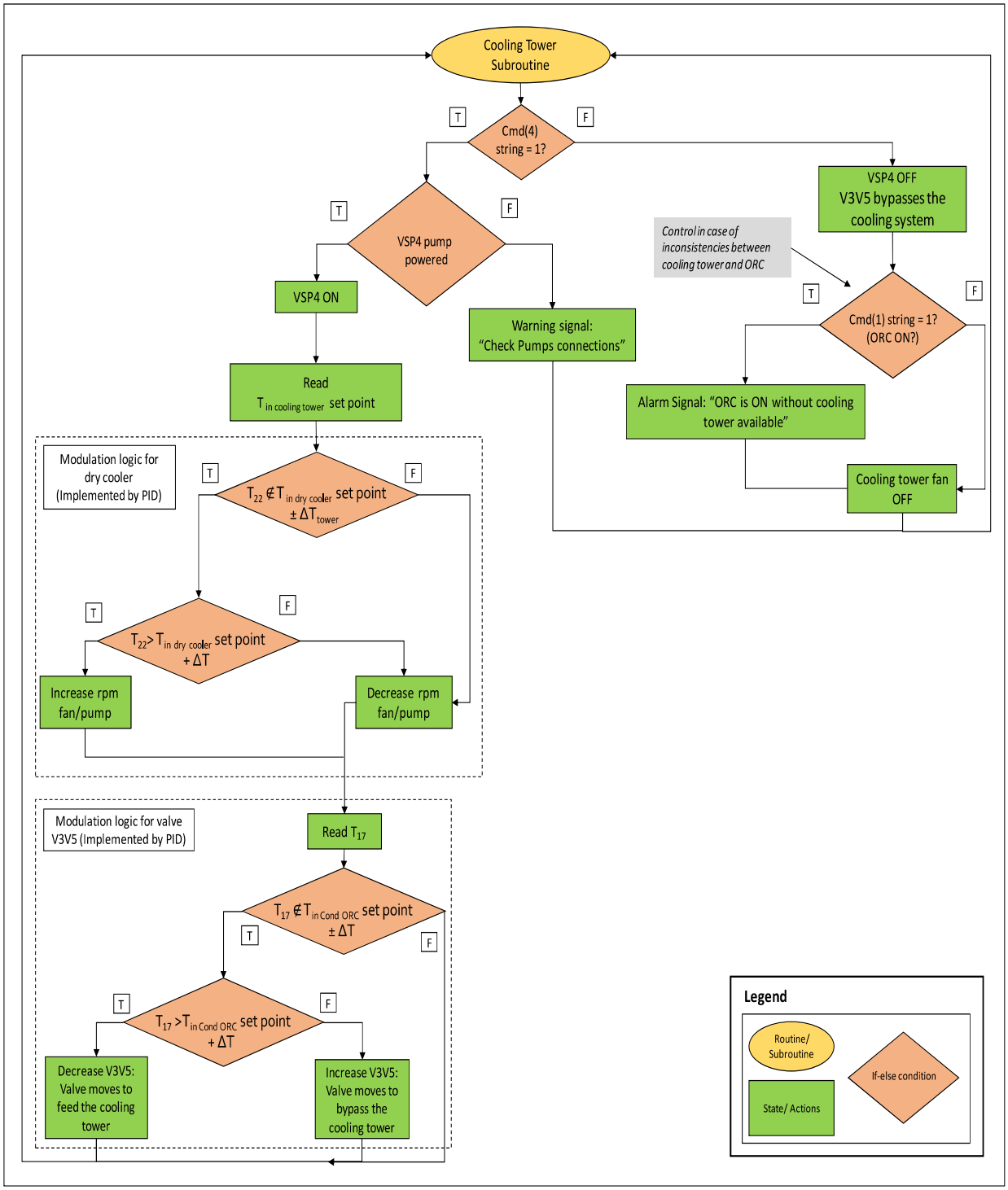

Figure 3.5: Flow chart of the cooling tower subroutine.

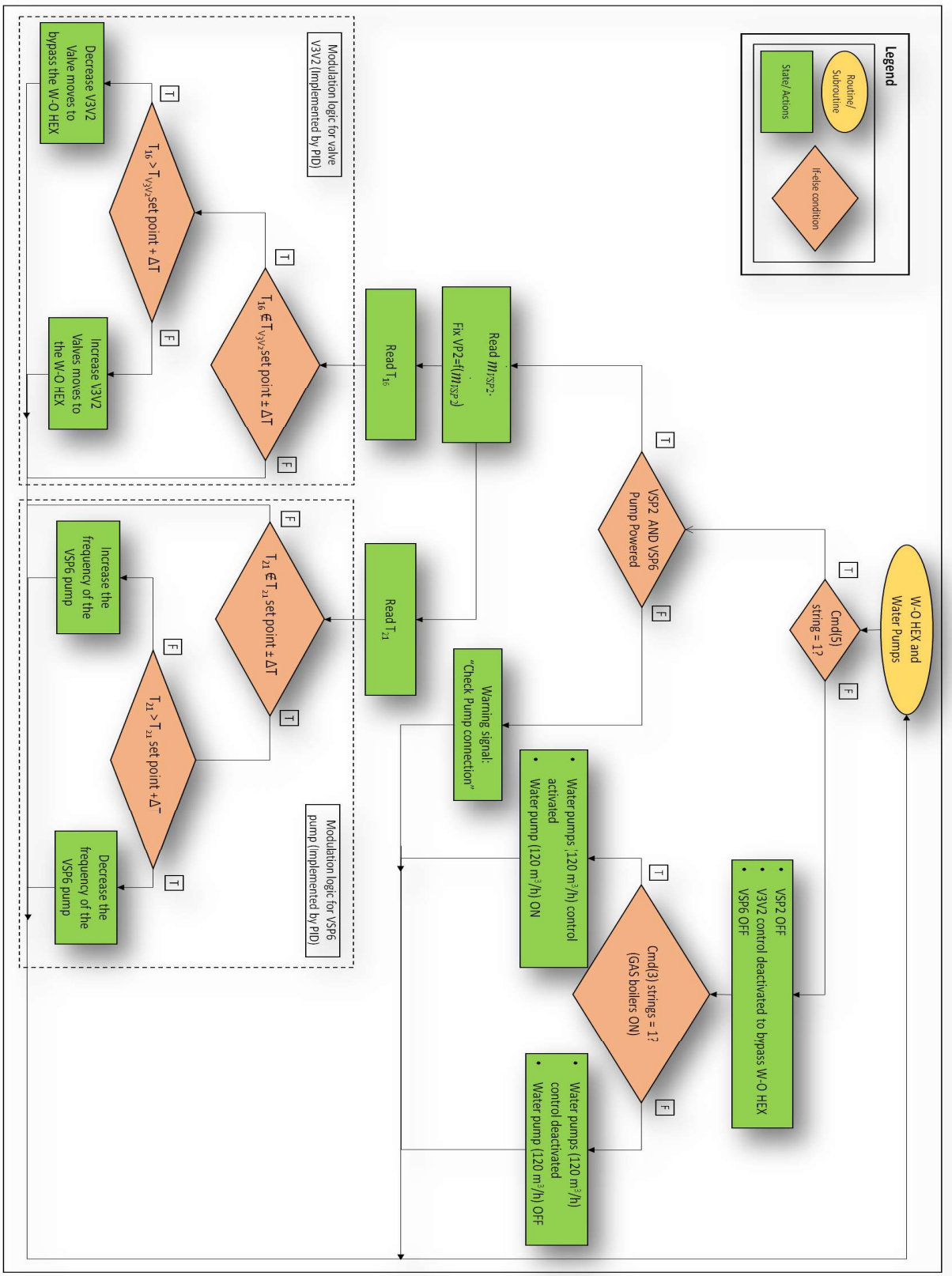

Figure 3.6: Flow chart of the water-oil heat exchanger subroutine.

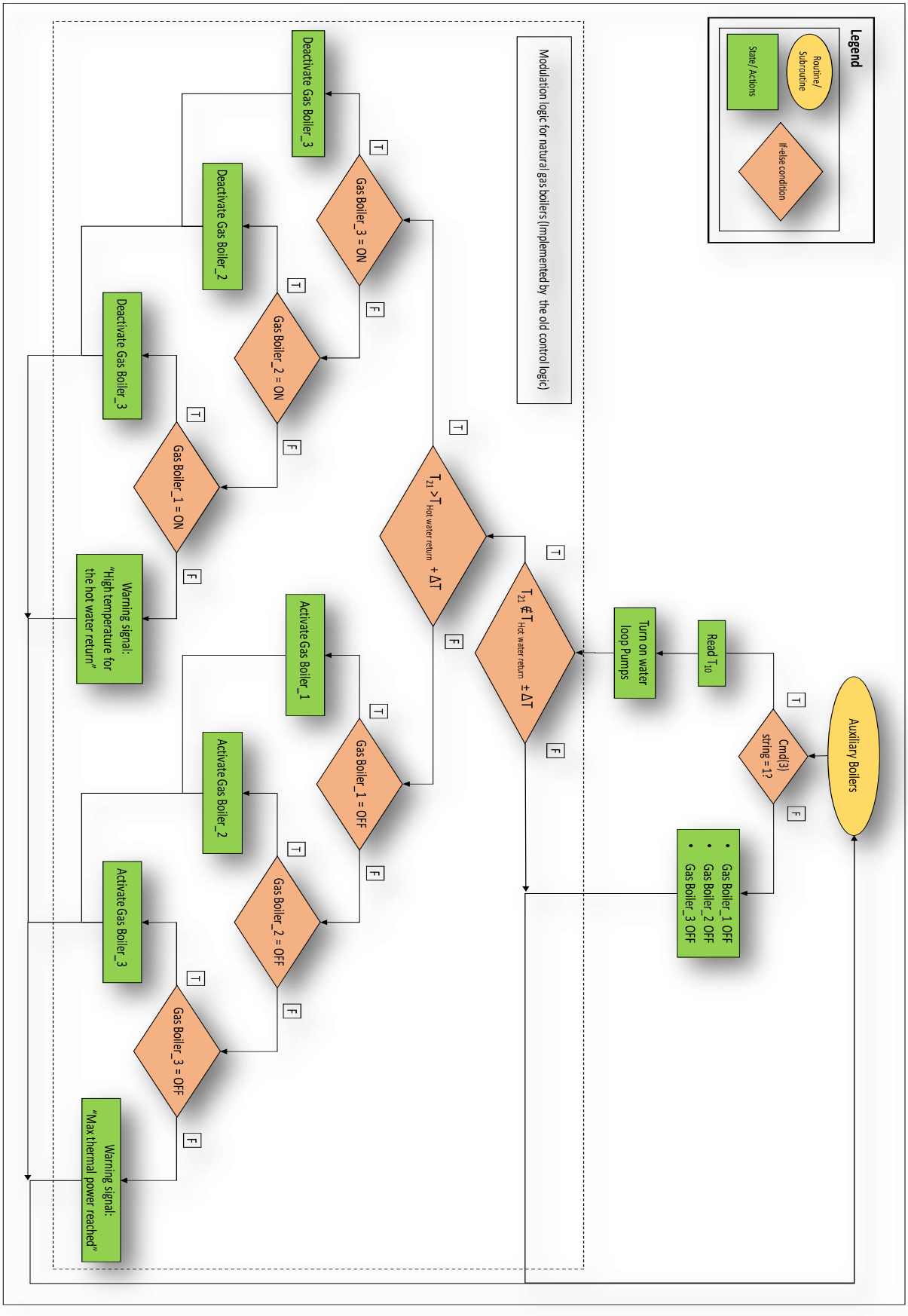

Figure 3.7: Flow chart of the auxiliary boilers subroutine.

3.3.6 Natural gas boilers subroutine

When the boilers are ON and when the temperature is under the allowed range of temperature, the old control logic system activates one supplementary gas boiler or increase its gas fuel rate consumption to increase the outlet temperature. Similarly, a temperature above the allowed temperature range implies a reaction of the gas boilers control logic which consists in decreasing the quantity of gas burned or shutting down one boiler to decrease the outlet temperature.

3.4 Working schemes

In this subsection, the control logic is applied for specific combinations of the Belgian layout components. A representation of the layout is given every time to show precisely the working schemes. The inactive components are showed in grey in all the figures and the active ones keep their own color (see Figure 3.1 for their initial color).

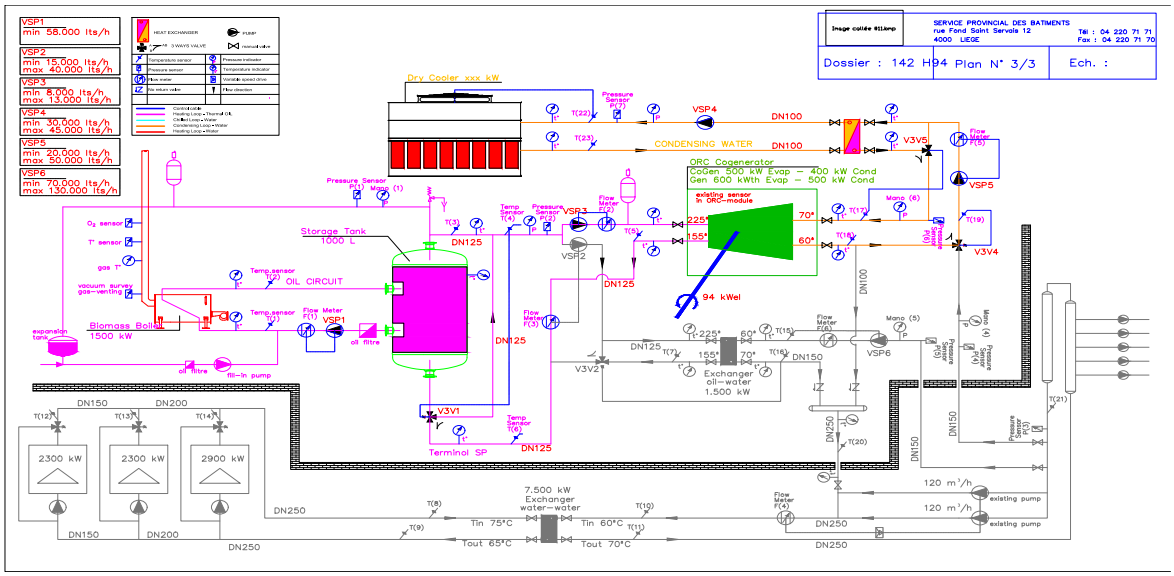

Figure 3.8: Working scheme : ORC generation mode and Dry Cooler.

During some periods of the year, the generation mode of the ORC will be used. Figure 3.8 is the illustration of the connections and the active components of this first considered configuration. As previously explained, the generation mode corresponds to a high production of electricity and a production of thermal power at a temperature really low making this power unusable. It means that this power has to be dissipated. The first working scheme considered (i.e the ORC working in generation mode) is mainly encountered during the summer when the building doesn't require any power at all. This configuration shouldn't be used often as the shutdown of the biomass is being considered when there aren't thermal power required by the building. The only components that are used in this configuration are the biomass boiler working at partial load to only produce the power needed at the ORC evaporator, the ORC, and the dry cooler to dissipate the power at the ORC condenser side. The illustration of this working scheme is showed in Figure 3.8 where the components unused are showed in grey.

This configurations is characterized by a consumption of 591kW at the ORC evaporator

for an oil inlet temperature of 225°C and a water inlet temperature of 20°C. The water outlet temperature corresponding is only 31°C and the thermal power has thus to be dissipated in the dry cooler. As there aren't fluctuations of thermal power demand or power production, it should work in steady state. Concerning the 3-way valves, shown in Figure 3.8, the 3-way valve *V3V4* is manually closed to bypass the distribution network where as the controller of *V3V5* modulates its aperture to extract the right thermal power released by the ORC (the *PID* output of the 3-way valves *V3V5* is constant and everything should work in a steady state).

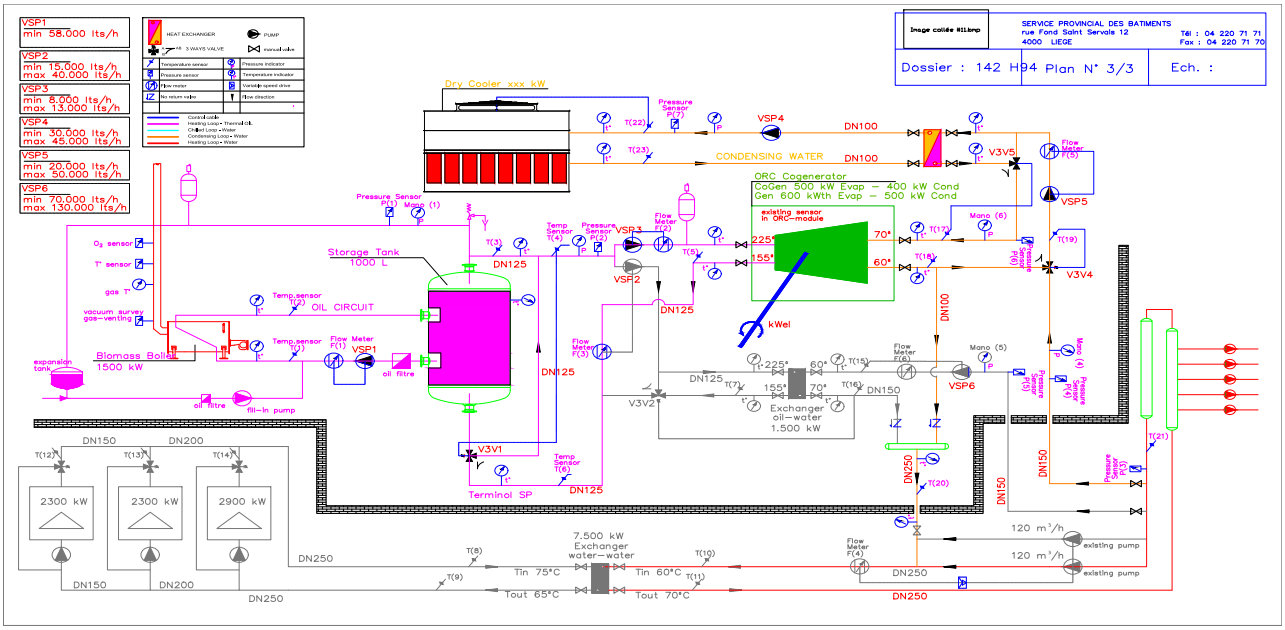

Figure 3.9: Working scheme : ORC cogeneration mode, Building and Dry Cooler.

The second scheme studied is illustrated in Figure 3.9. This working scheme corresponds to a low but non-null heating demand. To fulfil this low thermal demand, the ORC works in cogeneration mode. The water enters at 60°C in the ORC condenser and exits at 70°C from the condenser. After being heated, the water flow goes in the distribution network where only a fraction of its power is extracted. Contrary to the previous case, the 3-way valve *V3V4* is fully opened and a modulation of the three-way valve *V3V5* is needed to verify the power balance at every time step. The power balance is given by the following equations 3.1 and 3.2. This working scheme is encountered during the end and the beginning of the heating period (summer/autumn/spring).

$$\dot{Q}_{bm} = \dot{Q}_{ev,ORC} \tag{3.1}$$

$$\dot{Q}_{cd,ORC} = \dot{Q}_b + \dot{Q}_{dc} \tag{3.2}$$

Where $\dot{Q}_{bm}$, $\dot{Q}_{ev,ORC}$, $\dot{Q}_{cd,ORC}$, $\dot{Q}_b$ *and* $\dot{Q}_{dc}$ are respectively the thermal power for the biomass, the evaporator and condenser of the ORC, the building and the dry cooler.

The third working scheme is the most used during the year (3319 hours of this working scheme during the year 2015). It's the combination of the Biomass providing power to the ORC working in cogeneration and to the heat exchanger. In this case, the power extracted in the condenser isn't enough to fulfil the power requirement of the building and some extra power is exchanged in the heat exchanger oil-water 1500 kW. This latter working scheme is illustrated in Figure 3.10 and the different components work as followed:

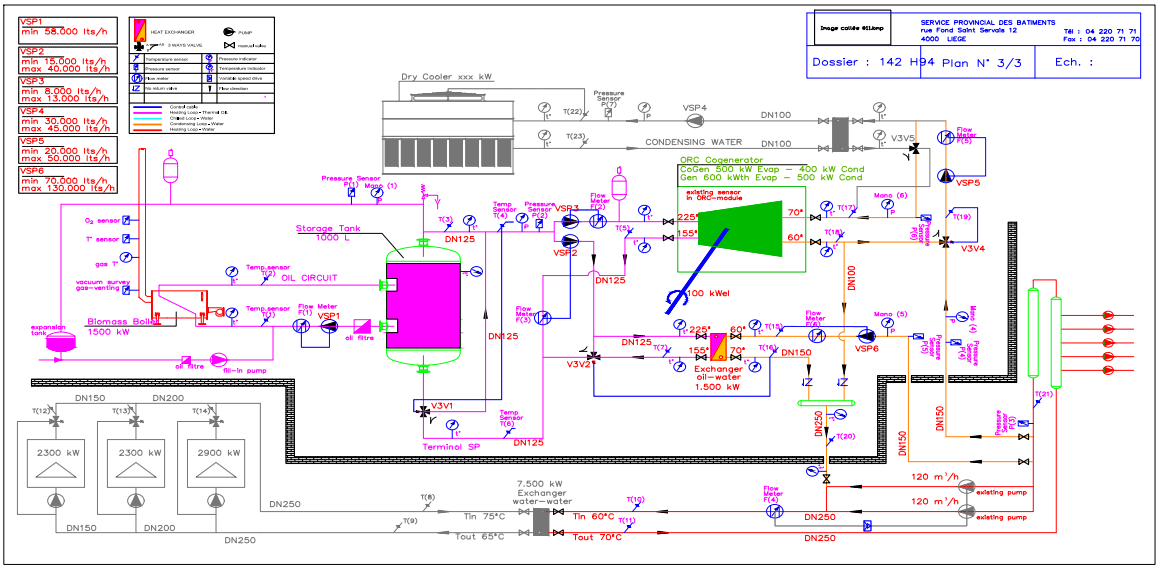

Figure 3.10: Working scheme : ORC cogeneration mode, W-O HEX and Building.

Three-way valves The valves *V3V4* and *V3V5* are completely opened. The three-way valve *V3V2* is modulated by the PID to reach the set point temperature T_{16}. If the temperature is lower than the set point, the aperture of the valve *V3V2* increases to increase the oil flow rate in the heat exchanger which leads to an increase of the water outlet temperature.

When the temperature is higher than the set point, the *PID* controller sends a signal to decrease the aperture of the valves and bypass the oil-water heat exchanger.

Concerning the three-way valve *V3V1* controlling the power produced by the biomass boilers, its aperture increases to extract more power from the biomass when the power exchanged at the heat exchanger increases.

Pumps All the pumps are working at a constant mass flow rate except the pump $VSP6$ which is modulated to meet the power demand. Depending on the pressure losses (whose vary with the aperture of the 3-way valves $V3V1$ and $V3V2$), the others pumps can make a slightly modification of their frequency to keep their mass flow rate at their nominal flow rate. Concerning the pump $VSP6$, it's controlled by a *PID* controller which increases the flow rate when the return temperature of the water (T_{21}) is lower than 60°C. Indeed, an increase of the flow rate implies a decrease of the HEX water outlet temperature which will induce a reaction of the component *V3V2*.

The next scheme studied is the scheme used during the coldest period of the year (in other words during the highest power demands which represent a bit less than one thousand hours in 2015). This case uses all the components available from the Belgian power plant except the dry cooler. This combination of components is illustrated in Figure 3.11. It ideally corresponds to the biomass boiler working at its maximal power and the extra power demand is produced by the natural gas boilers. This working scheme works as described as follow:

- All the three-way valves are fully opened and almost all the pumps are working at their nominal value.

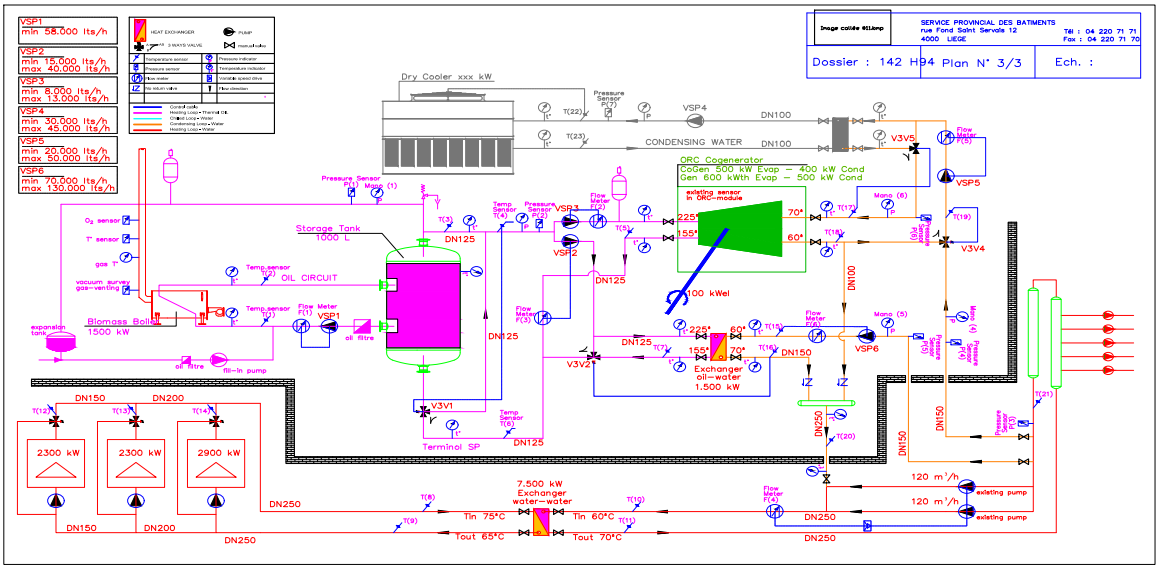

Figure 3.11: Working scheme : ORC cogeneration mode, W-O HEX, W-W HEX and Building.

- A frequency modulator is added to the existing pumps to use them as variable speed pumps. The existing pumps are thus modulated by a PID controller in the same way the pumps $VSP6$ was in the previously considered case. It means that its mass flow rate increases (respectively decreases) when the return temperature of the building T_{21} decreases (respectively increases).

- The three gas boilers provide the extra heating power required that the ORC and heat exchanger can not deliver. They regulate their power using the sensor T_{21}. Using the sensors measuring the outlet temperature of the water-water heat exchanger T_{11} is not allowed in this case because the maximal mass flow rate is limited and we then need a high temperature to keep the return temperature constant when the power increases. Moreover, this way of controlling showed the highest stability and the best results as it is shown in Chapter 5.

If any issue happens in the ORC or if one of the pieces is broken, the system has to modify its working scheme to be able to use the biomass boiler at its maximal power. Indeed, the biomass has to be used as much as possible before using the natural gas boilers. To do so, the pumps $VSP2$ and $VSP6$ increase their mass flow rate to be able to exchange a higher power in the water-oil heat exchanger without changing the functional temperature range. This is illustrated in Figure 3.12. In this last figure, the color of the natural gas boilers is cyan because they are used or not depending on the power required by the building. As shown in Figure 3.12, the dry cooler is OFF as there isn't any power to dissipate (considering there is no cooling demand).

The last scheme considered is illustrated in Figure 3.13. It corresponds to the old system working alone. This case has to be indeed considered because unexpected issues might happen in the new power plant (e.g. the shutdown of the biomass boiler) and instantaneous reaction are necessary to fulfil the power required. In old generation power plant, the pumps were working at their nominal value and the natural gas boilers were working like an ON-OFF system (it is described in detail in the subsection of Chapter 4 dedicated to the natural gas boilers).

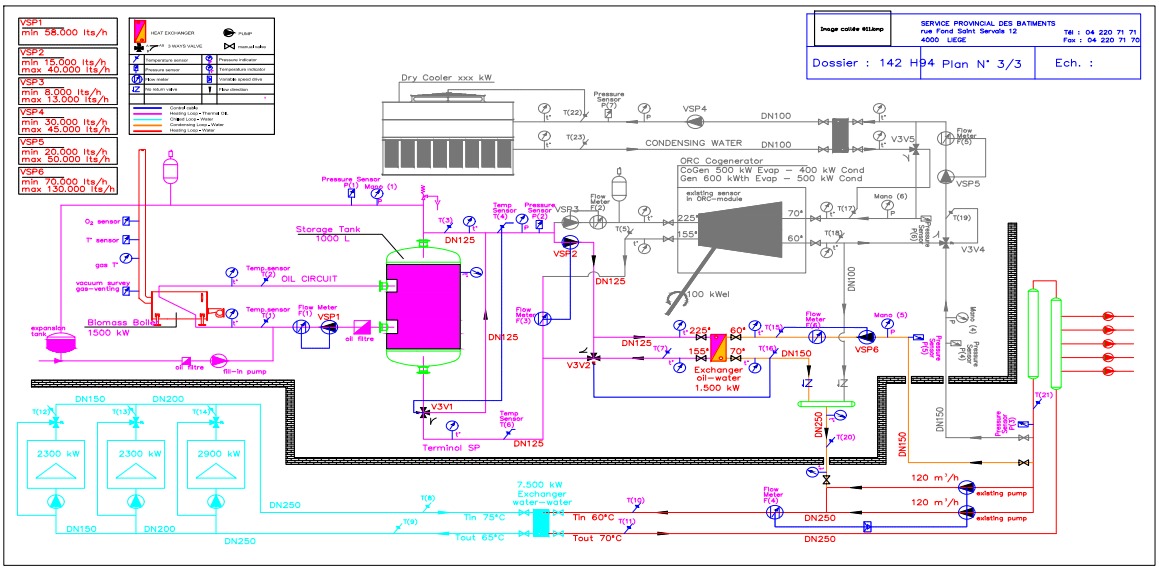

Figure 3.12: Working scheme : W-O HEX, W-W HEX and Building.

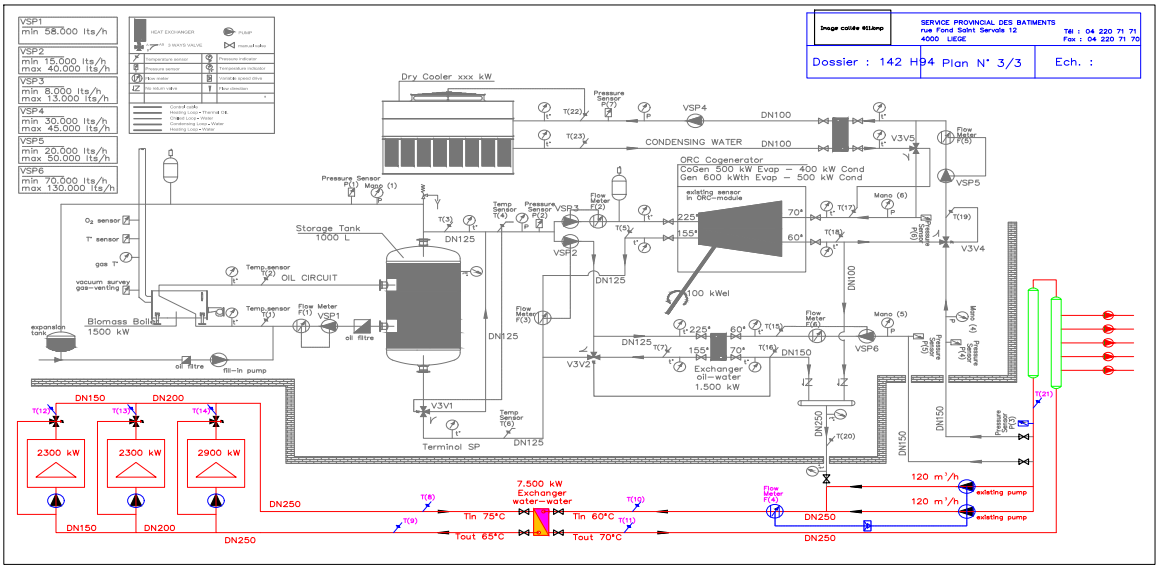

Figure 3.13: Working scheme : Previous Power Plant.

Chapter 4

Modelization and validation of the dynamic model

In this chapter, a detailed study of the components from the system layout is given. The beginning of the chapter is a description of the models used to implement each component and it is followed by a study of each model implemented in a dynamic environment (*Dymola*) to validate the results obtained.

4.1 Components from ThermoCycle

In Dymola language, an object-oriented software, many models of components already exit and they can be found in different libraries which most of the time are open-sources. In case one model doesn't exist, it's really easy to implement one based of the subcomponents that exist in these libraries. In the next pages, there is a list and a brief description of the models (or packages), from *Modelica* or *ThermoCycle*, that are used for the modeling of the power plant (Figure 3.1).

Two Flow1DimInc A component which represents the flow of an incompressible fluid through a pipe (its icon in *Dymola* is illustrated in Figure 4.2). This pipe is a simple one dimensional discretized pipe. Each sub division has its own heat flow, which is computed using the energy balance (equation (4.1)), through its thermal port. Moreover, this model includes one of the equation from the package **HeatTransfer** to consider a dependency of the heat transfer coefficient with the flow rate (**HeatTransfer** is explained in the next pages).

$$\dot{Q}_{tot} = A_i \dot{q} \qquad = V_i \rho \dot{h} + \dot{V}_i \rho (h_{ex} - h_{su}) \tag{4.1}$$

In this last equation 4.1, A_i, V_i and ρ are respectively the heat exchange area, the volume and the density of the fluid in the discretized finite volume. $\dot{Q}_{tot}$ is the total heat flow in the discretized element and $\dot{q}$ is the heat flux $[W/m^2]$. This equation is another form of the fundamental laws of the thermodynamics. The fundamental laws of thermodynamics that are used in this model are the mass and energy conservation (the momentum conservation is neglected). They are respectively given in equations (4.2) and (4.3).

$$\frac{dM}{dt} = \dot{M}_{su} - \dot{M}_{ex} \tag{4.2}$$

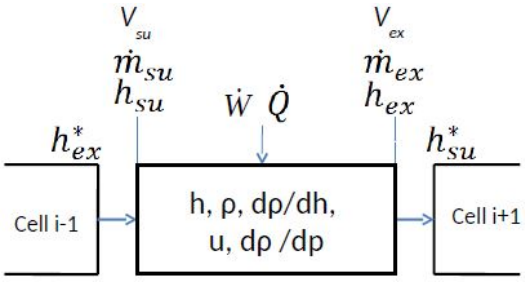

Figure 4.1: Fundamental thermodynamic law applied to a discretized cell[16].

$$\frac{dU}{dt} = \dot{m}_{su}h_{su} - \dot{m}_{ex}h_{ex} + \dot{Q} + \dot{W} \tag{4.3}$$

Indeed, the mass and energy conservation (equations (4.2) and (4.3) respectively) can be rewritten in simpler equations with the expressions of the internal energy $U = H - pV = Mh - pV$, the mechanical power $\dot{W} = p\frac{dV}{dt}$, the conservation of the mass for an incompressible volume $\dot{m}_{su} - \dot{m}_{ex} = 0$, $\frac{dp}{dt} = 0$ (incompressible fluid) and the annotations of Figure 4.1. The obtained equation is the equation (4.7) which is the same than the previous equation (4.1).

$$(\dot{m}_{su} - \dot{m}_{ex})h + m\frac{dh}{dt} - p\frac{dV}{dt} - V\frac{dp}{dt} = \dot{m}_{su}h_{su} - \dot{m}_{ex} * h_{ex} + \dot{Q} - p\frac{dV}{dt} \tag{4.4}$$

$$(\dot{m}_{su} - \dot{m}_{ex})h + m\frac{dh}{dt} - V\frac{dp}{dt} = \dot{m}_{su}h_{su} - \dot{m}_{ex}h_{ex} + \dot{Q} \tag{4.5}$$

$$with \quad \dot{m} = \dot{m}_{ex} = \dot{m}_{su}$$

$$m\frac{dh}{dt} - (\dot{m}_{su}h_{su} - \dot{m}_{ex}h_{ex}) = \dot{Q} \tag{4.6}$$

$$m\dot{h} + \dot{m}(h_{ex} - h_{su}) = \dot{Q} \tag{4.7}$$

This last equation can be written for every cell $[i]$. Additionally, the heat flux from one cell to the wall is given by $\dot{Q}[i] = U[i]A[i](T_{wall}[i] - T_{fluid}[i])$ where $U[i] = U$ seeing that the heat transfer U (computed by the model **HeatTransfer** described below) is considered as only depending on the mass flow rate.

CountCurr This component lets the user chose between using a parallel or counter flow inside the heat exchanger. If the counter current is chosen, this component simply swaps the order of the vector of temperature and heat flow. The icon representing this model in *Dymola* is showed in the upper part of Figure 4.3.

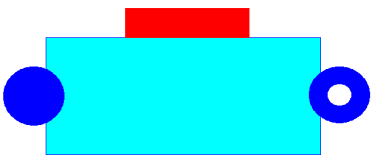

Figure 4.2: Interface of the Flow1DimInCModel.

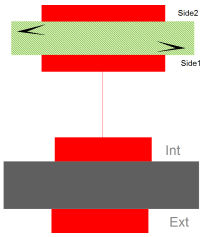

Figure 4.3: Interface of the models CountCurr and MetalWall.

MetalWall A component which represents the accumulation of energy in the metal wall situated between two fluid flows. For a wall divided in N nodes, the energy balance is given

by Equation (4.8).

$$\frac{m_{tot,wa}}{N}\dot{T_{wa}}[i]cp_{wa} = \frac{A_{ext}}{N}\dot{q}_{ex}[i] + \frac{A_{in}}{N}\dot{q}_{int}[i] \tag{4.8}$$

In the equation (4.8), the $m_{tot,wa}$ is the total mass of the wall, $\dot{T_{wa}}$ is the variation with time of the temperature of the wall, cp_{wa} is its specific heat capacity, $\dot{q}_{int}[i]$ and $\dot{q}_{ext}[i]$ are respectively the heat flow in and out of the component ($i = 1 : N$).

In this model, there is a boundary condition saying that there is no gradient of temperature ($T_{wa,int} = T_{wa,ext}$). The icon representing this model in *Dymola* is showed in the lower part of Figure 4.3.

HeatTransfer From the *Thermocycle* library, HeatTransfer is a package containing various methods to compute the heat transfer. This package is used everywhere a heat transfer is computed. Inside this package, there are many equations (like the equation (4.9)) which evaluate the variation of the heat transfer coefficient U with the mass flow rate.

$$U = U_{nom}\left(\frac{\dot{M}}{\dot{M}_{nom}}\right)^{n} \tag{4.9}$$

This last equation (4.9) is used in the model **Flow1DimInc** to include the variation of the heat transfer coefficient with the mass flow rate. The value of n is between 0.6 and 0.8 depending on the fluid [17].

Pump A model, illustrated in Figure 4.4, which prescribes the mass flow rate through itself whose value is the value of its input (blue triangle in the picture 4.4). This model quantifies the work necessary $\dot{W}$ with Equation (4.10). In this model, there is an option leaving a choice between considering or not the enthalpy gain due to the compression and the heating inside the pump.

$$\dot{W} = \dot{m}\left(\frac{p_{ex} - p_{in}}{\rho\eta_{is}}\right) \tag{4.10}$$

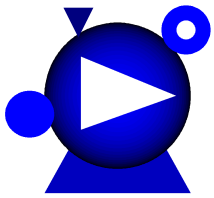

Figure 4.4: Interface of the pump.

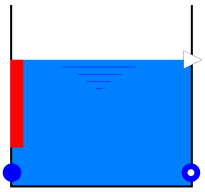

Figure 4.5: Interface of the OpenTank.

OpenTank This model, illustrated in Figure 4.5, corresponds to a storage of liquid fluid under a constant external pressure. The model *OpenTank* has one of the main interests in the whole system. It is a small model which is used to fix the pressure in a closed loop. An other way to fix the pressure is using the model *SinkP* from *ThermoCycle*. However, this last one doesn't include a heat transfer with the ambient contrary to *OpenTank* model where a choice can be made between the different heat transfer models from **HeatTransfer**.

Sensors As already said in the previous chapter, they are many sensors used for the control logic or for monitoring in the studied system. The sensors are really helpful when the thermodynamic variables are the enthalpy and the pressure which are less meaningful than a temperature. There exist many types of sensors in the *Modelica* library. The

Figures 4.6 and 4.7 are respectively the interface of the temperature and the mass flow rate sensor.

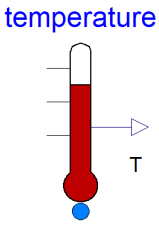

Figure 4.6: Interface of the temperature sensor.

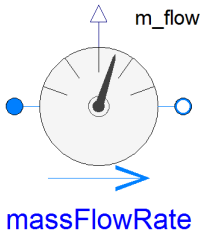

Figure 4.7: Interface of the mass flow rate sensor.

Source_Q A model which takes as input a heat flow value. This heat flow is divided by N where N is the number of discretized cells used in the component.

Valve This model creates pressure losses which directly affects the power needed by the pumps according to the equation 4.10. The equation used to evaluate the pressure losses is the equation 4.11. The hypotheses of this model are that the fluid is incompressible and that there are no thermal losses to the ambient. During this study of the power plant, the pressure drop is considered linear (equation 4.12). The interface of this model is showed in Figure 4.8.

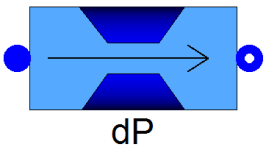

Figure 4.8: Interface of the valve.

$$\Delta P = h\rho g + k\dot{V} + \frac{1}{A^2}\frac{\dot{M}^2}{2\rho} \tag{4.11}$$

$$\Delta P = k\dot{V} \tag{4.12}$$

4.2 Study and validation of the components implemented

To validate the power plant model and prove that the obtained results are correct, all the parameters (used as inputs in all the sub-models) have to be close to the reality and each component need to be implemented with trustful models. That's why a precise analysis of each component has to be done. In the next subsections, all the sub models are studied separately and the results obtained are compared to the data sheet from the providers.

4.2.1 Heat exchanger

The model used to represent the heat exchanger is *Hx1DIncInc*, a model similar to the model *Hx1DInc* from the *ThermoCycle library*. It represents a counter-current plate heat exchanger where the two fluids are modelled as an incompressible fluid contrary to the component *Hx1DInc* where only one of the two fluids is modelled as incompressible. The sub-components, used to simulate the heat exchanger displayed in Figure 4.9, are listed below:

- Two **Flow1DimInc** which represents the flow of the two incompressible fluid through the heat exchanger.
- One **CountCurr** to make a choice between using a parallel or counter flow.
- One **MetalWall** which represents the inertia of the metal wall situated between the two fluid flows.

The connection of these three components is showed in Figure 4.10. Concerning the heat transfer and considering that the thermal resistance of the wall is negligible, the following equation can be used :

$$U_{global} = \left(\frac{1}{U_1} + \frac{1}{U_2} \right)^{-1} \tag{4.13}$$

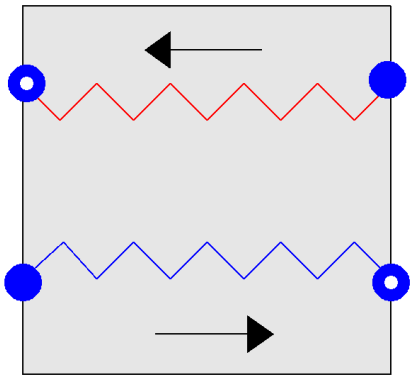

Figure 4.9: Interface of the heat exchanger.

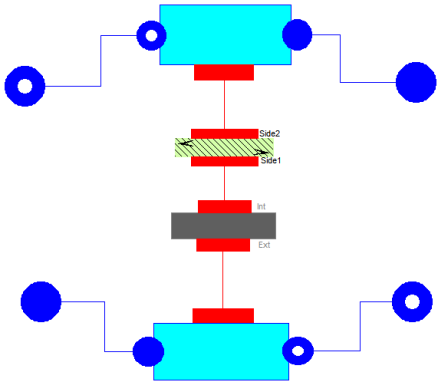

Figure 4.10: Inside view of the heat exchanger model.

The three heat exchangers from Figure 3.1 are implemented with this same model of plate heat exchanger. Indeed, all the heat exchanger can be modelled with incompressible flows as the three fluids can be considered incompressible:

- Therminol SP can be considered as an incompressible fluid as it is in liquid phase. Furthermore, according to the Ref.[18], the variation of the density can be expressed as a function of only the temperature.
- The hypothesis of water at a temperature between 60°C and 80°C considered as incompressible is one of the most usual hypotheses.
- Finally, according to the site Engineering ToolBox [19], the water glycol is also considered as incompressible due to his high bulk modulus (an expression of the variation of the density with the pressure).

4.2.1.1 Oil-Water heat exchanger

The nominal power of the heat exchanger Oil-Water is 1500 kW. All the parameters needed as input for the Oil-Water heat exchanger model were found using **SSP G7** (a program regrouping a list of data sheets of existing heat exchangers). The inputs of the software **SSP G7** are the heat load $[W]$, the inlet and outlet temperature $[°C]$ and the maximal pressure drop $[kPa]$. The inputs used for sizing are listed below:

- Head load 1500 W
- Water inlet temperature of 60 °C (set point temperature of the ORC condenser inlet)
- Water outlet temperature of 70 °C (outlet temperature of the ORC condenser)
- Thermal oil inlet temperature of 225 °C (set point temperature of the ORC evaporator inlet)

After having fulfilled the inputs, **SSP G7** suggests existing heat exchangers that correspond to our inputs. For each heat exchanger suggested, there are many data about it (a part of them are listed in table 4.1). The table 4.1 regroups all the data needed as inputs of the **heat exchanger** model and the one needed to compute the heat transfer.

Table 4.1: Physical characteristics and nominal working point of the heat exchanger Oil-Water 1500 kW.

	Hot Side	**Cold Side**
Fluid	Therminol SP	Water
Density $[kg/m^3]$	892	981.3
Mass flow rate $[kg/h]$	41 142.86	129 035.77
Inlet temperature [°C]	225	60
Outlet temperature [°C]	155	70
ΔT	70	10
Pressure losses $[bar]$	0.7	0.55
Heating Area $[m^2]$	5.11	5.11
Film coefficient clean/dirty	2987/2443 $[W/(m^2 * ^\circ C)]$	
Oversurfacing	24 %	

Using these parameters, a study was made to validate the heat exchanger model. The model used is illustrated in Figure 4.11 and consists of sources, sinks, sensors, one variable speed pump and the heat exchanger.

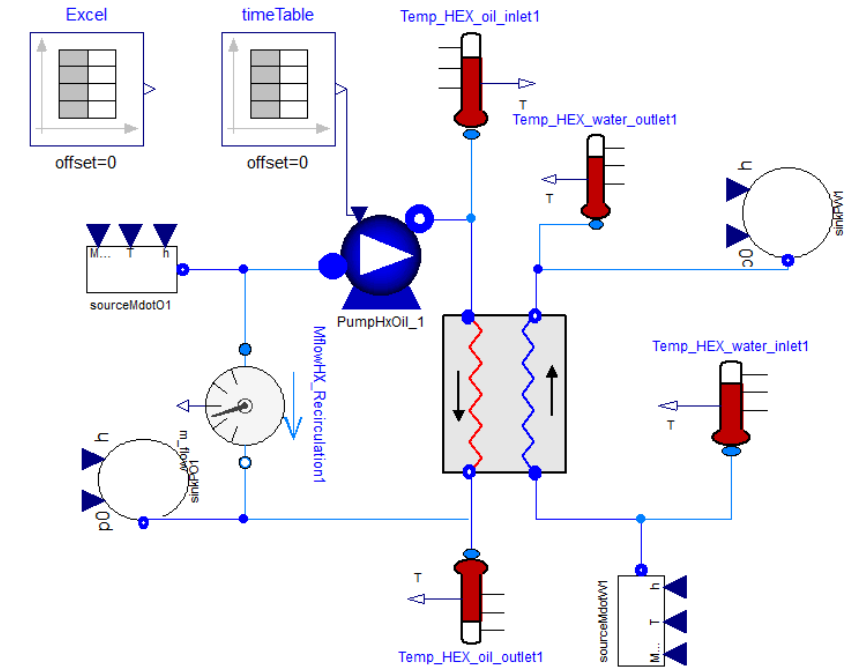

Figure 4.11: Small Dymola model used to study the heat exchanger.

To test the model, the inlet temperature and mass flow rate of both flows are fixed at their nominal value to compare the model with the technical data. As expected, the model gives a heat transfer of 1888 kW which is close to the nominal value of $5.11 * 2987 * 121.59 = 1856kW$. As the error is only 1.7% at the nominal conditions, the model can be considered accurate enough to model the heat exchanger.

4.2.1.2 Water-Water heat exchanger

The heat exchanger Water-Water is the heat exchanger of the old system. It means that it is now oversized for its new rule in the new system. Indeed, its nominal power was already oversized in the old system and now that it is only used as the backup of the new production system, it will never be used at its maximal capacity. Table 4.2 regroups the physical characteristics and the design working point of the plate heat exchanger.

Table 4.2: Physical characteristics and nominal working point of the heat exchanger Water-Water 7500 kW.

	Hot Side	**Cold Side**
Fluid	Water	Water
Volumetric flow rate $[m^3/h]$	332.6	218
Density $[kg/m^3]$	975.6	980.2
Inlet temperature [°C]	80	45
Outlet temperature [°C]	60	75
Internal volume $[m^3]$	0.10662	0.10662
Pressure losses $[kPa]$	98.5	49.6
ΔT	20	30
Mass flow rate $[kg/s]$	90.1346	59.3566
Plate Thickness	0.40 mm of Alloy 304	
Total heating surface $[m^2]$	83.7	
Global heat transfer coefficient	9884 $W/(m^2K)$	
Nominal power $[kW]$	7500	

With the nominal value inlet temperature and mass flow as input parameters, the model shows a difference of only 0.7% with the data sheet (the power transmitted is equal to 7450kW, 0.7% lower than the nominal value). Having no other data, the model can not be verified for other working points.

4.2.1.3 Water-Glycol heat exchanger

The Glycol-Water heat exchanger is the heat exchanger connecting the distribution loop to the dissipation loop. Table 4.3 regroups the physical characteristics and the design working point of this plate heat exchanger. With the inputs of this table (nominal inlet temperature and mass flow rate and the computed global heat transfer coefficient), the heat exchanger model (Figure 4.10) gives a power of 514.2 kW $\left(the\ error\ is\ only\ \frac{515-514.2}{515} = 0.15\% \right)$. In conclusion, the results obtained are good enough to validate the model and the parameters from this table.

Table 4.3: Physical characteristic and nominal working point of the Glycol-Water heat exchanger 515 kW.

	Hot Side	**Cold Side**
Fluid	Water	Glycol-Water
Volumetric flow rate $[m^3/h]$	45	47.7
Inlet temperature [°C]	50	30
Outlet temperature [°C]	40	40
Internal volume $[L]$	47.68	47.68
Pressure losses $[kPa]$	39.6	50
ΔT	10	10
Total heating surface $[m^2]$	40.8	40.8
Global heat transfer coefficient	1266 $W/(m^2K)$	
Nominal power $[kW]$	515	

4.2.2 Biomass

The two main aspects that are considered during the modelling of the Biomass are its long startup time and its huge inertia which leads to a particular power generation versus time curve illustrated in Figure 4.12. The different working conditions, explained in Chapter 3, like the minimal flow rate or the maximal temperature are not considered in this model as they are less constraining. In the reality, the control logic should send a warning signal to the operator if one of the conditions is not respected.

The model's interface of the biomass boiler is illustrated in Figure 4.13. Moreover, Figure 4.14 shows the components needed to implement the biomass and their connection. The subcomponents, used to simulate the biomass boiler, are listed below :

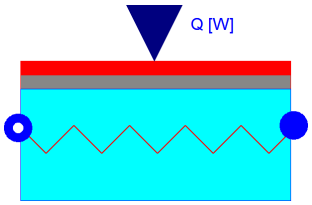

Figure 4.13: Dymola interface of the biomass boiler.

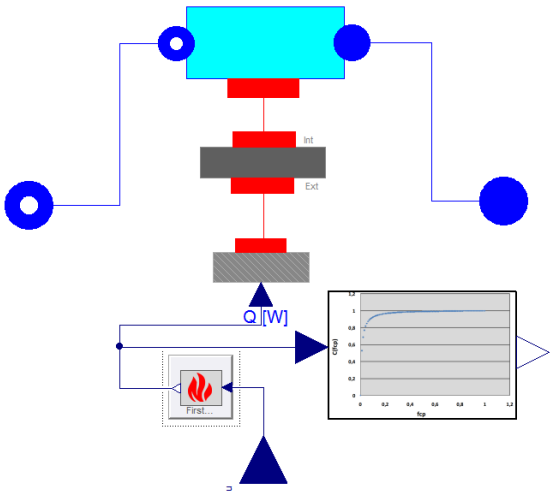

Figure 4.14: Inside view of the biomass model.

- One **Flow1DimInc** which represents the flow of the incompressible fluid through the biomass. It means it's representing the fluid flow and its heat flow with the wall connected to him. The heat flow is between the fluid and the gases produced during the combustion of the biomass with oxygen.
- One **MetalWall** which represents the inertia of the metal wall situated between the two fluid flows.

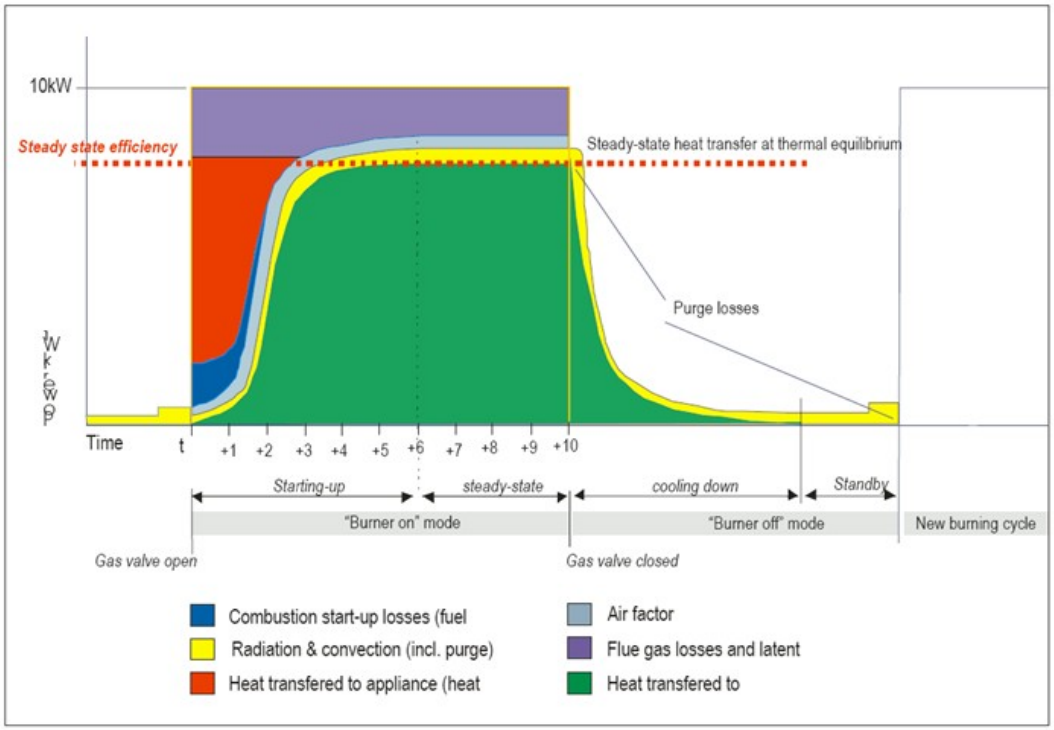

Figure 4.12: Heat transfer and losses during the combustion cycle of a biomass boiler [20].

- One **CombustionDynamic**, illustrated in Figure 4.15, is a component that allows the choice between a few different types of combustion dynamic. The icon of this model is illustrated in Figure 4.15.

Figure 4.15: Interface of the model CombustionDynamic.

Here is a list of the different types of combustion dynamic:

  - Constant power combustion $y = k * u$ where $k = \dot{Q}_{nom}$
  - Linear power combustion $\dot{y} = k * u$ where $k = \dot{Q}_{nom}/T_{startup}$
  - First order power combustion $\dot{y} = \dfrac{(k*u-y)}{T}$ where $T = T_{startup}/3$ and k= $\dot{Q}_{nom}$

  This small model is the most important one as it gives the shape of the power transmitted from the biomass to the fluid. The first order power combustion is selected to approach the boiler combustion dynamic (Figure 4.12).

- One **Source_Q** which takes as input the heat flow value $[W]$ computed by the **CombustionDynamic** model. It turns this number into a heat flux whose value is the heat flow divided by A (the heating area) and this heat flux is fixed to the **MetalWall** connected to component **Flow1DimInc**.

- One model, described in the next subsections, to have the quantity of biomass needed to produce the power. It takes the total power transmitted to the fluid (value $[W]$ computed by the model **CombustionDynamic**) and it computes the mass flow rate of biomass based on the efficiency.

The total inertia of the boiler is divided into the inertia of the model **MetalWall** and **Flow1DimInc** models. Indeed, the use of the internal volume of liquid inside the pipe and the mass of wall between the two fluids permits to add inertia in system. Based on data sheets from the boilers manufacturer *Babcock Wanson* [21] and on a study from *Cartif* [22], the following estimation of the biomass boiler inertia can be used:

- A mass of 9000 kg for the **MetalWall**. These walls are made in steel with a specific heat capacity of 502 $[J/(kg*K)]$.
- An internal thermal oil volume of 1200 litres.

4.2.2.1 Biomass boilers efficiency

Finally, according to J. Good, Th. Nussbaumer, J. Delcarte and Y. Schenkel [23], Ref. [20] and [24], a few terms can be defined to quantify the efficiency of the biomass boiler like the thermal, combustion and overall efficiency. The following definitions and equations stays in their easiest expression (detailed equations to compute the efficiencies and losses can be found here [23]) :

- The *thermal efficiency* $\eta_{thermal}$ is defined as the heat exchangers effectiveness between the fuel and the fluid. It's the ratio between the output energy (the energy given to the fluid $\dot{Q}_{fluid}$) and the energy given of the fuel gas $\dot{Q}_{fuel}$ (as shown in equation (4.14)). It comprises the heat exchanger type losses. They are losses to the ambient. Indeed, some heat generated from the combustion does not go to heat transfer medium (convection and radiation losses to the ambient).

$$\eta_{thermal} = \frac{\dot{Q}_{fluid}}{\dot{Q}_{fuel}} \left(= \frac{\dot{m} * (h_{f,out} - h_{f,in})}{\dot{m}_{gaz} * (h_{gas,in} - h_{gas,out)}} \right) \tag{4.14}$$

- Another definition of efficiency can be used to model the boiler efficiency. It's the *combustion efficiency* $\eta_{combustion}$ which is the burning process effectiveness. It shows the quality of the burner by measuring the quantity of unburned fuel and excess air in the exhaust gases and the quantity of input fuel.

- The *overall efficiency* η_{boiler}, also named fuel to fluid efficiency, is by definition as the ratio of output energy and input energy. The difference with the thermal efficiency is that all the losses, $\dot{Q}_{losses}$, (convection/radiation to the ambient and unburned fuel) are considered in the overall efficiency. This efficiency is showed in the equation (4.15). It comprises the thermal efficiency, the ambient losses and the combustion efficiency.

$$\eta_{boiler} = \frac{\dot{Q}_{fluid}}{\dot{Q}_{in}} = \frac{\dot{m}_f * (h_{f,out} - h_{f,in})}{\dot{m}_{BM} * ncv_{BM}} \tag{4.15}$$

$$\eta_{boiler} = 1 - \frac{Q_{losses}}{Q_{in}} + \frac{Q_{gain}}{Q_{in}} \tag{4.16}$$

  where $\dot{m}_{BM}$ is the mass flow rate of fuel $[kg/s]$ and ncv_{BM} is the Net Calorific Value *NCV* as the products of combustion contains water vapour and that the heat in the water vapour isn't recovered. The first equation (4.15) shows the direct method of determining the boilers efficiency and the equation (4.16) shows the indirect method. This direct method is the most interesting as all its terms are easy to find.

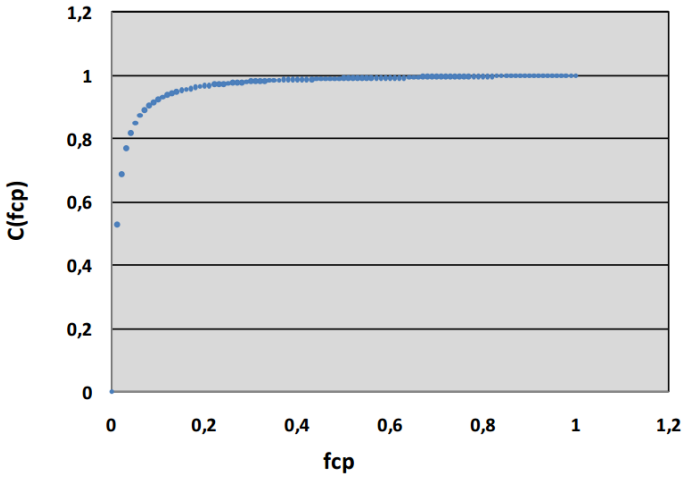

Figure 4.16: Variation on efficiency in function of partial load ratio($0 \leq f_{cp} \leq 1$) [25].

4.2.2.2 Biomass consumption

The biomass consumption is one of the keys factors to find the running cost of the installation. To compute it, the equation (4.15) can be adapted in case of a Partial Load Ratio ($PLR = \frac{\dot{Q}_{fluid}}{\dot{Q}_{nom}}$) as followed :

$$\dot{m}_{BM} * ncv_{BM} * \eta_{PLR} = \dot{Q}_{fluid} \tag{4.17}$$

$$\dot{m}_{BM} = \frac{\dot{Q}_{fluid}}{ncv_{BM} * \eta_{PLR}} \tag{4.18}$$

$$\tag{4.19}$$

The partial load efficiency η_{PLR} depends on internal factors (type of boilers etc.) and also on external factors like the inlet fluid temperature and the fluid mass flow. For this reason, the partial load efficiency of the boiler is hard to find for the specific case studied. Furthermore, it is also difficult to get it from manufacturers. The solution is to express η_{PLR} as a function of the nominal efficiency $\eta_{PLR} = C(PLR) * \eta_{nom} = C(f_{cp}) * \eta_{nom}$ as explained by Pedro M. Aranda F. [25]. A typical curve of the efficiency correction factor $C(f_{cp})$ is showed in Figure 4.16 for a specific boiler.

The curves of Figure 4.16 is using two different equations depending on the partial load factor f_{cp} (one for f_{cp} above 30% or one for the f_{cp} under 30%). The extremely low efficiency for PLR below 30% can be explained with the equation 4.16 where the term $\dot{Q}_{losses}$ are almost constant. Indeed as stated in [20], these losses depend on the temperature of the boilers for the convection and radiations losses to the ambient (constant losses) and depend on the combustion process effectiveness (low effectiveness during the start-up of the boilers - variable losses).

Considering that the ORC is supposed to be activated as soon as the biomass is ON, the biomass boiler should never work under 30% of its nominal capacity. According to Pedro M. Aranda F. [25], a simplified equation can be used in this part of the graph :

$$C(f_{cp})_{f_{cp} \geq 0.3} = \frac{1}{\eta_{nom}} * \left(\eta_{nom} - \frac{\eta_{nom} - \eta_{30\%}}{1 - 0.3} * (1 - f_{cp}) \right) \tag{4.20}$$

where f_{cp} is the partial load ratio; η_{nom} is the overall efficiency at his nominal capacity and $\eta_{30\%}$ is the overall efficiency at PLR 30%. Using the equation (4.20) and $\eta_{PLR} = C(f_{cp}) * \eta_{nom}$,

the equation (4.19) becomes :

$$\dot{m}_{BM} = \frac{\dot{Q}_{fluid}}{cp_{BM} * \left(\eta_{nom} - \frac{\eta_{nom} - \eta_{30\%}}{1 - 0.3} * (1 - f_{cp}) \right)} \tag{4.21}$$

$$\dot{m}_{BM} = \frac{\dot{Q}_{fluid}}{cp_{BM} * \left(\eta_{nom} - \frac{\eta_{nom} - \eta_{30\%}}{1 - 0.3} * (1 - \frac{\dot{Q}_{fluid}}{\dot{Q}_{nom}}) \right)} \tag{4.22}$$

Ana I.Quijano, Cecilia Sanz and Fredy Velez [26] have made a detailed study about the different biomass boilers existing, local market for the boilers and the biomass and a economical study about the use of biomass boilers. According to this report [26], the type of biomass used in the Belgian demo site should be wood pellets. The following values are used to find the consumption of biomass and its associated price:

- A specific energy cp_{BM} of 4150 $kcal/kg$ (value between 4000 and 4300 $kcal/kg$ as suggested in Ref.[26]).
- Biomass expected price in Belgium: 275.6 €/ton (TVA included) according to Raymond Charlier [27].
- A nominal efficiency η_{nom} of 90% and a partial load efficiency $\eta_{30\%}$ of 85%. These value are estimated with the boilers manufacturer D'Alessandro Termomeccanica [28].
- $\dot{Q}_{nom} = 1500kW$ according to the sizing of the biomass boiler.

4.2.3 Organic Rankine Cycle

A complete implementation of the ORC with a detailed study of the evaporator and condenser (two phase changes in total), a pump and a turbine would lead to a system more complex. Moreover, the characteristics of the elements inside the ORC installed in the new power plant are unknown. The implementation would be based on too much hypothesis. Indeed, the ORC installed has its own control logic (based on the condensation and evaporation temperatures and the secondary flow rates) and it is sealed in a box (there are penalties if it is opened). It acts then like a black box. That's why its implementation is thus based on characteristic curves equations provided by the ORC's manufacturer. These curves are for specific flow rates on both evaporator and condenser sides. These flow rates are respectively $13m^3/h$ and $37m^3/h$ and the internal control logic should stop the ORC if the flow rates are different than these values. The following equations can be used to determine the oil and water outlet temperature, the electrical power generation and the efficiency:

$$\begin{aligned} T_{o,out} = & -160,098174650338 + 3,26482367478462 * T_{o,in} \\ & - 1,11924814360188 * T_{w,in} - 0,00861131836983239 * T_{o,in}^2 \\ & + 0,0011896293553043 * T_{w,in}^2 + 0,0059159249149304 * T_{w,in} * T_{o,in} \end{aligned} \tag{4.23}$$

$$\begin{aligned} P_{el} = & 378,703922659974 - 4,52283805808272 * T_{o,in} \\ & + 0,397942892699653 * T_{w,in} + 0,0145862000859525 * T_{o,in}^2 \\ & - 0,00772385071383634 * T_{w,in}^2 - 0,00226518144606598 * T_{o,in} * T_{w,in} \end{aligned} \tag{4.24}$$

$$P_{el,gross} = P_{el} - P_{el,pumpORC} \tag{4.25}$$

$$\dot{Q}_w = \left(\dot{Q}_o - P_{losses}\right) - P_{el,gross} = \left(\dot{Q}_o - \frac{\dot{Q}_o * \beta}{100}\right) - P_{el,gross} \tag{4.26}$$

$$T_{w,out} = T_{w,in} + \frac{\dot{Q}_w}{\dot{m}_w * cp_w} \tag{4.27}$$

$$\eta_{el} = \frac{P_{el,gross}}{\dot{Q}_o} \tag{4.28}$$

$$\eta_{th} = \frac{\dot{Q}_w}{\dot{Q}_o} \tag{4.29}$$

where η_{el} and η_{th} are respectively the electrical efficiency and the thermal efficiency of the ORC, $P_{el,gross}$ is the gross electrical power $[kW]$, $P_{el,pumpORC}$ is the electrical consumption of the pump inside the ORC ($0.5[kW]$), P_{el} is the net electrical power $[kW]$, β is the ORC losses in terms of percentage of the evaporator thermal power $[\%]$, $\dot{m}_w$ is the mass flow rate of the secondary fluid in the condenser $[kg/s]$, cp_w is the specific heat of water $[kJ/(kg*K)]$, $T_{o,out}$ [°C] and $T_{w,out}$ [°C] are respectively the outlet temperature of oil and water. *Rank*, the provider of the ORC, also gave the temperature range for which the correlations are valid. These results would only be trustful when the oil inlet temperature is comprised in the range $[215°C; 225°C]$ and when the water inlet temperature is in the range $[20°C; 60°C]$. And according to the ORC supplier, a maximal error of 15% is expected for the temperature outside the designed ranges.

The ORC's icon is shown in Figure 4.17. In this picture, there are:

- Two fluid ports inlets and outlets (one of each type for the water and thermal oil).
- Three outlets for the electrical power, the power extracted from the thermal oil and the power delivered to the water in the condenser.
- One input to consider the operational range of the ORC (temperature and flow rate have to be in the right range). If all the conditions aren't respected, the main control logic send a signal read by the ORC who turns/stays OFF until it is in the working conditions.

Figure 4.17: Dymola interface of the ORC.

These latter conditions, for the activation or deactivation of the ORC, are less strict than $T_{o,in,ev} \subset [215°C; 225°C]$ and $T_{w,in,cd} \subset [20°C; 60°C]$ to have a system more stable. In reality, the ORC can work at higher and lower temperatures but the correlations are not certified any more by *Rank*. For this last reason, larger ranges of temperatures are accepted for the thermal oil and the water. However, the thermal oil should avoid exceeding the temperature of 250°C for safety operations. Indeed, the ORC working fluid has been tested during 7 days and degradation has been noticed by Dupont [29]. In the next pages, the thermal power required at the evaporator, produced at the evaporator and the electrical power generated are shown for various evaporation and condensation temperatures.

4.2.3.1 Extrapolation of the characteristic curves

As the provider of the ORC advises to keep the secondary flow rates at their design value for a question of stability, the flow rates are imposed during the whole simulation. However, even if the mass flow rates are constant, the temperature won't and it is interesting to study the behaviour of the ORC for a wider range of temperature. The Figure 4.18; 4.19 and 4.20 are the results of the characteristic curves extrapolated to a wider range of temperature. These figures show that an increase (respectively decrease) of the evaporation temperature increases (respectively decreases) the generation of electricity, the required power by the evaporator and the extracted power in the condenser. A decrease of the condensation temperature has the same effect on the power generation and consumption than a increase of the evaporation temperature. Furthermore, the evaporation temperature should stay high to have a high electrical efficiency and keep thermal demand at the evaporator nearby $450kW$ (and keeping then a good biomass boiler efficiency).

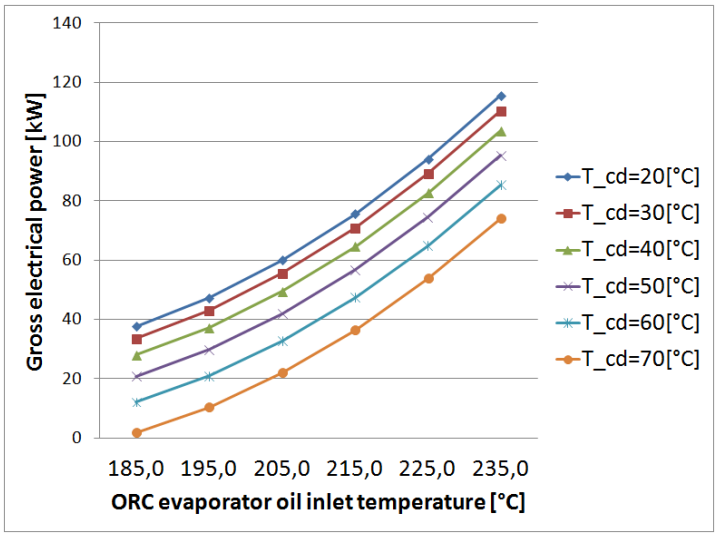

Figure 4.18: ORC electrical power generation for different condensation and evaporation temperatures.

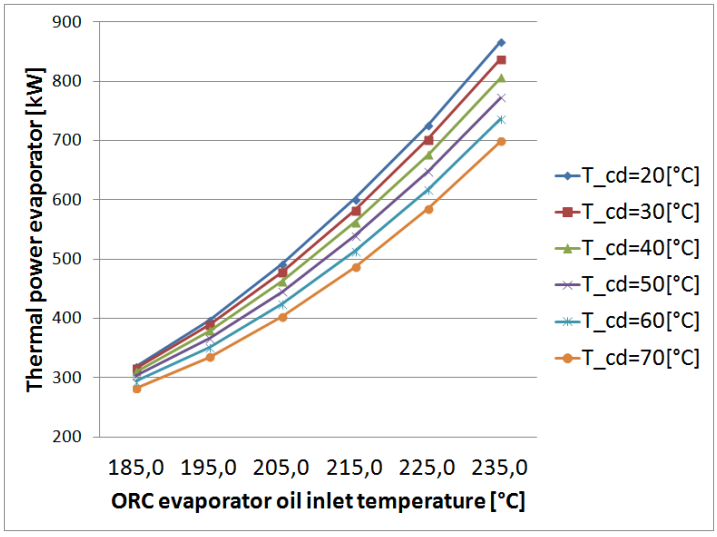

Figure 4.19: ORC thermal power consumption for different condensation and evaporation temperatures.

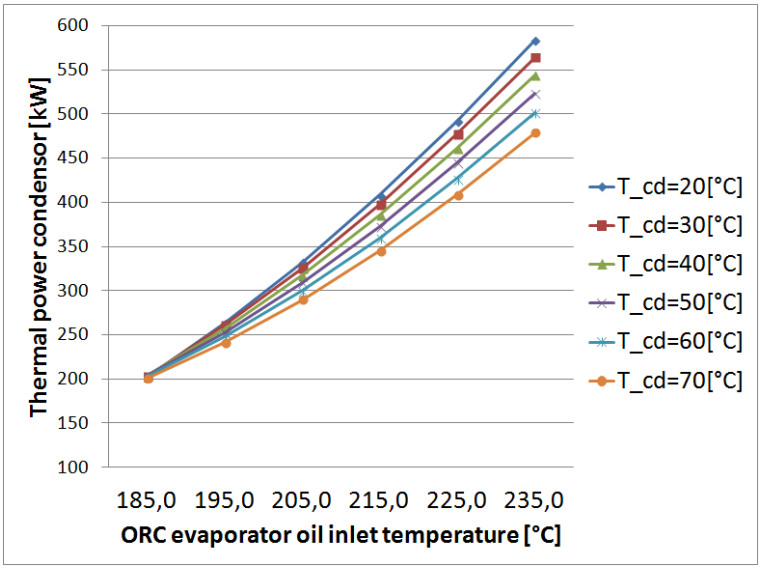

Figure 4.20: ORC thermal power generation for different condensation and evaporation temperatures.

Using equations instead of a detailed model doesn't take into account the inertia of the ORC. However, the inertia of the ORC is not really important due its low value (in comparison with the one of the biomass boiler or the building) and due to the high mass flow rate going through the evaporator and the condenser. It means that the temperature of the walls change almost instantly when the inlet temperature of the evaporator (or condenser) changes. Furthermore, the inertia can be ignored as the 3-way valves *V3V1* and *V3V5* are modulated to keep the temperature T_4 and T_{17} constant all the time. Furthermore, no values are known for the ORC installed to implement the inertia. Once the power plant will be running, the ORC model could be improved with a calibration of the system.

4.2.4 Building

The different blocks of the building, presented in Chapter 2, were not modelled to avoid having a stiff model. Undeniably the modelling of all the 7 blocks (including the 8 hydraulic circuits for indoor heating (radiators) and 3 for ventilation units) would have lead to a complex system and it would thus have been impossible to make long simulations of the power plant. Moreover, with the data received from the building's owner, it was possible to represent the heat distribution pipes and the heat distribution units with a simple model. Indeed, the data received contains the power required for heating each block of the building.

The power required by each block was measured every ten minutes from September 2014 to April 2016. Meters were used to measure the water flow and temperature difference at the depart/return of the distribution loop. This power, $\dot{m} * cp_w * \Delta T$ is then equals to Q_w and is linked to the power demand $Q_{tot,block}$ with the equation (4.30). The power demand from the data is given in kW and it comprises the sum of the power demand from each block ($Q_{tot,block}$), the thermal losses ($Q_{losses,pipes}$) and the inertia of the distribution pipes ($\frac{dQ}{dt_{system}}$).

$$\dot{m}_{meas} * cp_w * (T_{in} - T_{out}) = Q_w = Q_{tot,block} + Q_{losses,pipes} + \frac{dQ}{dt_{system}} \tag{4.30}$$

In this last equation, $Q_{tot,block}$ is the power needed to heat the different blocks, $Q_{losses,pipes}$ is the power lost in the heat distribution network and the term $\frac{dQ}{dt_{system}}$ is the effect of inertia. The term $\frac{dQ}{dt_{system}}$ comprises the walls' inertia of both the pipes and the heat exchangers of the heat distribution units. Considering that the power Q_w is known, the building can be modelled with one model **Source**$_Q$ heating one *Flow1DimInc*. The internal volume of the tube *Flow1DimInc* is fixed to the volume of water inside the distribution loop. This last term can not be neglected as there are about 29.451 m^3 of water inside the pipes in the distribution loop of the system. This value was computed during a study made by Roberto Ruitz and Matteo D'Antoni [15] with an assumption of 5 litres/kW for the radiators and real data for the pipes and coils (AHUs). The model is showed in Figure 4.21 and its interface is illustrated in Figure 4.22.

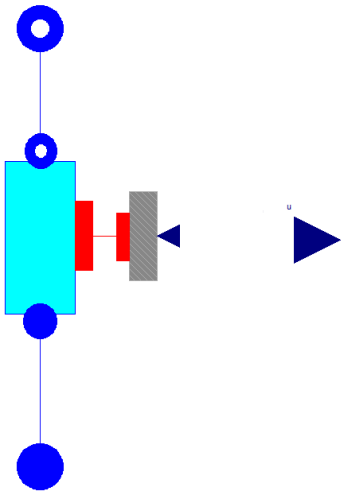

Figure 4.21: Model of the building.

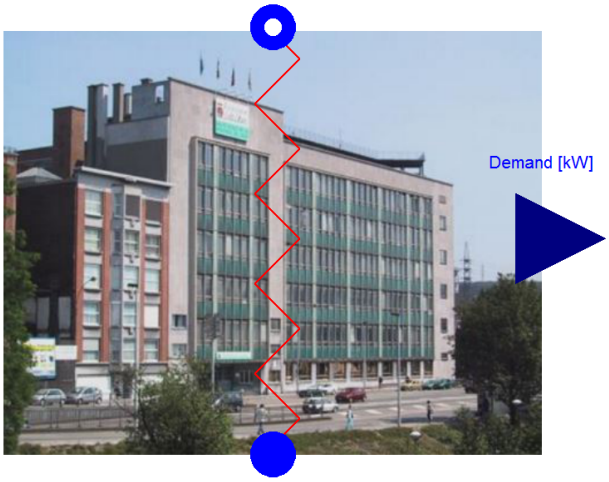

Figure 4.22: The interface of the building in Dymola.

A detail implementation of the building to take into account the electrical consumption of the circulating pumps, the thermal losses in the distribution loop and the indoor air quality control is not included however it should be treated in a future work.

4.2.4.1 Power demand curve

During this thesis, the aim was to obtain detailed results even if it implies long simulations. As previously said, the biomass boiler should start in the beginning of the heating period and stays ON until the end of the heating period. The heating period represents about 8 months (there are four months, between the 15th May and the 15th September, when the building doesn't require any thermal power). To reduce the simulation time to its minimum while keeping a good accuracy, 12 days were simulated (one typical day per month). Each day is made based on an average of all days of the month and some supplementary modifications to use the dry cooler and natural gas boilers in right proportions. Once this power demand curve is obtained, it can be smoothed using the continuous derivative interpolation. The obtained curve is illustrated in Figure 4.23. Finally, this curve is used as an input of the model *Buiding* previously modelled.

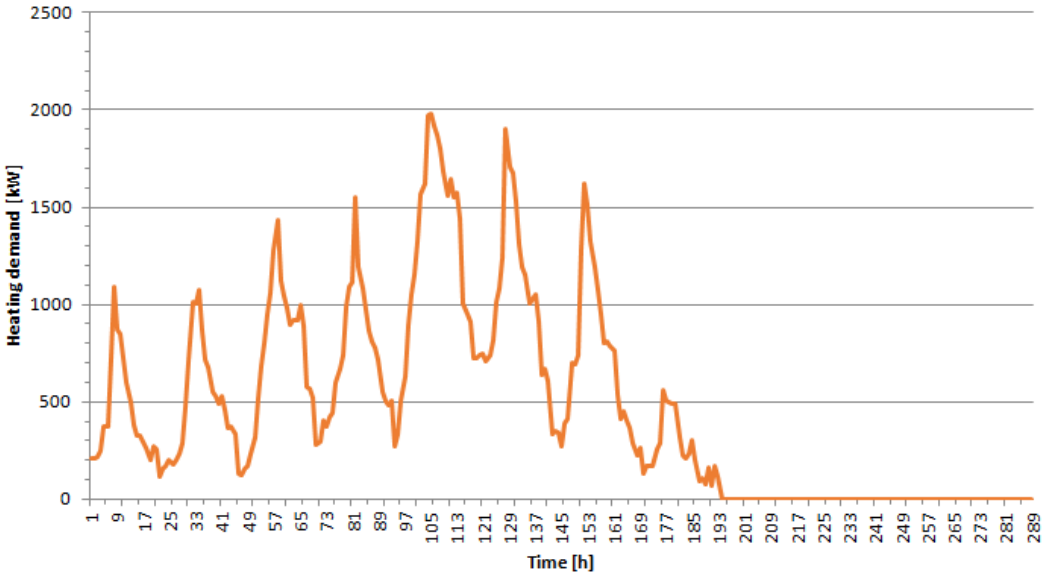

Figure 4.23: Fluctuation of the building power consumption during the year.

4.2.5 Dry cooler

The dry cooler, a finned tube heat exchanger, uses a water glycol mix fluid to carry power from the heat exchanger Water-Glycol to the air. The water-glycol fluid is implemented in *Dymola* with a table containing its properties (see Appendix A). The hypothesis of this implementation is that it is a compressible fluid and it is based on the production information of the ethylene glycol-based mixed with water (Ref. [30]). The subcomponents used to implement the Dry cooler and the interface of the dry cooler in Dymola are shown respectively in Figure 4.24 and 4.25.

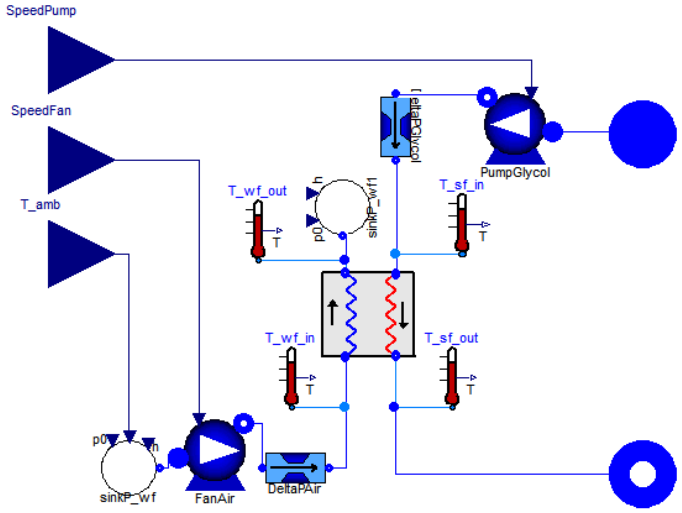

Figure 4.24: Model of the Dry Cooler.

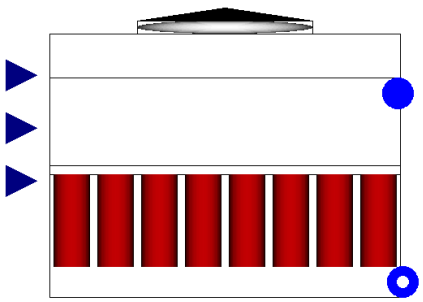

Figure 4.25: Dry cooler interface.

The model of the *Dry Cooler* is pretty simple. It's composed of :

- Two **pump** models: one to fix the air flow rate (the model represents the blower/air fan in reality) and one for the glycol-water mix flow (a real pump in this case).

- One **valve** for each flow to consider the pressure losses in the heat exchanger. The pressure losses are supposed linear with the volumetric flow rate and their sizing is based on received data from Raymond Charlier [31].
- A few temperature sensors to verify the behaviour.
- A heat exchanger whose parameters were fixed with the data sheet. The overall heat transfer coefficient $U = U_{nom}\left(\frac{\dot{m}}{\dot{m}_{nom}}\right)^{n}$ between the fluid and the wall. The value of n must be around 0.8 for the glycol-water and 0.6 for the air [17].

The pump, named *PumpGlycol* (Figure 4.24), circulates the fluid from the water-glycol heat exchanger to the dry cooler. As a component of the dry cooler and according to the dry cooler's manufacturer, it should always work at its nominal flow rate. From the different possible ways of controlling the power dissipated in the dry cooler (see Chapter 2), the control that achieves the highest electricity consumption reduction isn't oblivious. The suggested solution is a regulation of the power dissipation by decreasing/increasing the rotational speed of the fans with a *PID* controller modulating the speed of the fan depending of the output temperature of the dry cooler. The controller of the fan depends on the *PID* controller of the ORC condenser as follows:

- When the ORC condenser inlet temperature is higher than the set point, the valve increases the flow inside the water-glycol heat exchanger which increases the outlet temperature of the glycol-water. When the temperature increases, the *PID* controller reacts by increasing the air flow rate.
- In contrary, when the cooling demand decreases, the *PID* controller decreases the speed of the fans until zero when there is no power to dissipate.

4.2.5.1 Working behaviour outside its nominal value

The dry cooler would almost never be used at its nominal conditions. In fact, the inlet temperature is not necessary equal to the design temperature (45°C) and the power dissipated will thus be different (the inlet temperature depends on the control strategy adopted and this is studied in the next chapter). In theory, the dry cooler will only be used to dissipate the exceed power produced during the cogeneration mode (considering a heating demand lower than the heat released at the condenser) as there are no cooling demand.

The nominal working point of the dry cooler is characterised by a nominal power of 570.5kW (from the data sheet). For this working point, the implemented model gives a power of 570.6 kW. The model also gives a power dissipated of 519 kW for a different working point of the installed dry cooler. This value is only 2,4% higher than the value of the provider (507kW)(other technical data of the same dry cooler [32]). Considering the model gives quite good results, it's interesting to look the behaviour of the dry cooler outside its designed point. The power released is shown in Figure 4.26 for different air flow rates with the inlet temperature of the two fluids constant (25°C for the air and 45°C for the glycol water). To dissipate a thermal power lower than 570kW, the necessary air flow rate decreases faster than the heat transfer as expected. The electrical consumption decreases also faster than the heat transfer which leads to a dry cooler more efficient in partial load. According to the data sheet, the Energy Efficiency Ratio, calculated with the equation (4.31), is equal to 60 at the nominal working point and its variation is showed in Figure 4.27. This figure shows that the EER reaches 100 for a power dissipation of 300kW to finally decreases really fast for lower power

dissipation. Indeed, the suggested control strategy is a constant glycol-water flow and therefore the electrical consumption of the pump is constant.

$$EER = \frac{Q_{cooling}}{P_{el,tot}} = \frac{Q_{cooling}}{P_{el,f} + P_{el,pump}} \tag{4.31}$$

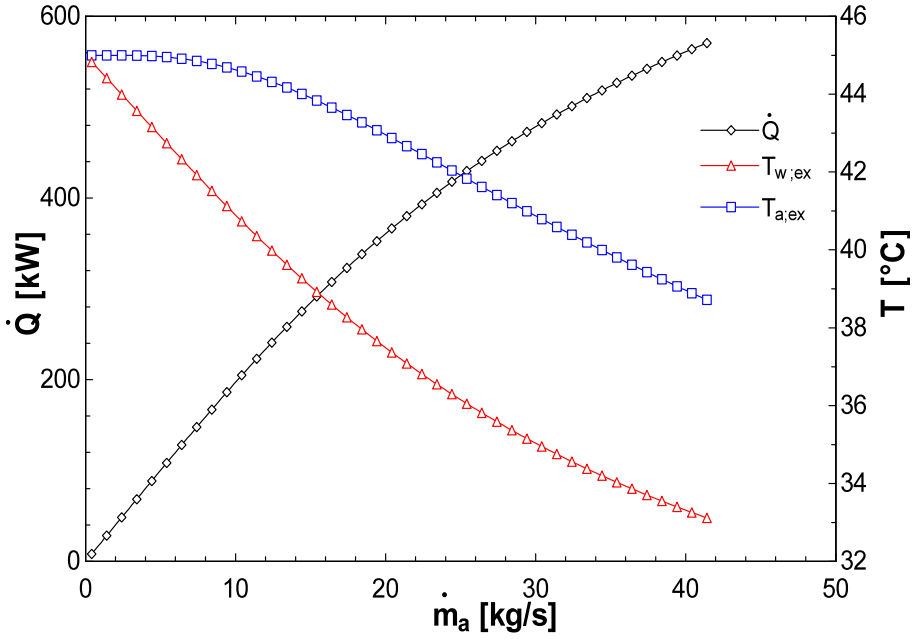

Figure 4.26: Fluctuation of the power dissipated with the air flow rate.

Once experimental data are available, a tuning of the model should be considered to represent better the cross-flow heat exchanger. As the model gives good results for the two working points available, the implemented model can be considered accurate enough to study the whole power plant without inducing to much errors. Finally, to have this system working smoothly, the *PI* controller of the fan has to have a slower reaction speed than the *PI* controller of the 3-way valve *V3V5*.

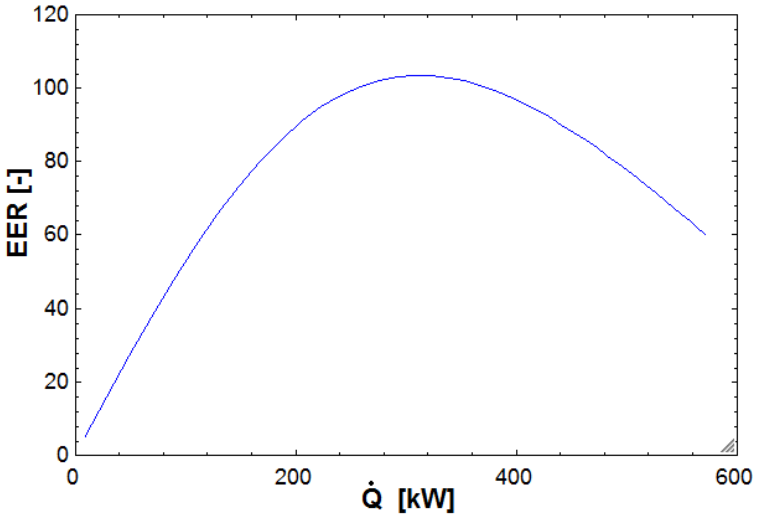

Figure 4.27: Fluctuation of energy efficiency ratio with the power dissipation.

4.2.6 Gas Boilers

The gas boilers are characterized by a short reaction time and so by an easy regulation. The implementation of the three gas boilers and the control logic in *Modelica* is easier than the modelisation of the biomass. However the results obtained with the model have to be as real as possible. That's why the parameters have to be chosen precisely. A gas boilers works in the same ways as a biomass boiler with a shorter reaction time. That's why the three gas boilers of the systems (see the layout illustrated in Figure 3.1) are modelled using the model implemented for the biomass boiler. The main difference will be in the value of the inertia and it's start-up time. These values are known from previous studies [15].

In the next subsection, an explanation of the old control logic is described and it's followed by a detailed analysis and a validation of the results.

4.2.6.1 Implementation of the old control logic

The old control logic is running in a simple way. The old control logic, which isn't supposed to change unless modifications are absolutely needed, is modulating the boilers like an ON-OFF system. Each of the three gas boilers can work with 0%, 69% or 100% of their nominal power. Here is an explanation of how the activation cascade of the natural gas boilers works, and how the amount of power generated by the boilers varies with time depending on the boundaries conditions:

- The initial step is the activation of all the pumps. When the sensors in the distribution network indicate that the demand isn't equal to zero, the header is turned on and all the pumps are turned ON and work at their nominal mass flow rate.
- The next step is one boiler turned ON at low gas flow rate. If the demand stays higher than zero for 60 seconds and if the storage situated in the distribution network is not able to give the necessary power, the first boilers is activated at low gas flow rate 136 m^3/h. This is the first step of the power generation. The boiler 1 produces 1564 kW which is about +-69% of its nominal capacity 2268 kW.
- If the power asked is still higher than 1564 kW (this corresponds to a temperature lower than the set point temperature), the second boilers is also turned ON at low fuel gas rate after a delay of 60 seconds (delay starting after the activation of step 1). The results shows that the delay in the activation cascade is really important for the stability and for the simulation speed of the model as it will avoid having transition of state every seconds. The second step of the activation cascade is two boilers at low gas flow rate. The equivalent power is 3128 kW.
- When the temperature measured by the sensors stays lower than the set point for an additional 300 seconds, the first boiler works at high gas flow rate (232 m^3/h) which is equal to 100% of its maximal capacity 2268 kW. The second boilers stays at a low fuel gas rate (1564 kW). The total power produced at this step is 3832 kW. If this generated power is still not enough to fulfil the thermal demand, the next stage is activated after 300 seconds of delay starting up after the activation of this previous step.
- The next stage is the two first boilers at high gas flow rates. The total power produced is 4536 kW.
- During some extreme period of year, the power produced by the first two boilers might be not enough. That's why the third boiler can be activated if two conditions are fulfilled.

The first condition is the same condition as before (temperature measured lower than the temperature set point) and the second condition to active the third boiler at low gas flow rate (129 m^3/h) is an ambient temperature lower than -5 °C. This stage is activated after 180 seconds when both conditions are fulfilled. This stage corresponds to two boilers at high gas flow rate (total power of 4536 kW) and the third at low gas flow rate (1484 kW) to generate a total amount of 6020kW.

- The last step is the three boilers working at high gas flow rate. The third boiler is operated at high gas flow rate of 257 m^3/h for a power of 2956 kW. The total power generated is 7492 kW which is much higher than the power required by the building. In theory, the last two stages of this cascade won't be necessary any more in the new generation layout as the biomass is supposed to replace one of the old gas boilers. And there is again a 180 seconds of delay with the previous stage.

The implementation of this control logic is done using the package *StateGraph2* and *Blocks* from *Dymola* and it is based on the paper [33]. The following components are used to implement this activation cascade:

Step Step that can be an initial step or not. An initial step is the step which is active when the simulation starts.

Transition Transition with(/without) a fire condition or with(/without) boolean condition. This transition can be instantaneous or delayed depending on what is needed.

BooleanExpression Block with a time varying output (*Boolean* output).

Timer Small block which measures the time from which the boolean input becomes true.

GreaterEqualThreshold Block which makes a comparison of its input value and its defined parameter.

Each boiler has a minimal operating time of 120 seconds for the low gas flow rates and an operation time of 2 seconds at least for the high gas flow rates. This supplementary condition can be considered as a condition to shut down the boilers and starts the descending sequence of the activation cascade. It's modelled using the component **Timer** from the library *Modelica* which is able to measure the time elapsed between the moment when its boolean input becomes true and the current time. Its output is the number of seconds and it's connected to a comparison component. The latter output is true once the number of seconds, computed with the timer is bigger, than 120 for the low flow rate and 2 seconds for the high flow rate. Finally, this output signal is used as a input of the transition to reach a lower power production stage. The components and their connections are shown in Figure 4.28. Despite this condition on the minimal working time, there is no other regulation during the cascade descending except that the temperature still has to be higher than the set point temperature.

With *StepWithSignal* from the library *StateGraph*, the minimal working time is considered but not the condition $T_{measured} > T_{SP}$. One solution to consider both conditions at the same time is the combination of the little loop like illustrated in Figure 4.29 and the component **BooleanExpression** whose output is true when we are inside the loop. This loop determines if we are above or under the set point temperature. In other words, it determines if we have to increase the power generation or decrease it while the time elapsed since the activation of the boiler is computed in order to respect the minimal operation time.

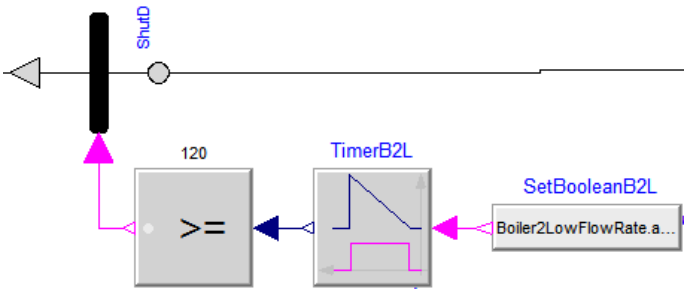

Figure 4.28: Dymola model for the computation of the time delay.

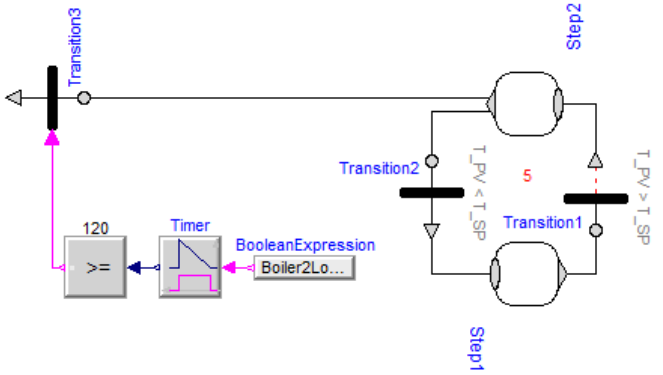

Figure 4.29: Illustration of a delayed transition with a condition.

To have a better behaviour, some modifications were required. Indeed, the working scheme of the gas boilers system implemented in *Dymola* leads to many changes of state for some specific power. For a power required by the building between two levels of the power generation cascade, the system would work like an ON-OFF system. The next part of the thesis is dedicated to a detailed analysis of the results obtained.

In Figure 4.30, the Boolean input *Powered* is true or false depending if the natural gas boilers are necessary or not to fulfil the heating demand. The three other inputs are the ambient temperature, the measured and set point temperature of the natural gas boilers. The four outputs are the three inputs of the natural gas boilers named CS_{BM1}; CS_{BM2} and CS_{BM3} which are respectively the power produced by the three gas boilers and the output CS_{pump} is the input of all the pumps.

4.2.6.2 Analysis of the old thermal production system

The whole building is separated in small blocks (see Figure 2.1). Each block has its own set point temperature which is different depending on the ambient temperature set point and the mass flow through the distribution units. Each subdistribution system is controlled by a 3-way valve which makes a regulation to have the right temperature. The set point temperature of the previous distribution system is the maximal value between the highest set point temperature and a theoretical load curve (depending on the outdoor air temperature). This maximal value obtained is modified with a correction based on the demand of the ventilation groups. This latter determination of hot water production set point temperature is illustrated in Figure 4.31.

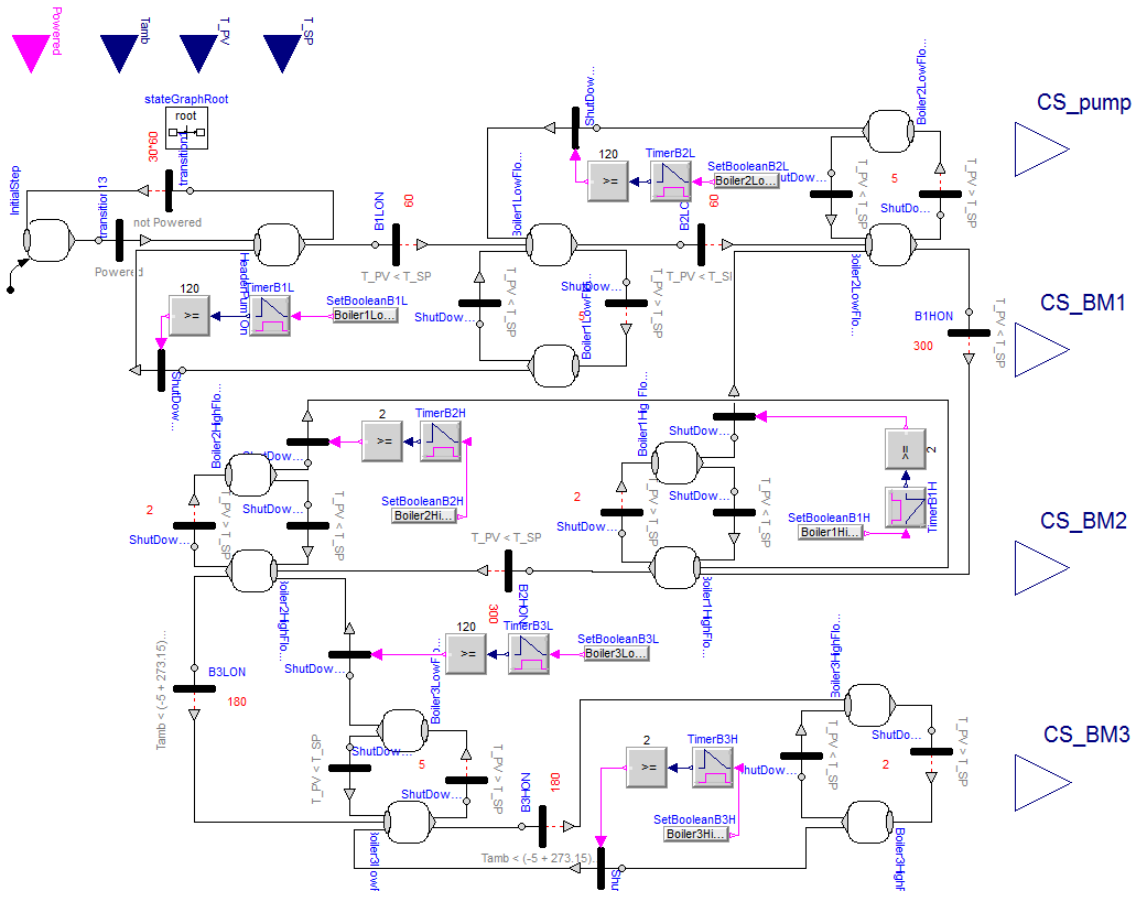

Figure 4.30: Model implemented for the control logic of the three gas boilers.

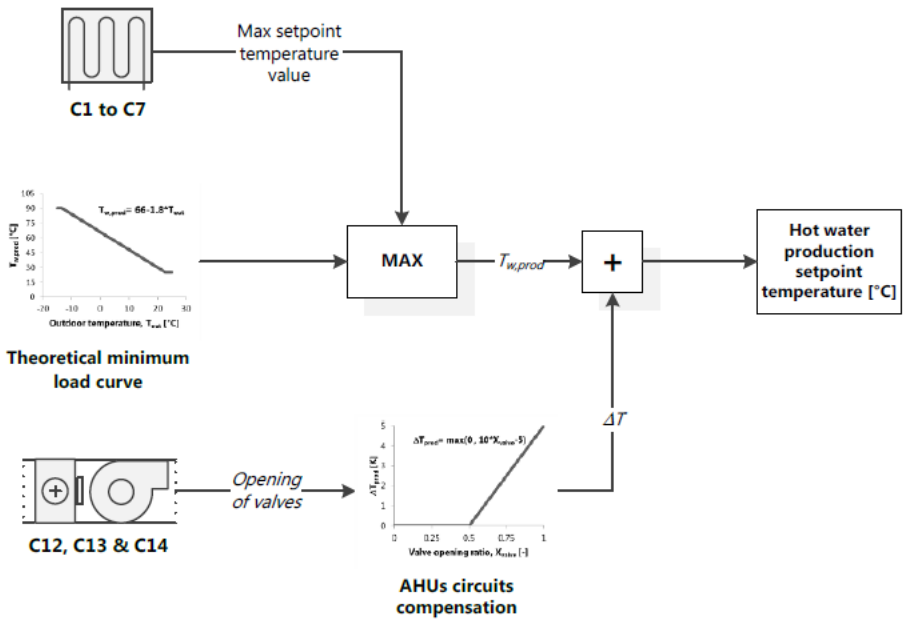

Figure 4.31: Determination of the hot water production set point temperature.

In the retrofitted system, the water outlet temperature of the building (in red in Figure 4.32) should be equal to the temperature set point of the ORC condenser (60°C as first hypothesis) to

avoid using the dry cooler and to have the ORC working at its nominal cogeneration condition. For this reason, during the validation of this component, the controlled temperature of the old control logic is the return temperature (ringed in red in Figure 4.32) and it is fixed to 60°C (instead of the value computed with Figure 4.31).

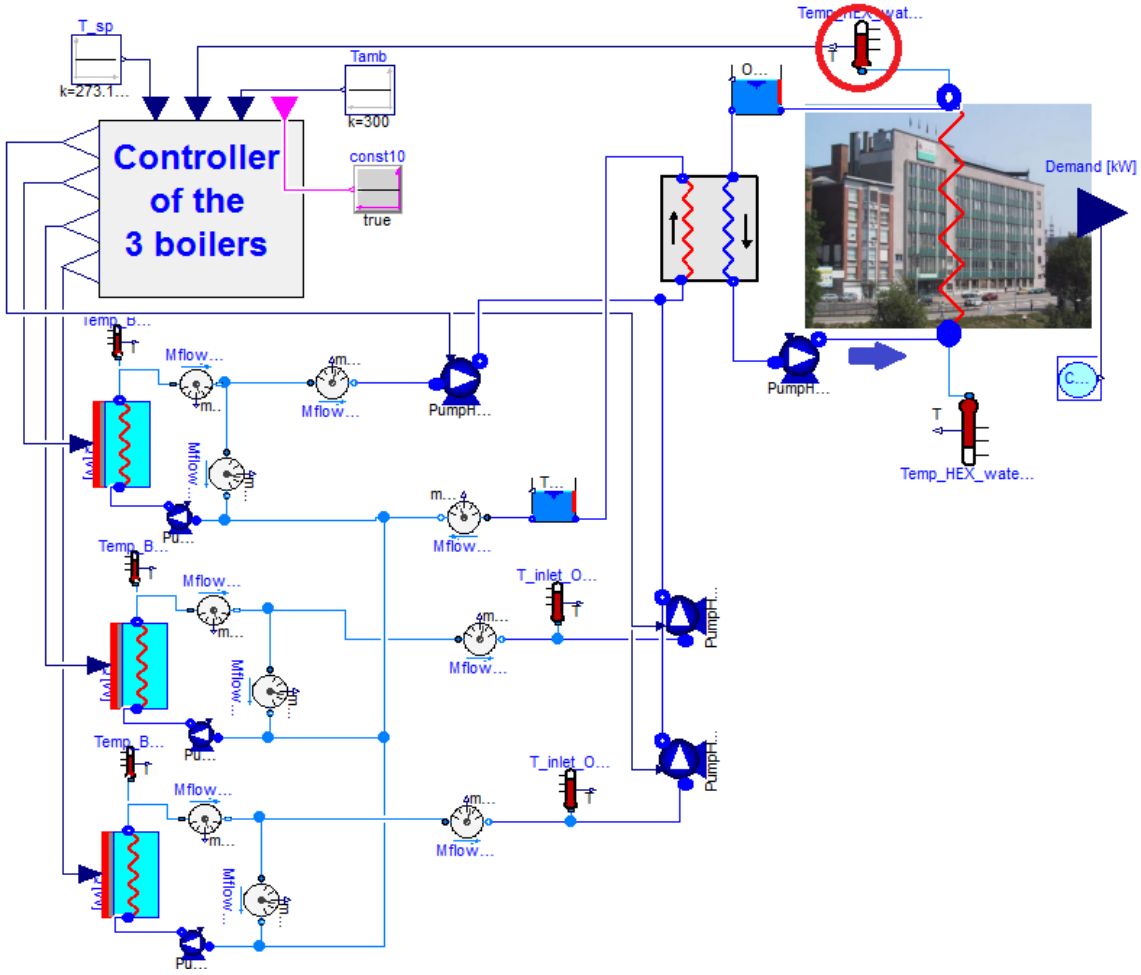

Figure 4.32: Illustration of the Dymola model used to study the old power plant.

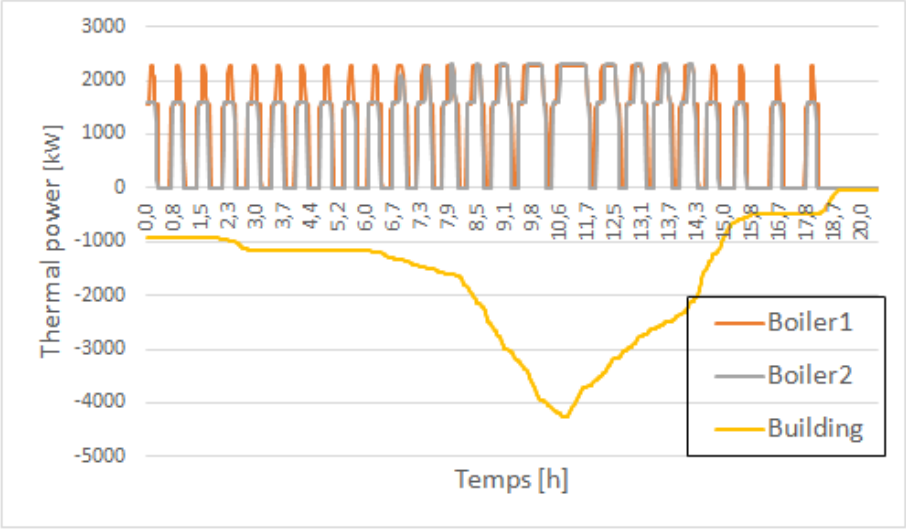

Figure 4.33: Thermal power production of the old power plant.

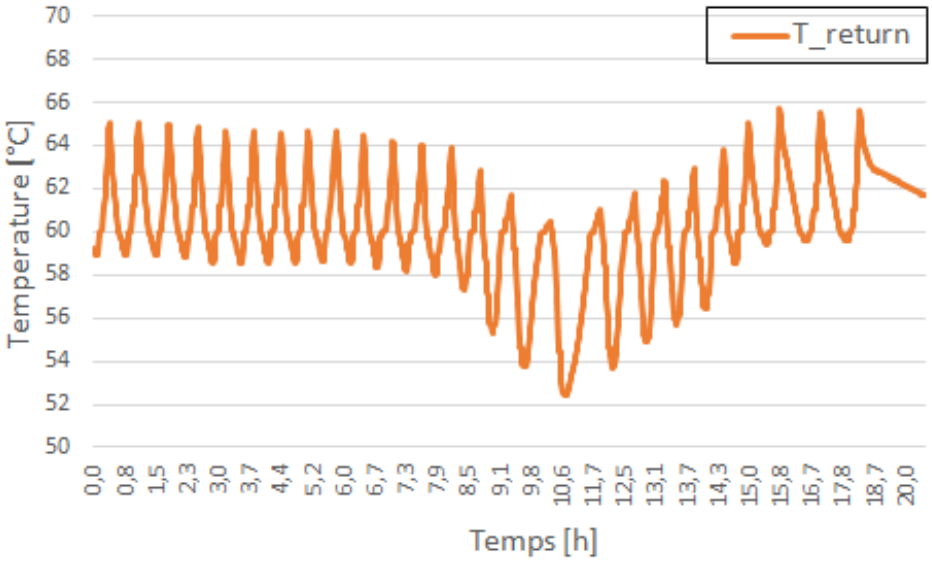

Figure 4.34: Fluctuation of the temperature due to the ON-OFF system.

Figure 4.33 shows the power generation of the boilers for a hypothetical power consumption from the building (the third boiler is not illustrated as it is not used). The system is able to fulfil the demand all the time. However, due to its ON-OFF feature, there is also a fluctuation in temperatures shown in Figure 4.34. This fluctuation is more or less 6°C above or under the set point.

This difference of power production/consumption is mainly due to the activation cascade characterised by a slow activation speed and a fast shutdown of the natural gas boilers. As soon as the temperature is high enough, the fluctuation of temperature has no impact in distribution network. Indeed, the water loops are composed of a high mass flow rate combined with a 3-way valve to control the partial water recirculation to reach the desired distribution temperature (the partial recirculation is shown in Figure 2.1).

The temperature fluctuation due to the use of the natural gas boiler (see Figure 4.34) has a huge impact on the future results. Indeed, once the natural gas boilers are activated, they heat the water loop above the set point temperature and in reaction, the biomass boiler decrease its generation of power and/or the dry cooler dissipates some power to keep constant the inlet temperature T_{17}. To solve this issue, a modification of the activation and deactivation cascade delay can be considered to have a faster reaction time and a better regulation. With this last simplification, the behaviour of the temperature is improved at the cost of really slow simulation and lower robustness (due to faster variations of thermodynamics states). Another possible simplification to produce the right amount of power and so to keep the right temperature is using gas boilers modulated by a *PID* controller or using the gas boilers to generate power only when the biomass boiler can not produce it as it should be the case. This last simplifications means that the power generation is equal to $Q_{GN} = Q_{Building} - Q_{BM}$. Moreover, the three gas boilers can be modelled with one equivalent boiler. The model obtained with these last simplifications was the fastest to simulate. It also gives good temperature behaviour which allows studying the power plant in detail in Chapter 5 without having fluctuation in the temperature every time the gas boilers are ON.

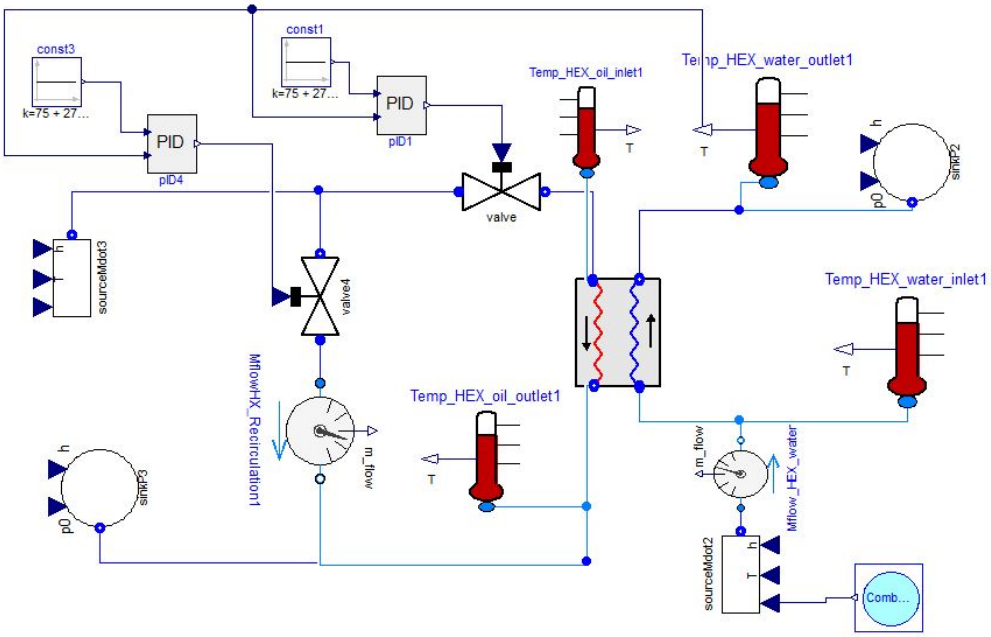

Figure 4.35: Dymola model used for the reference case of the 3-way valve study.

4.2.7 Three-way valves

As shown in Figure 3.1, they are many 3-way valves and valves in the layout. This might lead us to simulation issues during the compilation or during the initialization. To avoid having simulation errors or slow simulations (due to system hard to solve with the large number of valves used in the power plant (Figure 3.1)), the 3-way valves are replaced by an equivalent model.

The pump model used fixes the mass flow rate and does not depend on the pressure losses in the different components. The head pressure gain in the pumps is only used to compute the electricity consumption. It is different from the reality where we have to use a combination of 3-way valves and simple valves to have the right total pressure losses, given by the equation 4.32, to have the desired mass flow $\dot{m}$ in the elements. Indeed, the flow rate depends on the characteristic curves of the pumps ($\dot{m}$ is a function of the pressure losses for a fixed rotation speed).

$$\Delta P_{tot} = \Delta P_{component} + \Delta P_{Valves} + \Delta P_{3WaysValves} + \Delta P_{Pipes} \tag{4.32}$$

Many configurations were studied to get the same results as the one obtained using two valves controlled by two *PID* controllers (this is quite good approximation of how a 3-way valve works). The model, illustrated in Figure 4.35, is the model whose results are the reference case for the comparisons with others alternative studied configurations.

The two controllers, illustrated in Figure 4.35 and named *pID1* and *pID4*, have almost the same parameters as inputs with an opposite outputs. The equation (4.33) explains precisely the value of the output of two PID controllers:

$$y_{pID1} = 1 - y_{pID4} \tag{4.33}$$

The model giving exactly the same results is shown in Figure 4.36. It's composed of two pumps instead of one pump and a 3-way valve. The second pump, named *PumpHxOil_1* (see

Figure 4.36), acts like a valve by limiting the flow going through itself. The two configurations can be explained as follows:

One Pump + one 3-way valve The aperture of the 3-way valve is modified to increase/decrease the pressure losses to reach the right mass flow in the heat exchanger. The aperture depends on the nominal flow rate of the associated pump and the eventual pressure losses in others components (heat exchanger in this case).

2 Pumps The first pump has the same nominal flow rate as the previous case and the *PID* controller has the same role as previously. In this case, it directly fixes the mass flow rate of the "fake pump" to reach the right set point. This configuration does not take into account the pressure losses that affect the consumption of the pumps (equation (4.10) where the variation of pressure is given by the equation (4.32)).

This new configurations has still many interests as listed below:

- We can easily implement the zero flow which could be problematic if the valves aren't written correctly.
- The implemented model is easier to solve as it uses fewer components (see Figure 4.35 and 4.36).
- The implemented model of the power plant can not be accurate concerning the pressure losses seeing that the terms ΔP_{Valves} and ΔP_{Pipes} from the equation (4.32) are unknown (e.g., uncertainties for the length pipes). Indeed, increasing voluntary the pressure losses might be necessary if the mass flow rate is modulated with a variation of the pressure and not with a variation of frequency ($\dot{m} = f(Hz, \Delta P)$).
- The new system is much faster. With the same inputs, the model of Figure 4.36 takes only 13.4 seconds whereas the system with the 3-way valve from the Figure 4.35 take 20.7 seconds. This difference means that the alternative system decreases the simulation time of 35.2%.

This simplification allows us to decrease drastically the time needed for the simulation as there are many 3-way valves in the whole system. It also makes the system more robust with the fast variation of the mass flow encountered during the implementation of the control logic.

4.2.7.1 Sizing of the valves

The new model of the power plant will thus not take into account the pressure losses due to the 3-way valves. Once the main model gives the mass flow rate in each component necessary to reach the set point temperature, a small model takes these flow rates as inputs and compute the pressure drops. The pressure drop found is the lower bound as it considers only the pressure losses in the components and not in the pipes. The separation of the power plant simulation in two models, one for the power generation and distribution, and one for the pumps consumption, makes the model more stable and decrease drastically the simulation time as previously said. With the few data available, the pressure losses were supposed linear and computed with the equation (4.34)

$$\Delta P = k * \dot{V} \tag{4.34}$$

where $\dot{V}$ is the volumetric flow rate $[m^3/s]$. The parameter k is computed using the nominal pressure losses and/or the nominal pump consumption and they are listed in Table 4.4.

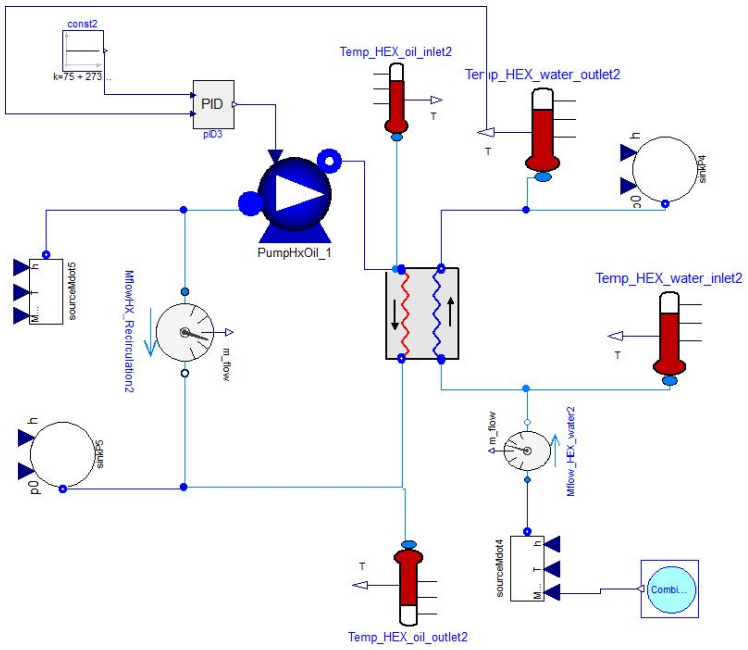

Figure 4.36: Dymola model of the alternative configuration of the 3-way valve.

Table 4.4: Value of the k parameter from the equation (4.34).

	WO Hex Oil Side	WO Hex Water Side	DC Hex Glycol mix Side	DC Hex Air Side
Value of k $[kg/(s*m^4)]$	$4,796E6$	$1,506E6$	$7.923E6$	4.401
	WW Hex GN Side	WO Hex Cold Side	GW Hex Glycol mix Side	GW Hex Water Side
Value of k $[kg/(s*m^4)]$	$1,066E6$	$8,19E5$	$3,76E6$	$3,17E6$

4.2.7.2 Consumption of the pumps

During this thesis, the pumps were considered modulated by a *PI* controller to have the desired mass flow rate/temperature (further information about the frequency variation of a pump are given in [34] for a heat pump when the ambient temperature changes). Using them as variable speed pumps (with an inverter to have lower flow rates) should be considered because a good regulation of the frequency saves energy. There are other ways of regulating the mass flow (e.g. increase of the pressure losses or recirculation) but they are less efficient [35].

To estimate the consumption of the pumps, the following assumptions were made concerning the pumps and the electrical consumption (equation (4.10)) :

- All mass flow rates are possible with a regulation of the pump's frequency.
- The isentropic efficiency of the pump, η_{is} is 70% and it is supposed constant at partial load.
- The pressure losses are supposed linear.

4.2.8 Thermal losses

The thermal losses to the surrounding air are one of the main parameters that need to be considered during the study of power plant. The thermal losses regroup the thermal losses of the tank and of the pipes. They are only function of the temperature and they can be considered constant as the temperature is controlled by many *PI*. Once the thermal losses are modelled, a study is made to determine the optimal set point temperatures. Indeed, a high temperature means higher thermal losses and a lower electrical consumption whereas lower temperature leads to higher power consumption and lower thermal losses.

4.2.8.1 Oil tank

The total resistance to the heat transfer between the oil inside the storage of $1m^3$ (cylinder shape) and the surrounding air is given by the following equation [36]:

$$\frac{1}{AU_{tot}} = \left(\frac{1}{h_1 A_1} + \frac{ln(r_2/r_1)}{2\pi k_1 L} + \frac{ln(r_3/r_2)}{2\pi k_2 L} + \frac{1}{h_2 A_3} \right) \tag{4.35}$$

where r_1 and r_2 are respectively the inner and the outer diameter of the tank wall, r_3 is the external diameter of the insulation, A_1 is equal to $2\pi r_1 L$ and k is the thermal conductivity (subscript 1 for the metal layer and 2 for the isolation). The convection heat transfer coefficient h, the insulation thickness and the conductivity of the insulation are known ([37] and [38]). Concerning the height and the radius, they are found with the thickness of the insulation and the internal volume. Finally, the global heat transfer coefficient can be written for the inner diameter of the wall:

$$U_{tot} = 2 * \pi * r_1 * L * AU_{tot} \tag{4.36}$$

Concerning the ceiling of the tank, the global heat transfer coefficient is found using the equation for an isolated horizontal wall :

$$AU = \frac{1}{h * A} + \frac{x}{k * A} \tag{4.37}$$

where x is the thickness of the insulation. The interface of the oil tank, *StraTank* from *ThermoCycle*, is shown in Figure 4.37.

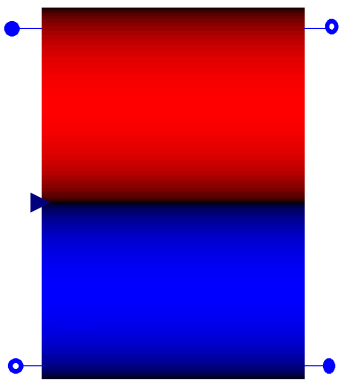

Figure 4.37: Interface of the stratified tank.

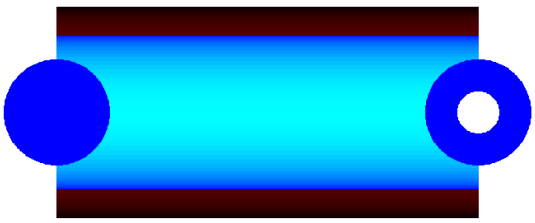

Figure 4.38: Interface of the isolated pipe.

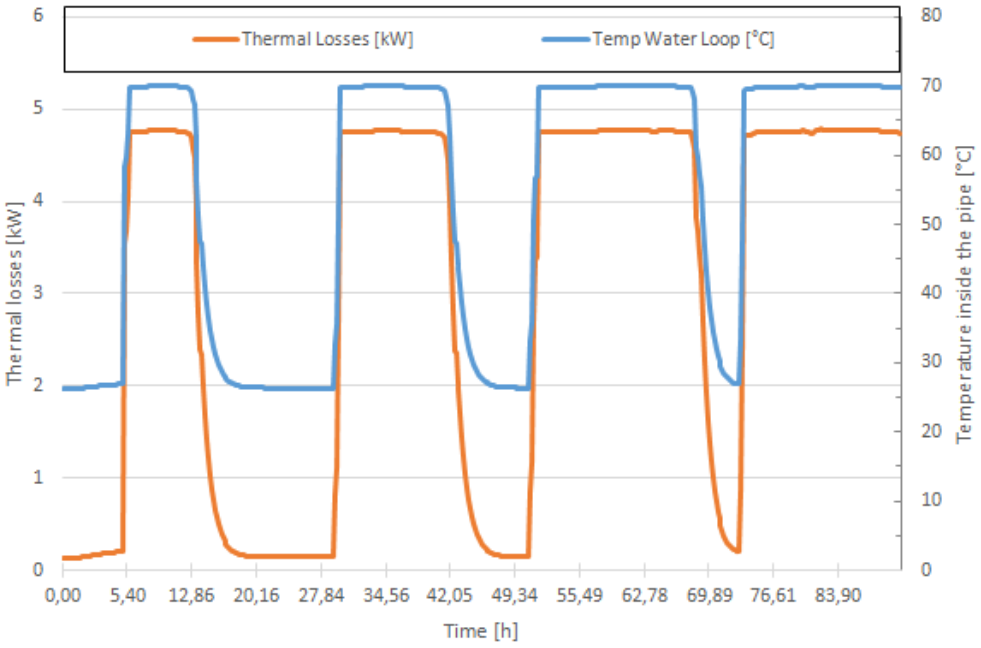

Figure 4.39: Variation of the thermal losses with the temperature for an isolated pipe.

4.2.8.2 Insulated pipes

The resistance to heat flow is principally due to the insulation and the heat transfer from the pipe to the air and it can be expressed with the following equation [36]:

$$\dot{Q} = \frac{T_1 - T_\infty}{\frac{ln(r_3/r_2)}{2\pi L k_2} + \frac{1}{h_2 2\pi r_2 L}} \tag{4.38}$$

The length and the diameter of each pipes, and the thickness and the conductivity of the insulated layer of each pipe are known thanks to the technical specifications [38]. The interface of the model can be seen in Figure 4.38. Depending on temperature inside the oil storage and depending on the thermal oil and water loop temperature, the thermal losses of the pipes and the oil tank represent between 0.5% and 2% of the nominal power of the biomass boiler. The thermal losses of the tank with the surrounding air are almost constant ($400W$) whereas the thermal losses of the pipes are variable.

The behaviour of the pipe connecting the oil-water heat exchanger to the building is illustrated in Figure 4.39. This picture shows that when there is no flow inside the pipe, the stationary water inside the pipe is cooled down. In consequence, the amplitude of the thermal losses decreases. After 5-6 hours, the pipe is at the ambient temperature and has to be heated up to the desired temperature when there is a thermal demand from the building. This means that the water inside the specific pipe ($4.6m^3$ for a pipe $260m$ long) consumes a fraction of the power generated just to reach the desired temperature and this is the case each time we switch ON-OFF the pump $VSP6$.

4.2.9 Validation of the main biomass control logic

As previously said, the biomass is directly connected to an oil tank which behaves like an energy storage. The tank and the 3-way valve from Figure 2.5 are principally used to

compensate the lack of fast reaction from the biomass boiler. The model used to simulate the tank is a stratified tank with 4 ports. The equivalent model of Figure 2.5 is showed in Figure 4.40 (compounds from the left side of the red line). It uses:

- two pumps for the equivalent 3-way valve (whose maximal mass flow is the sum of the mass flow through the ORC evaporator and the water-oil heat exchanger),
- the building model (=sink of power) to represent both the ORC and the oil-water heat exchanger,
- the oil tank and the biomass.

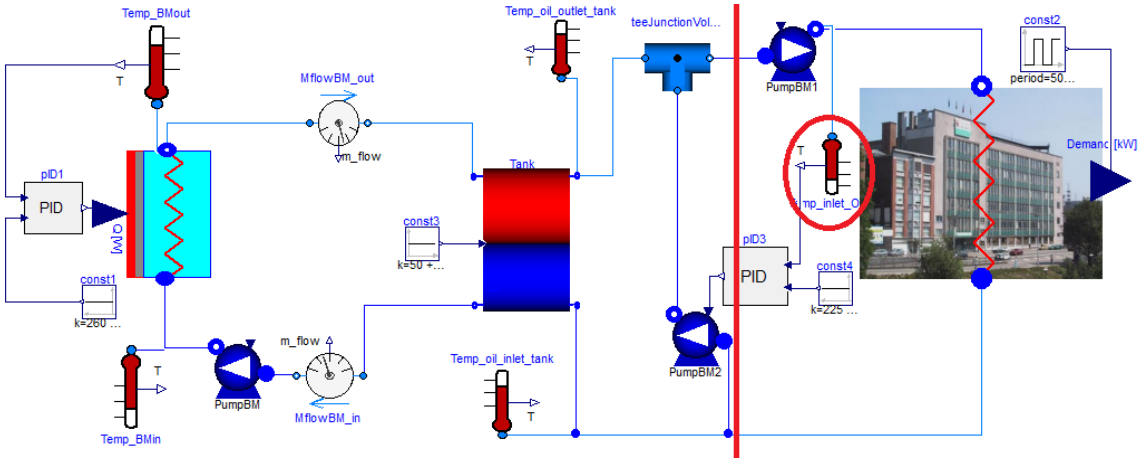

Figure 4.40: Model of the biomass and its oil tank.

This small study shows that the set point temperature encircled in Figure 4.40 can be kept constant with a control logic working above the biomass internal control logic. This is shown in Figure 4.42 where the thermal oil temperature in the main loop (annotations from Figure 2.5) is constant while the outlet temperature of the biomass is fluctuating depending on the power required (shown in Figure 4.41). Here is a list of the behaviours of the system:

- If the oil tank is big enough, the 3-way valve can compensate the slow variation of the biomass boiler. Considering a fast reaction of the 3-way valve, it is thus possible to keep the fluid flow to the main loop at 225°C and provide the thermal power instantaneously. The total power delivered is the sum of the power from the biomass and from the oil tank:

$$\dot{Q}_{delivered} = \dot{Q}_{BM} + \dot{Q}_{tank} \tag{4.39}$$

$$= \dot{Q}_{BM} + V_{tank} * \rho_o * cp_o * (T_t - T_{t+1}) \tag{4.40}$$

  where T_t is the temperature in the tank at time t. The fluctuation of these terms are illustrated in Figure 4.41 and 4.42.

- The volume required to keep a constant temperature is illustrated in Figure 4.43. It decreases:
  - If the variation of the thermal demand is fast.
  - When the amplitude of the fluctuation decreases.

– With a decrease of the start-up time of the biomass. This is explained by a lower capacity required to fill the gap between the production and consumption curves (see Figure 4.41).

- It means that the combination of a well-sized oil storage, biomass boiler and the controlled 3-way valve *V3V1* can deliver the right power all the time even if the thermal demand changes really fast.

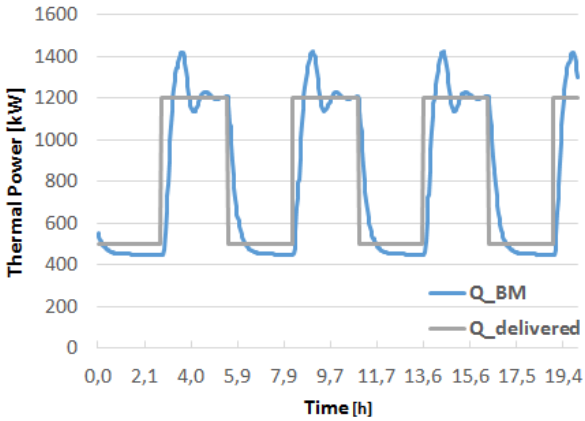

Figure 4.41: Variation of the power production when the power plant has a fast variation of thermal power consumption.

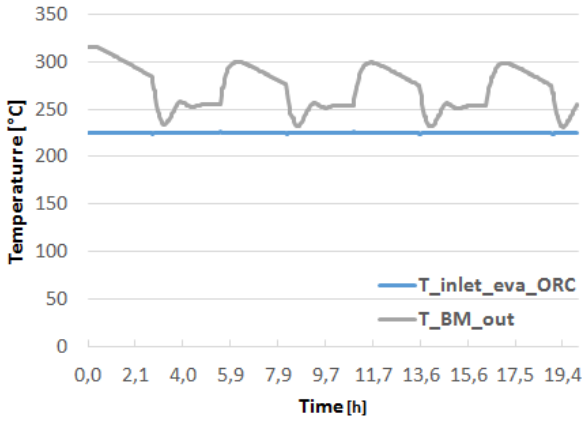

Figure 4.42: Variation of temperatures when the power plant has a fast variation of thermal power consumption.

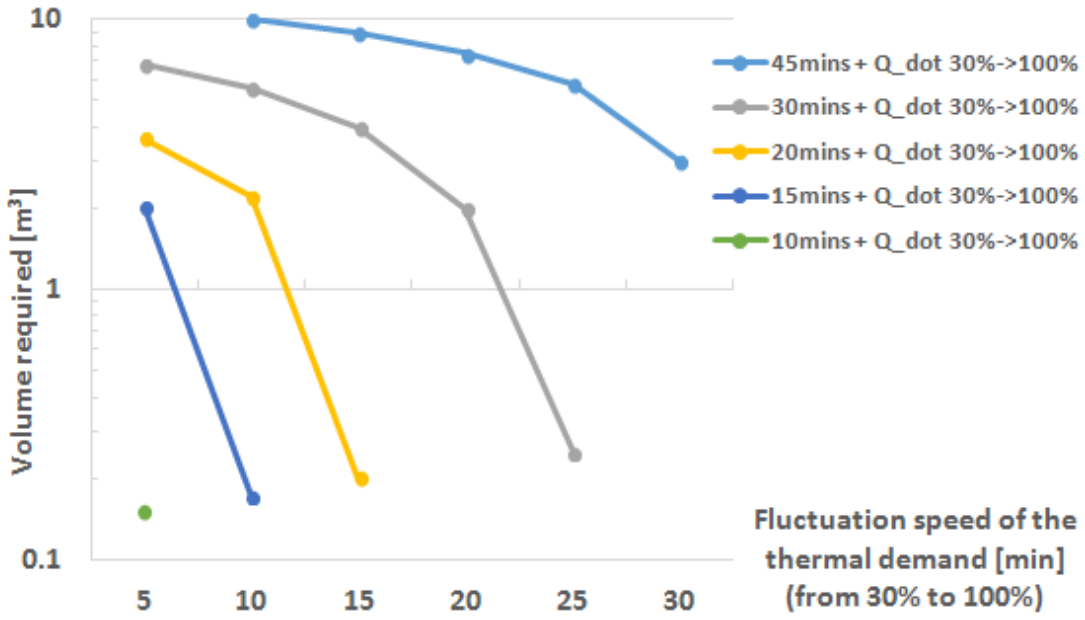

Figure 4.43: Variation of volume required to compensate the slow Biomass' reaction as a function of the reaction time of the biomass and the variation's speed of the thermal demand.

Chapter 5

Optimisation and analysis of the power plant

The study of the whole power generation system was realised step by step. Indeed, the first configurations showed some issues regarding the thermodynamics behaviour. To find a solution to these issues, the layout was modified one step at a time. The aim of this chapter is to show and explain why improvements of the first considered layout were necessary.

In the next sections, a detailed description of the configurations considered is given. It's followed by a thorough investigation of the results and by some possible improvements to the layout. These improvements aim to solve one or all the issues of the configuration. The next part of this chapter is about the installed power plant. It starts with a optimisation of the dry cooler, the control strategy and the working temperatures. Finally, this chapter ends with small studies about the profitability of the power plant.

5.1 First configuration

5.1.1 Distinctive features

The first configuration studied, illustrated in Figure 5.1, works as described below:

- The pump $P2$ works at his nominal flow and the 3-way valve *V3V2* makes a modulation (with a *PI* controller) on its aperture to regulate the water outlet temperature of the W-O HEX T_{16}.
- The pumps $P3$ and $P5$ work at their nominal value and the 3-way valve $V3V5$ is controlled with a *PI* controller to have the right temperature at the condenser (60 °C in the case of cogeneration mode).
- Concerning the cooling of the working fluid, a first proposition is to make a regulation on the fans speed with variable speed fans. The fans of the installed dry cooler should be controlled by an internal control logic. Furthermore, the dissipation of power is also controlled with another control system working in parallel (a modulating the 3-way valve *V3V5* of the HEX G-W).
- When the power delivered by the condenser of the ORC isn't enough to fulfil the heating demand of the building, one of the two "existing pumps" is activated and the fluid goes through the HEX W-O $1500kW$.

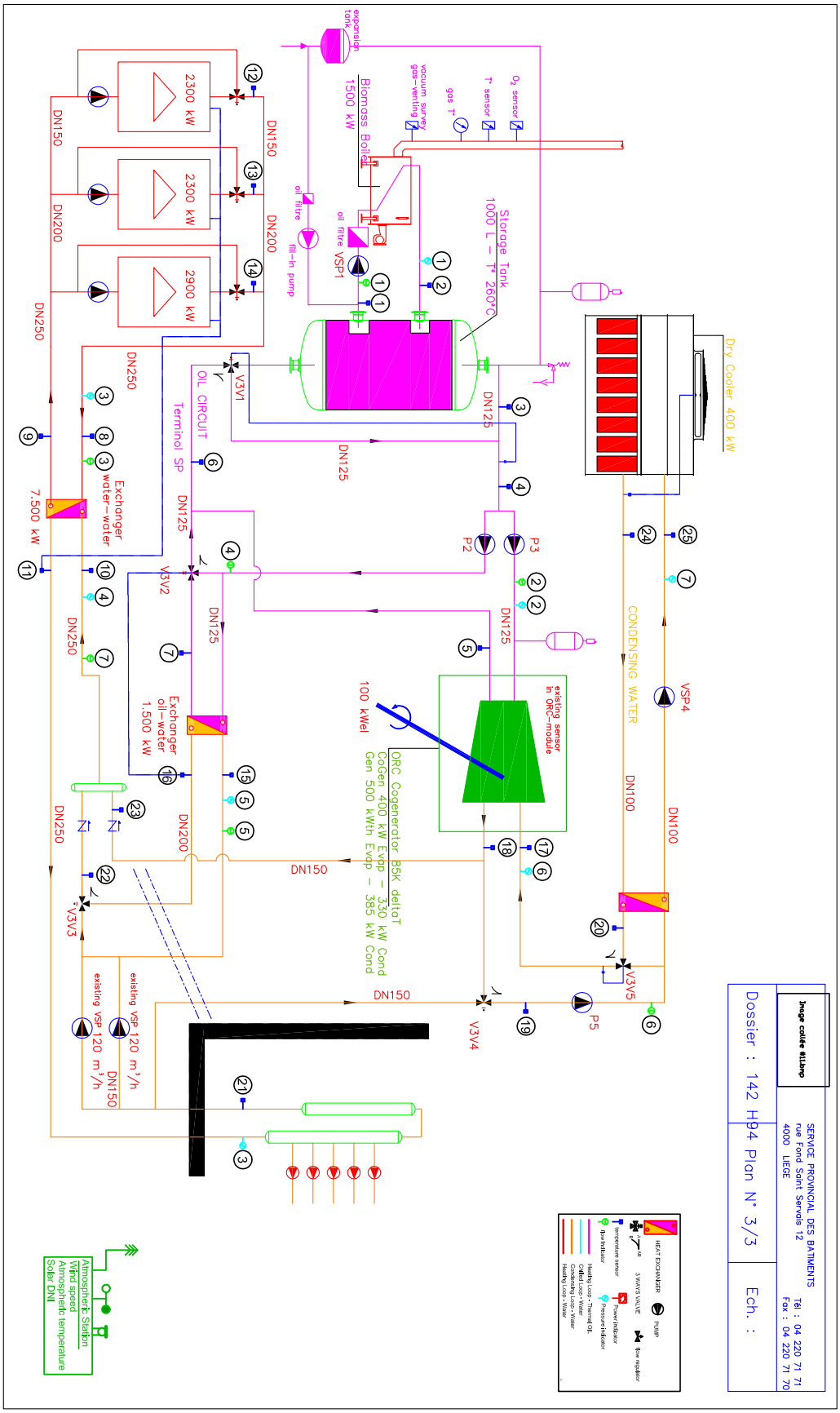

Figure 5.1: Illustration of the first layout.

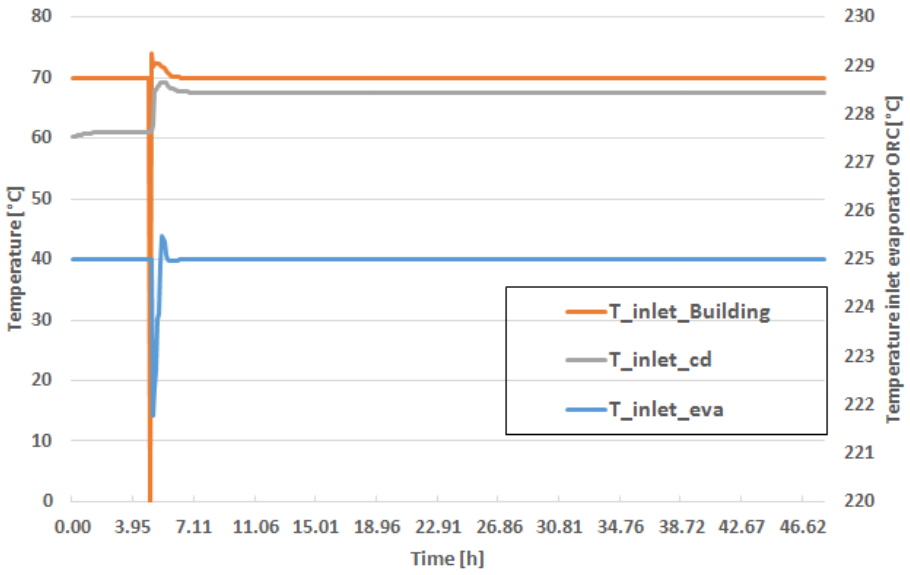

Figure 5.2: Increase of the temperature $T_{21}(T_{inlet,cd})$ due to wrong control system.

If the power available from the oil-water heat exchanger isn't enough, the set point temperature of the sensors T_{16} isn't reached. The sensor T_{11} reads a lower temperature than $T_{sp,17}$ (fixed at a lower value than $T_{sp,16}$ to avoid using the natural gas boilers in normal operation). In consequence, the natural gas boilers are activated to increase this temperature. With the reaction of the gas boilers, the power balance is verified all the time with the appropriated combination of the components regardless the heating demand. The power balance is showed in the following equation:

$$\begin{aligned} \dot{Q}_b &= \dot{Q}_{bm} + \dot{Q}_{ng} + \dot{Q}_{dc} \\ \dot{Q}_b &= \dot{Q}_{ORC,cd} + \dot{Q}_{HEX,w-o} + \dot{Q}_{HEX,w-w} + \dot{Q}_{dc} \end{aligned} \tag{5.1}$$

- The aperture of the valve *V3V1* is modulated to reach the set point of the temperature sensor T_4

In the next subsection, the results obtained are presented in terms of the balance of power, mass flow and temperature. The first issues are illustrated and a possible justification about the malfunctioning is given.

5.1.2 Results obtained and drawbacks

There are many issues encountered with this layout. Some of them are linked to a wrong control of the layout. Here is a list of these issues:

The first issue When the power asked overpasses the power available from the ORC condenser, one of the existing pumps starts and extracts thethermal power necessary to reach the set point ($T_{set,point,16}$) fixed at 70 °C. In terms of power, there aren't any problems and the power balance is respected. The following equation is a special case of the equation (5.1) where the terms from the water-water exchanger is neglected.

$$\dot{Q}_b = \dot{Q}_{ORC,cd} + \dot{Q}_{HEX,w-o} + \dot{Q}_{dc} \tag{5.2}$$

However, as the pumps are only working at their nominal flow rate, there is an issue in the temperatures. The water coming back from the building (sensor T_{21}) is warmer than the set point of the inlet ORC condenser. The controller of the cooling tower makes thus a modulation on the aperture of the valve $V3V5$ to reach the right temperature. This previous problematic can be explained as followed:

A constant mass flow rate, combined with a temperature of $T_{sp,16}$(70°C in this case) fixed by the controller of the 3-way valve $V3V2$ and a temperature from the building (T_{21}) ideally equal to $T_{sp,17}$, leads to a constant power exchanged $\dot{Q}_{HEX,w-o}$ which is impossible. The results (Figure 5.2) show that the temperature T_{21}, which is also the input temperature of the W-O HEX, increases to extract a lower power. However, as the water returning from the building is hotter than the set point temperature of the condenser, the controller of the dry cooler reacts by extracting some power. That means that we are producing power to dissipate it further. This is shown in Figure 5.3.

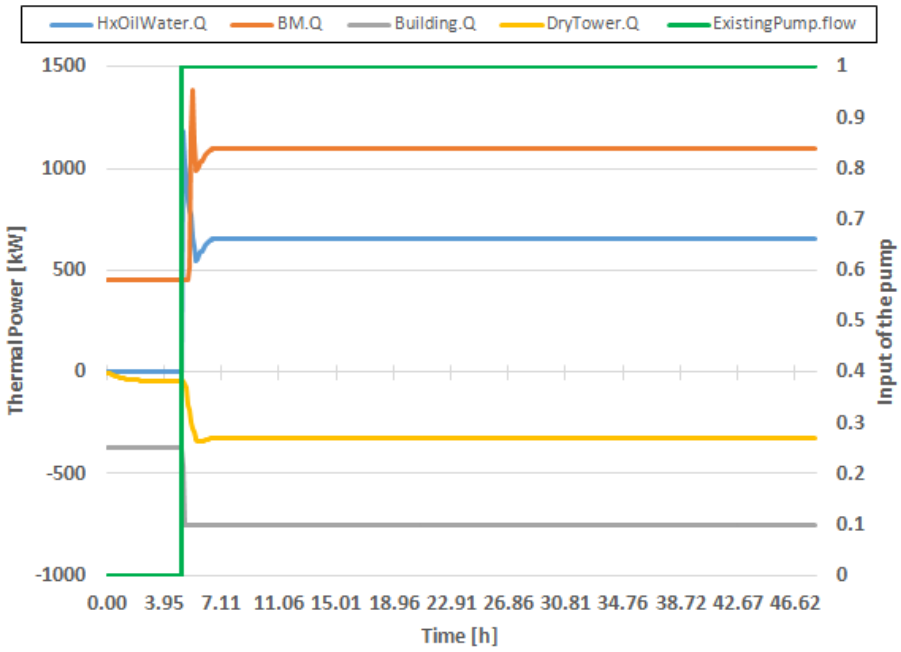

Figure 5.3: Activation of the dry cooler even if the building power required *Building.Q* is high.

Issue 2 When the power required is bigger than the power available from the new power plant (ORC + W-O HEX), the water flow rate through the heat exchanger increases (activation of the second pump of the existing pumps) and so does the oil flow rate in response to the *PI* controller of *V3V2*. The increase of the mass flow rate is shown in Figure 5.4 where the parameter $ExistingPump.flow$ slightly increases when the building power demand *Building.Q* overpasses the power available from the ORC and the HEX W-O.

In consequence, the oil flow rate increases to fulfil more power which leads to a higher total power extracted. As the power extracted from the Water-oil heat exchanger increases, the temperature decreases in the whole thermal oil loop. The decrease of temperature in the thermal oil loop resulting of this issue is illustrated in Figure 5.5. Due to the excessive extraction of power in the heat exchanger combined to a limited power production from the biomass boiler, the evaporation temperature decreases to extract less power in the ORC. Furthermore, if the temperature decreases too much, the ORC is stopped (for a temperature lower than the *"minimal authorized value"* for the *ORC*).

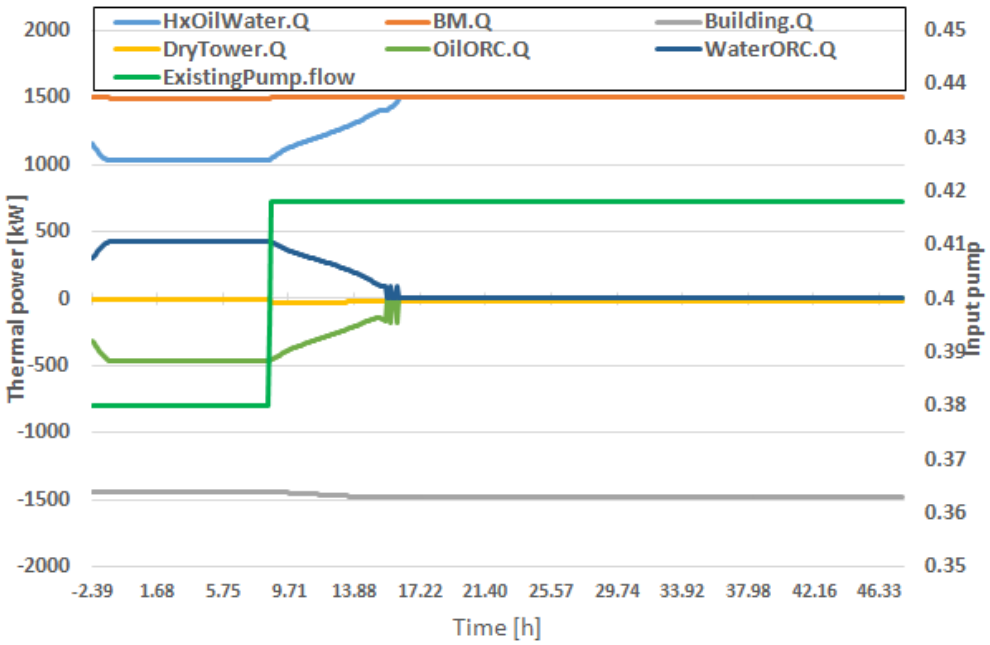

Figure 5.4: Activation of the dry cooler even if the building power required *Building.Q* is high.

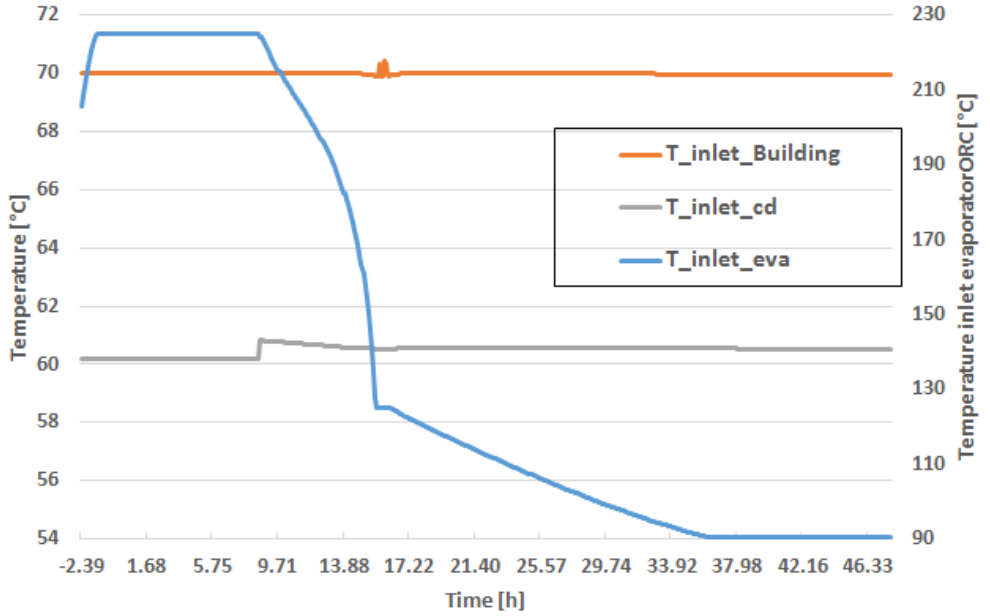

Figure 5.5: Activation of the dry cooler even if the building power required *Building.Q* is high.

5.1.3 Improvement of this configuration

Concerning the first issue, a modification in the layout is necessary. The first solution is to use a variable speed pump instead of a pump working at its nominal condition $120m^3/h$. The other solution consist to accept a temperature lower than 70°C in the input of the building and use the temperature sensor T_{21} to control the aperture of the 3-way valve *V3V2*. With one of these modifications, the second issue is not yet solved for the high thermal demand ("higher than the capacity of the biomass"). Indeed, if the existing pumps are now variable, the water flow rate keeps increasing with the thermal demand (ΔT is constant between T_{16} and

T_{17}). In reaction of the controller of V3V2, a higher mass flow of thermal oil is redirected through the heat exchanger and more power are extracted which will decrease the thermal oil temperature. In case if the pumps are working at their nominal flow rate with the other control, the thermal oil flow rate also increases when the thermal demand increases until we extract too much power.

To limit the impact of the second issue, a sizing of the pump $P2$ is necessary. Indeed, the flow rate of this pump is not known and the actual value is too high. The sizing is done for the future layouts studied and as it is shown in the next subsection, the lower flow rate of the next configurations solves this issue. The sizing of the pumps depends on the characteristic of the heat exchanger and so, it is necessary to do a new one for each exchanger considered during the sizing. Furthermore, a sizing of the 3-way valve $V3V2$ is also necessary. Indeed, it should be completely open only when $1500kW$ are extracted in the oil-water heat exchanger. It means that the aperture of the valve *V3V2* has to be limited and keeps a small bypass of the flow in the normal working condition (it is shown in Figure 5.8).

5.2 Second configuration

5.2.1 Distinctive features

The second configuration studied tries to solve the previous issues. This new configuration has two important modifications and many small modifications on all the components. Those small modifications are principally made on the inertia of the components and on their physical characteristic to reach a more realistic model. The two main improvements to the previous layout are:

- A sizing of the pump P_2 is realized and the optimal mass flow found is 6.42 kg/s (value computed with the data available during the study of this configuration). To determine this flow rate, a simple version of the power plant is used. The Dymola model is shown in Figure 5.6. As previously explained in the last chapter, the valve $V3V2$ (see Figure 5.1) is replaced by a pump for many different reasons. This pump, named *PumpHxOil_2* is modulated by an *PI* controller like the valve is in reality. Furthermore, its maximal flow rate is 4.26 kg/s when the ORC is working and its maximal flow rate is the nominal flow rate of pump $P2$ to extract $1500kW$ in case if there are issues in the ORC. The sizing of $P2$ and $V3V2$ is made using the maximal water flow rate calculated with the following equation (respectively 5.3 and 5.4).

$$\dot{m}_w = \frac{\dot{Q}_{Hex,w-o}}{\Delta T * cp_w} = \frac{\dot{Q}_{biomass} - \dot{Q}_{eva,ORC}}{\Delta T * cp_w} \tag{5.3}$$

$$\dot{m}_w = \frac{\dot{Q}_{Hex,w-o}}{\Delta T * cp_w} = \frac{\dot{Q}_{biomass}}{\Delta T * cp_w} \tag{5.4}$$

  Using those equations to obtain the water mass flow rate guarantees:

  - having the right water outlet temperature fixed at 70 °C,
  - avoiding a too big extraction of power
  - and keeping the desired set point temperature 225°C whatever the thermal demand

- The pumps "Existing pumps" are used as variable pumps (with a inverter).

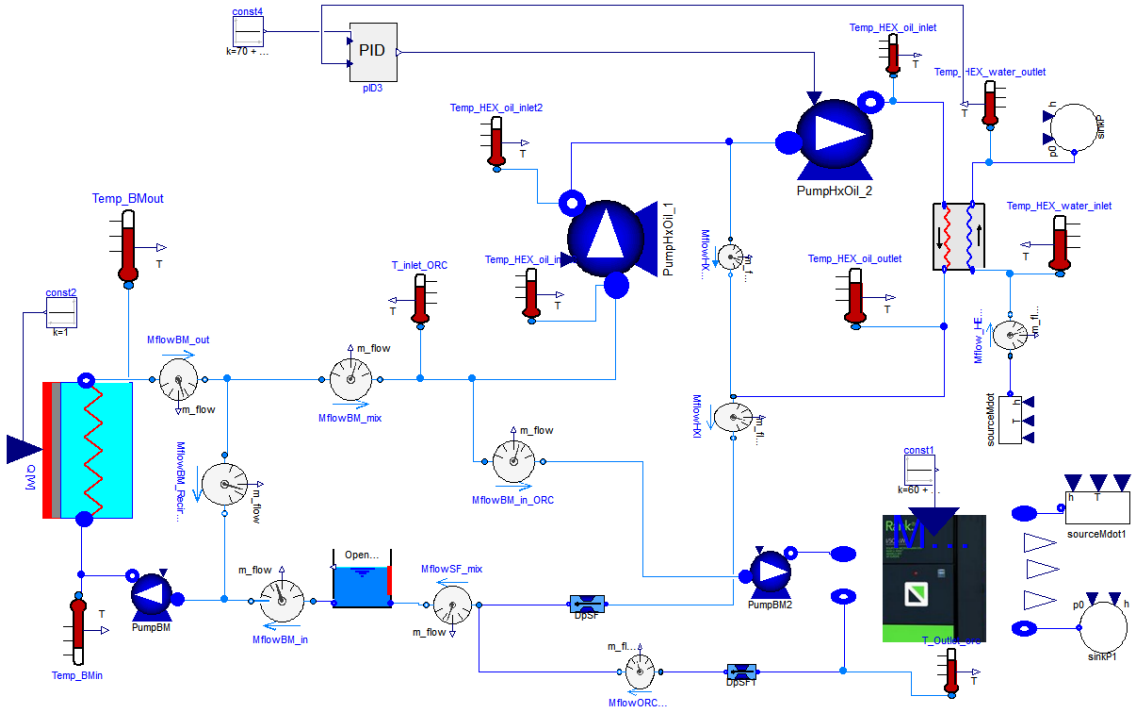

Figure 5.6: Illustration of the model used for sizing the pump *PumpHxOil*_1 (named *P*2 in the Figure 5.1).

The mass flow rate in the two pumps, illustrated in Figure 5.7, shows that it works indeed like a 3-way valve (bypass in the beginning and one hundred percent of the flow through the heat exchanger when we extract $1500kW$). Figure 5.8 shows that when the ORC is stopped (at 4000 seconds), the water can extract more power in the water-oil heat exchanger with the conditions than the valve $V3V2$ redirects all the oil flow through the heat exchanger. In these pictures, the water flow rate increases slowly which leads to a slow increase of $HExOilWater_Q$ and $PumpHxOil_2.flow_{in}$ (seeing that the ΔT is fixed, when the water flow rate increases, it implies an increase of the thermal power delivered).

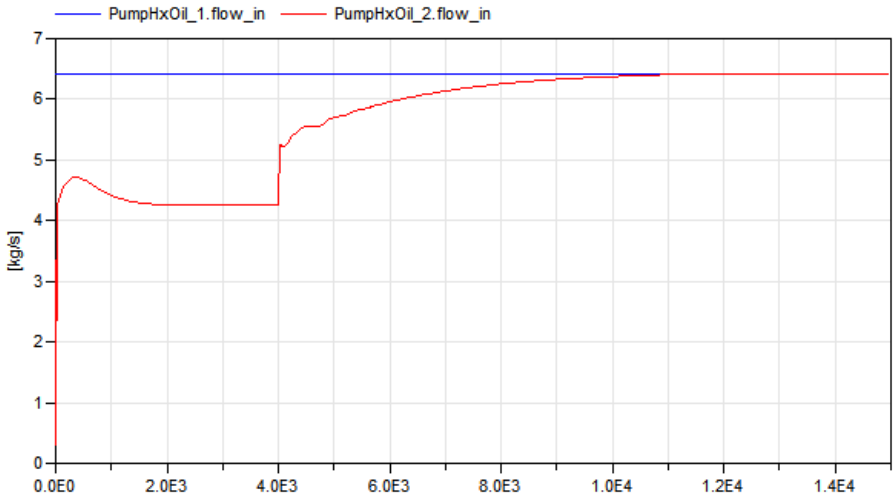

Figure 5.7: Mass flow rate profile over time.

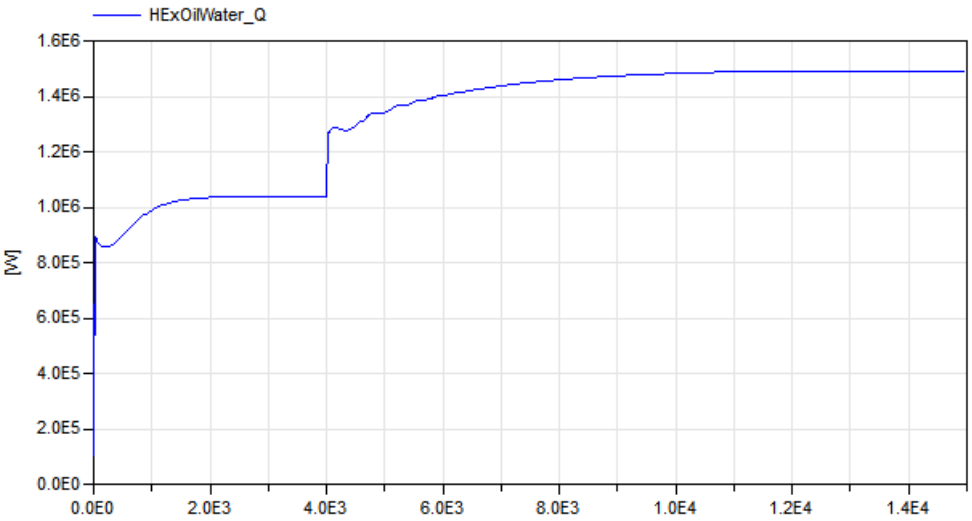

Figure 5.8: Heat exchanged over time.

5.2.2 Results obtained and drawback

With the modifications, the simulation of the power plant gives better results as expected. The set point temperatures are kept constant for almost all the thermal possible demand proving that the actual sizing and its associated control logic is working. The only residual problem is the fluctuation of temperature due to activation of the natural gas boilers.

5.3 Suggested layout for the implementation on-site

This part of the work has more constrains and the sizing of the different components is limited. Indeed, the next configuration studied is the layout installed in the building in Liège due to the fact that the Belgian demo site was under construction during this work and the layout of the Belgian building has been decided and can not be modified anymore. This means that the disposition and the physical properties of the pumps and the other components are fixed (and known). This section consists in a study of the installed layout and the suggested control strategy. The suggested layout by the partners "Province de Liège" is shown in Figure 5.9 and the Dymola model is illustrated in Figure B.1 (Appendix B). It incorporates some of the improvements suggested and there are others modifications in the layout and in the control strategy. In the next subsection, the issue of this proposed control logic is explained.

5.3.1 Drawback

The main issue concerning this power plant layout is the control logic of the Oil-Water heat exchanger. Indeed, the controlled parameters are not chosen correctly:

Issue 3 The proposed control system should use the sensor T_6 (see Figure 5.9) to control the aperture the 3-way valve. The control system is supposed to open or close the 3-way valve depending of the heat exchanger power demand to keep a fixed temperature T_6 :

$$(\dot{m}_{VSP2} + \dot{m}_{VSP3}) * cp_{o,T6} * T_6 = \dot{m}_{VSP3} * cp_{o,T5} * T_5 + \dot{m}_{VSP2} * cp_o * T_{V3V2} \quad (5.5)$$

$$= (\dot{m}_{VSP2} + \dot{m}_{VSP3}) * cp_{o,T4} * T_4 - \dot{Q}_{ev,ORC} - \dot{Q}_{Hex,WO} \quad (5.6)$$

.

This control system isn't working as both the mass flow rates (of the pumps VSP2 and VSP3) and the power consumed in the ORC evaporator $\dot{Q}_{ev,ORC}$ are constant ($\dot{Q}_{ev,ORC}$ only depends on the ORC inlet temperatures (T_4 and T_{17}) which are supposed constant). Indeed, this last equation shows that the temperature T_6 only depends on the power exchanged in the water-oil heat exchanger $\dot{Q}_{Hex,WO}$. And if the *PI* controller tries to keep it constant, it leads to a constant extraction of power and that is not what is desired. A small consequence of this is that the 3-way valve *V3V2* can not be modulated using a sensor placed after it. Indeed, the same issue is encountered if we place the sensors before the mix of the flows from the pumps $\dot{m}_{VSP2}$ and $\dot{m}_{VSP3}$.

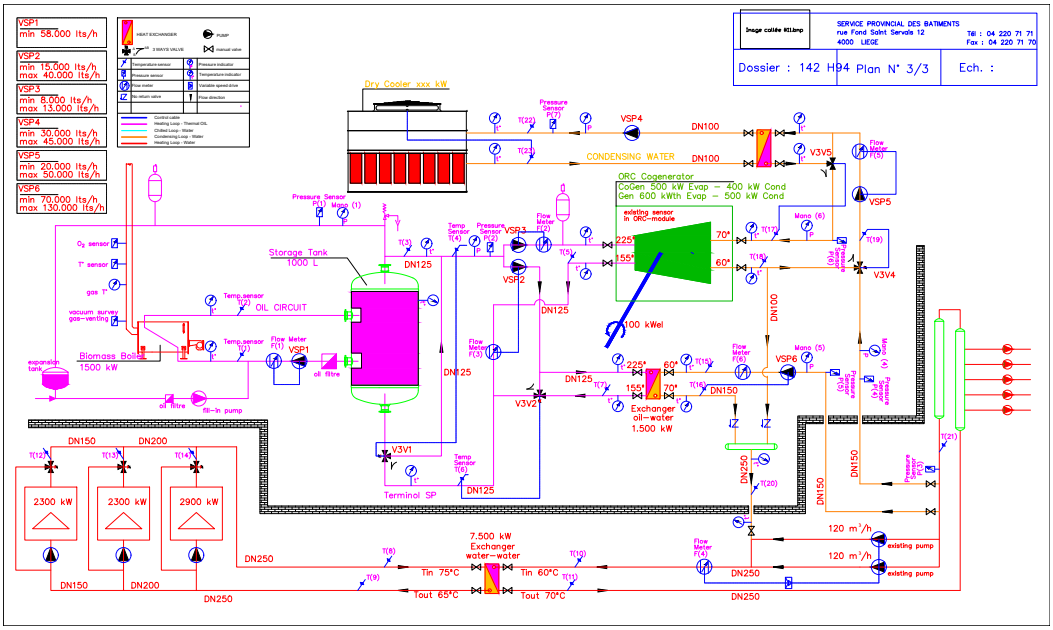

Figure 5.9: Illustration of the proposed layout.

5.4 Improvement of the installed layout

This section starts with some propositions and possible modifications to the control strategy to improve the stability and the efficiency of the power production system and finishes with an optimisation for some of the working schemes presented in Chapter 3.

5.4.1 Modification of the dry cooler control

As previously explained in Chapter 2, there are many possible control methods to modulate the power dissipated [6] [12] [13]. The one proposed by the provider is based on a regulation of the fans speed (Figure 5.9). A study was made to find the optimal control system to increase the efficiency of the dry cooler (and thus the efficiency of the whole system). All other things being equal, the system stability of the system was enhanced when the set point temperature was the sensor T_{22} (DC inlet temperature) instead of the sensor T_{23} (DC outlet temperature). Four control strategies are studied:

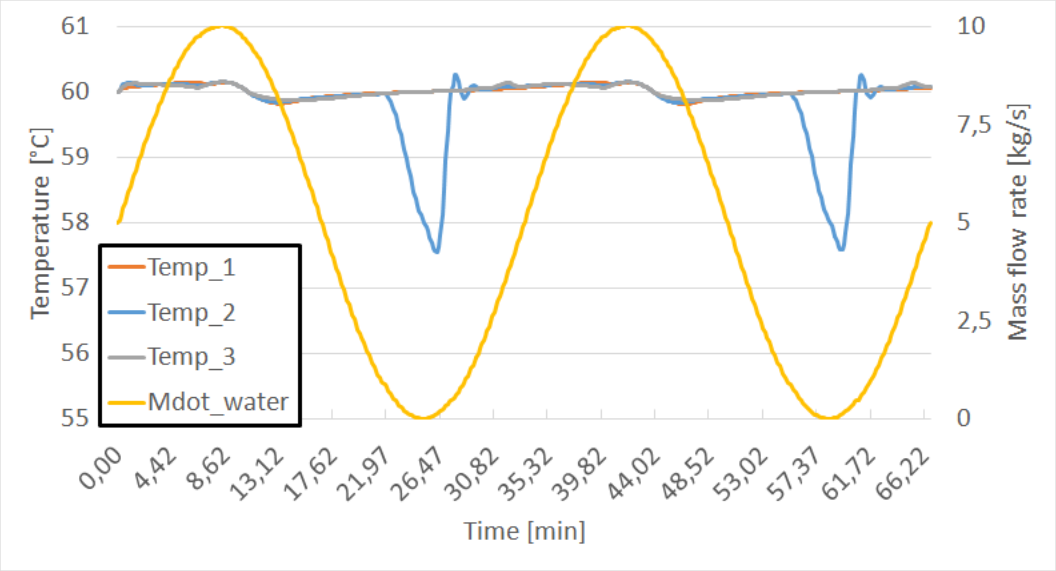

Figure 5.10: Fluctuation of the controlled temperature over time.

No control The fans and the pump are working at their nominal flow rates all the time. In the whole power plant, the dissipation of power is only controlled with the 3-way valve *V3V5* (Figure 5.9). This configuration is the simplest and it is the reference case study. In the three next configurations, the power dissipation is controlled using both the 3-way valve *V3V5* and an internal control.

Case 1 In this case, the air flow rate is constant inside the dry cooler and the dry cooler inlet temperature is controlled by a *pI* controller modulating the glycol-water flow rate (i.e variation of the frequency of the pump). When the cooling demand decreases, the controller of the valve *V3V5* bypasses the heat exchanger. The glycol-water outlet temperature of the heat exchanger decreases and as a reaction, the *PI* decreases the flow rate of the glycol-water mix to decrease de dissipation of power inside the dry cooler

Case 2 Contrary to Case 1, Case 2 uses variable speed fans and a constant glycol-water pump. Its *PI* controller reacts the same ways as the case 1.

Case 3 In the last configuration considered, both the fans and the process pump are used as a variable pump (with an inverter).

To compare those configurations, a water flow rate at 70°C is applied to the G-W HEX connected to the Dry Cooler (the hot water flow rate varies sinusoidally as illustrated in Figure 5.10). The temperature (its set point is 60°C) and the electricity power consumption are respectively showed in Figure 5.10 and 5.11. Figure 5.10 shows that the temperature is kept close to its set point thanks to the regulation. The only exception is Case 2 where a slight decrease in temperature happens when there is no cooling demand (zero mass flow). Indeed, this specific control logic keeps constant the glycol-water flow at its nominal value and when the fans are turned OFF, a power is exchanged between the inertia of the DC and the G-W HEX. This leads to an increase in the wall temperature of the dry cooler and a decrease in temperatures of the heat exchanger wall (situated between the Glycol-Water mix and the water distribution loop).

Concerning the power consumption of Figure 5.11, a summary is made in Table 5.1. To obtain these values, the pressure drops are considered linear with the mass flow rate, and the

fans and the pump have a hypothetical constant isentropic efficiency of 70% for their nominal and partial load.

Table 5.1: Total electricity consumption.

Case	Consumption $[kWh_{el}]$	Consumption reduction $[\%]$
No Control	10.866	0
1	9.02831	14.571
2	4.8307	55.545
3	3.6915	66.029

As predicted, modulating the dry cooler is more interesting than keeping the pump and fans at their nominal value. Furthermore, Table 5.1 shows than a frequency regulation on the fans is more interesting (55.5% of consumption reduction) than modulating the power dissipation with only a regulation of frequency of the water-glycol pump (14.5%). This can be proved with the nominal consumption of the fans that is much higher than the nominal consumption of the water-glycol pump (see Figure 5.11). Indeed, modulating only the fans or the process fluid pump means that the other component stays at its nominal flow rate even if the cooling demand is low. Finally, a decrease by 66% of the electricity consumption is achieved with a modulation on both the fans and the pump. This percentage of consumption reduction is even bigger when the power demand stays low for a long period.

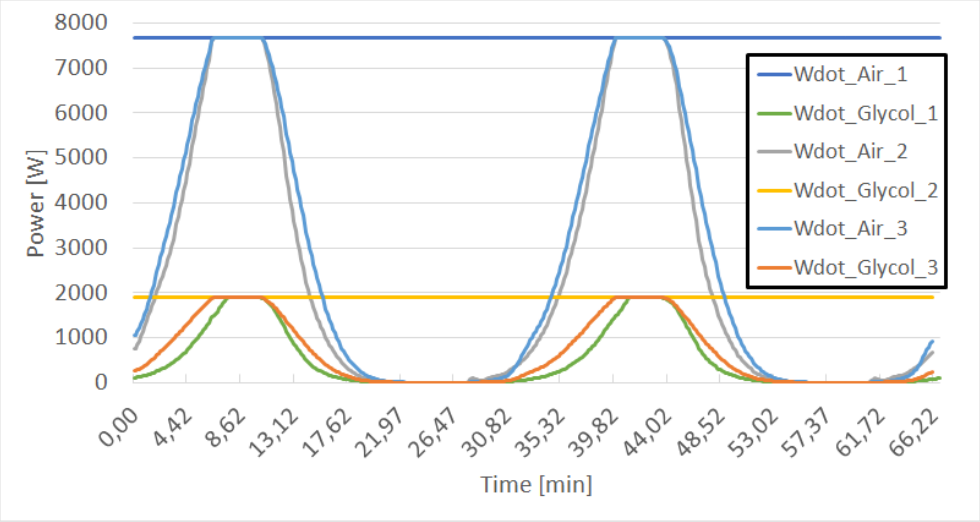

Figure 5.11: Electrical power consumption over time.

In conclusion, this small study showed that it is more interesting to control both the frequency of the pump and fans.

5.4.1.1 Optimisation of the dry cooler

There are many factors influencing the performance of the dry cooler. To optimise the control method, the set point temperature of the dry cooler is latter determined case by case (e.g. the working schemes are studied separately during the temperatures optimisation). The area of the G-W HEX is a parameter influencing the efficiency. Indeed, if sizing is still under consideration, the heating area has to be studied because it influences the reachable temperature T_{22}(considering a pinch depending on the area) and in consequence, it modifies the DC

efficiency. Finally, the ratio between the two flow rates is also one parameter having a huge influence as it is demonstrated in the previous subsection. Many studies are available concerning the optimisation of a dry cooler like G. Barigozzi, A. Perdichizzi and S. Ravelli [39] who have developed a *Matlab* code able to find the optimal combination of the fan speed and the cooling water pump speed. According to [39], the modulation of fans and pumps rotational speeds leads to maximal reduction of power consumption whatever the operating conditions may be. A few possible ratios between the two flows are considered. However, to avoid having a stiff system, the studied ratios are simple and they are based on a single *PI* controller.

The results of this optimisation, shown in Table 5.2, demonstrate that it was more interesting to increase faster the glycol-water flow rate in respect to the air flow rate. Indeed, to dissipate more power, an increase of the water-glycol flow rate leads to a smaller electrical consumption. The best ratio air-glycol, for the cooling demand studied, is given by the equation:

$$\dot{m}_{glycol} = min\left(\dot{m}_{glycol,nom}\ ,\ 1.13 * \sqrt[0.8]{\left(\frac{\dot{m}_{air}}{\dot{m}_{air,nom}}\right)^{0.6}} * \dot{m}_{glycol,nom}\right) \tag{5.7}$$

Table 5.2: Dependence on the electricity consumption with the glycol-air ratio.

Glycol-air ratio	Consumption $[kWh_{el}]$	Consumption reduction $[\%]$
$\left(\frac{\dot{m}_{glycol}}{\dot{m}_{glycol,nom}} = \frac{\dot{m}_{air}}{\dot{m}_{air,nom}}\right)$	4.958	0
$\left(\frac{\dot{m}_{glycol}}{\dot{m}_{glycol,nom}}^{0.8} = \frac{\dot{m}_{air}}{\dot{m}_{air,nom}}^{0.6}\right)$	4.936	0.44
equation (5.7)	4.908	1

Table 5.2 shows that a higher consumption reduction is achievable with an optimised glycol-air flow ratio. However, the percentage of reduction is small for a more complex control strategy (which has a longer simulation time and leads to a stiff system when it is combined with the whole power plant model). To keep a simple model, the air-glycol flow ratio is fixed to $\left(\frac{\dot{m}_{glycol}}{\dot{m}_{glycol,nom}} = \frac{\dot{m}_{air}}{\dot{m}_{air,nom}}\right)$ and only the air flow rate is controlled with one *PI* controller. In the reality, there is no limitation (stability of the system and simulation time) and a faster increase of $\dot{m}_{glycol}$ has to be considered before increasing too much the air flow rate.

5.4.2 Optimal control strategy

Table 5.3 regroups all the control logics studied. The first part is about the two first configurations of this chapter and the second part regroups the different control strategies considered for the installed power plant. In this table, sensors are in blue when the are only used to activate and deactivate the pumps (i.e. when the power delivered in the ORC condenser is not enough to fulfil the building demand, the temperature T_{21} decreases and the *PI* controller reacts with the activation of the pump **VSP6** and with the activation of the pumps **EP** when the power demand is really high). Concerning Configuration 8, the existing pumps are in red because they were not activated during the simulation of 12 typical days even if they were controlled by a *PI*. The difference between each configuration is briefly explained below:

Configuration 4 The first modification considered to the **configuration 3** is using the sensors T_{15}(=T_{21}) to modulate the $V3V2$ aperture. An unexpected issue happened due to a wrong control system:

Table 5.3: Different control strategies considered.

Configuration	Sensor **V3V2**	Flow rate **VSP6**	Sensor **VSP6**	Flow rate **Existing Pumps (EP)**	Sensor **EP**	Results
1	T_{16}	Absent	/	ON/OFF	T_{21}	Issue 1 and 2
2	T_{16}	Absent	/	Variable	T_{21}	No issue
2'	T_{21}	Absent	/	ON/OFF	T_{21}	No issue
3 "suggested"	T_6	Variable	T_{16}	ON/OFF	T_{21}	Issue 3
4	T_{16}	Variable	T_{16}	Variable	T_{21}	Issue 4
5	T_{15}	ON/OFF	T_{21}	ON/OFF	T_{21}	No issue
6	T_{15}	ON/OFF	T_{21}	OFF	/	No issue
7	T_{16}	Variable	T_{15}	ON/OFF	T_{21}	No issue
8	T_{16}	Variable	T_{21}	Variable-OFF	T_{21}- /	No issue

- **Issue 4** The controlled parameters are not chosen well. If the building power demand increases, the water inlet temperature of the Oil-Water heat exchanger decreases. Everything else kept constant, the water outlet temperature decreases. This system as thus two possible reactions depending on the reaction speed of the two controllers. It can increase the oil flow rate inside the heat exchanger to increase the power exchanged and/or it can increase the water mass flow rate to keep the outlet temperature constant. In the two cases, the outlet temperature T_{16} is the desired temperature. However, if only the oil flow rate increases, the inlet temperature T_{15} stays low while the thermal demand increases $\dot{Q} = \dot{m}_w * cp_w * (T_{sp} - T_{15})$. Concerning the increase of water flow rate, the temperature T_{15} decreases less as $\dot{m}_w$ has increased. In fact, both flow rates (water and oil) will increase in both cases because increasing the flow rate of only one of the two sides doesn't increase enough the heat transfer. In conclusion, in both cases, the temperature T_{15} isn't controlled and isn't equal to the nominal value of 60°C.

Configuration 5 It is the simplest configuration. The pumps **EP** and **VSP6** are working at 0 or 100% of their nominal flow rate depending on the power demand.

Configuration 6 In this configuration, the pump **VSP6** is working ON-OFF like in the previous configuration and the existing pumps **EP** are kept OFF. This leads to a higher temperature in the inlet of the building and this is more in accordance with the previous control system (old power plant, illustrated in Figure 2.1), which was using high temperatures according to values found with the old control (illustrated in Figure 4.31).

Configuration 7 The control strategy is based on a regulation of the pump **VSP6** and the existing pumps working at 0 or 100% of their nominal flow rate. Contrary to the **configuration 1** which uses the same sensor for the control, this control system does not have issues as the water pump **VSP6** is variable which avoids the *Issue 1* (for a building power requirement $\dot{Q}_b > \dot{Q}_{ORC,cd}$) previously explained and the existing pumps now only feed the $7500kW$ heat exchanger connected to the natural gas boilers. Keeping them working at their nominal flow doesn't lead to the *Issue 2* ("dropping of temperatures in the thermal loop") because the thermal oil loop and the water loop are not connected through the water-oil heat exchanger.

Configuration 8 This configuration is similar to the **configuration 4**. Indeed, this configuration has only an alternative control method for the pump **VSP6**. The *PI* controller modifies the frequency of this pump using the sensor T_{21} and tries to keep its value around

the desired temperature. As already said before, this solution showed that the existing pumps weren't used as the mass flow rate of the pump **VSP6** is already high enough to fulfil the power for the 8 days representing the 8 months of the heating demand.

5.4.2.1 Economical study

Each configuration of Table 5.3 has different levels of temperature seeing that the mass flow rate is different in each case. In consequence, the difference consists mainly in the electrical consumption of the pumps and in the biomass consumption due to different thermal losses. To compare the different control strategies, some hypotheses are necessary:

- The set point temperatures are the same for each configuration and the ORC works with the same temperatures at the evaporator and at the condenser of the ORC during the whole heating period.
- As previously said, the price of electricity, wood pellet and natural gas are respectively 215 €/MWh$_{el}$, 275.6 €/tonne and 25.223 €/MWh (TVA included) [27].
- The electricity generated by the ORC is totally self-consumed.
- In Belgium, the government gives green certificates *GCs* depending of the reduction of carbon dioxide emissions (1 every 456 kg of CO_2 saved). The reference case concerning the electricity and the heating is respectively a Combined Cycle Gas Turbine *CCGT* with an efficiency η_{el} of 47% and a natural gas boiler with a efficiency η_{th} of 98%. The emission of CO_2 for natural gas and wood pellets are respectively 251 and 91 kg/MWh.
- The CO_2 emissions savings, the electricity generated and the associated number of GCs is computed every three months [40]. In other words, the equations (5.8) and (5.9) are computed every three months.
- There is an upper limit of 2 GCs/MWh_{el} produced with the ORC and each *GCs* can be sold 65 €/ units.
- The ratio between the electrical own consumption of the biomass boiler and its nominal thermal power supplied is 1% [1].

With these hypotheses, it is possible to determine the profits of the power plant using the following equations:

$$\begin{aligned} Profit &= Reference\ Price - New\ Price \\ &= \frac{Q_b}{0.98} * 25.223 - (M_{BM} * 275.6 - GCs * 65 - El_{net} * 215) \end{aligned} \tag{5.8}$$

$$with\ GCs = min\left(2; \frac{(\frac{Q_{building}}{\eta_{th}} + \frac{P_{el,ORC}}{\eta_{el}}) * 251 - M_{BM} * ncv_{BM} * 91}{451}\right) \tag{5.9}$$

Where M_{BM} is the daily mass of biomass required, Q_b is the integral of the thermal power demand [MWh] ($\dot{Q}_b * time$), EL_{net} $[MWh_{el}]$ is the integral of the net electrical power P_{net} (from equation (5.10)) and *GCs* is the number of green certificates *GCs*. Using the equations (5.9) and (5.8), the yearly profit of the studied configurations 5,6,7 and 8 (Table 5.3) are found for the following set point temperature :

[1] In [41], a ratio of 3% is suggested.

- Evaporation temperature of the ORC T_4 equal to 225°C.
- Condensation temperature of the ORC T_{17} equal to 60°C.
- Temperature of dissipation T_{22} equal to 55°C.

Table 5.4: Comparison of the control strategies studied for a simulation of 240 days and one year. The *Heating period* represents the 240 days of heating demand.

	Pumps Consumption Heating period $[MWh_{el}/year]$	Reduction Heating period $[\%]$	Biomass Consumption Heating period $[tonne]$	Yearly benefits Benefits if positive Heating period [€]	Yearly benefits Benefits if positive One Year [€]
5	126.29	0%	114.7	-101439	-139184
6	121.71	3.76%	114.2	-100779	-138694
7	111.15	11.99%	118.1	-99357	-137265
8	106.68	15.53%	117	-98046	-135915

The table 5.4 regroups the total electrical consumption of the pumps, the quantity of fuel necessary and the associated yearly running cost. From this table, the total electrical consumption shows an important decrease when the pumps are working as variable speed pumps (up to 15.53%). The table also shows an increase of the biomass consumption when the pumps work as variable pumps. This last phenomenon is due to higher temperatures in the water loop. Indeed, in the last two cases (7 and 8), the temperature T_{16} is controlled to have 70°C whereas the two first cases only control the temperature T_{15} to have T_{cd} equal to 60°C. This difference leads to a temperature T_{16} variable (which is most of the time lower than 70°C). In consequence, the thermal losses to the ambience are lower in the first two cases due to their lower temperatures. In conclusion, controlling the flow rate of the pumps showed a reduction in the electrical consumption as predicted and a higher consumption of biomass due to higher temperatures and thermal losses. Seeing that the quantity of biomass burned is different with a small variation of temperature, the next step is to modify the set point temperatures of the optimal control logic (configuration 8). In the next subsections, this last aspect is studied with parametric studies to try reaching a better cost efficient power plant.

5.4.3 Parametric study

Many parameters influence the efficiency of the system and some of them can be modified to optimise the power plant's efficiency. Indeed, the efficiency of the power plant depends on:

- The quantity of biomass burned which depends on the temperature in the different loops (thermal losses) and on the thermal demand and the biomass combustion efficiency which is variable with the load.
- The electricity generated with ORC depending on the evaporation and condensation temperatures.
- The total electrical consumption which is also a function of temperatures (for a fixed thermal demand).

Each term of the equation (5.8) is variable with the building's thermal demand and it is then interesting to see their evolution. The variation of the net electricity with the thermal

demand is illustrated in Figure 5.12, the number of *GCs* and the quantity of biomass burned is showed as a function of the thermal demand in Figure 5.13. The profits of the power plant are computed using the equation (5.8) and are illustrated in Figure 5.14. From this last figure, the optimal working condition (thermal demand of 389kW which is equal to Q_{cd}) gives a benefit of -51€ per day. For this specific working point, the profits are null if the biomass buying price is 255€/tonne of woods pellets (<=>52.8€/MWh). All the figures are shown for a set point temperature of evaporation, condensation and dry cooler's inlet temperature of respectively 225°C; 60°C and 55°C. The graphs stop for a heating demand of 1418kW because the profits are constant for a higher thermal demand (i.e. using of the natural gas as previously).

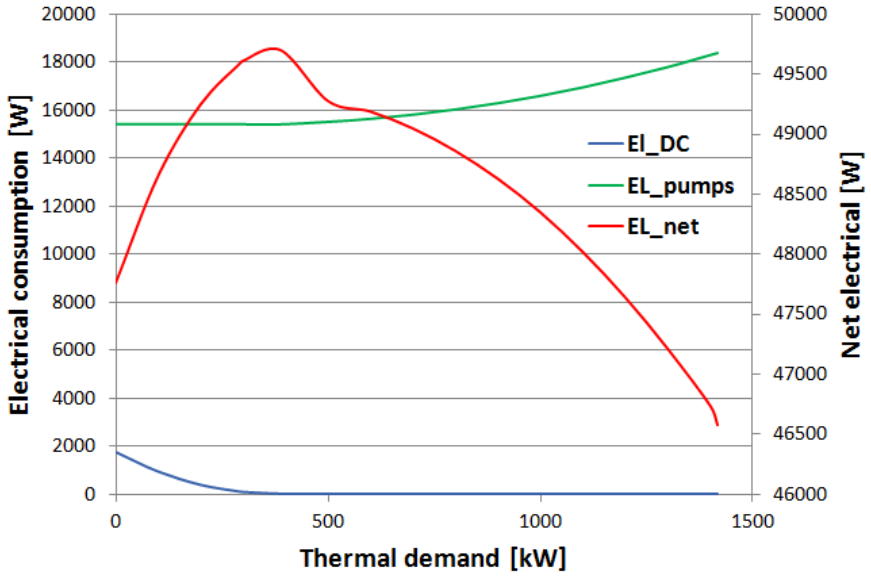

Figure 5.12: Evolution of the electrical consumptions as a function of the thermal demand.

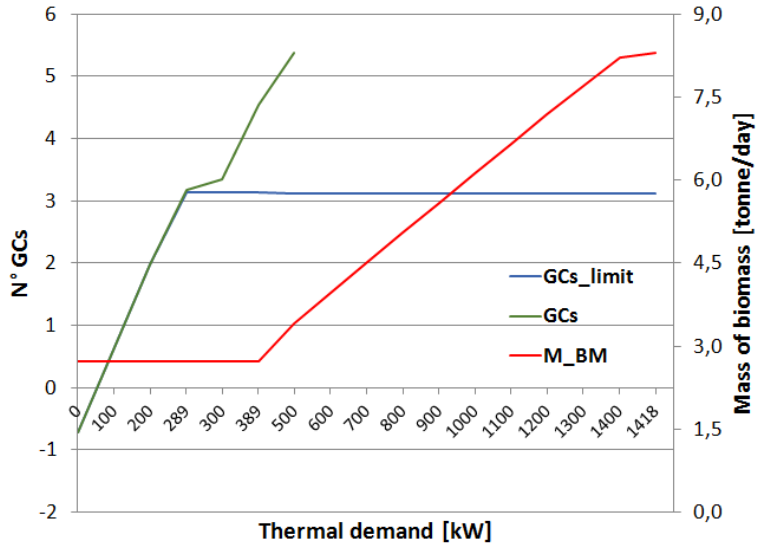

Figure 5.13: Number of GCs and mass of biomass burned as a function of the thermal demand.

The net electricity of the Figure 5.12 is given by the following equation:

$$P_{net} = P_{el,ORC} - P_{pumps} - P_{DC} \tag{5.10}$$

where $P_{el,ORC}$ is the electrical power out of the ORC, P_{pumps} is the electrical consumption of all the pumps and P_{DC} is the electrical consumption of the dry cooler. In the low thermal demand (lower than $Q_{cd} = 389kW$), only the pumps $VSP1$, $VSP2$ and $VSP5$ are used at their nominal flow rate and so the electrical consumption of the pumps is constant. Concerning the electrical consumption of the dry cooler, it is decreasing for an increase of the thermal demand as predicted due to a lower power to dissipate.

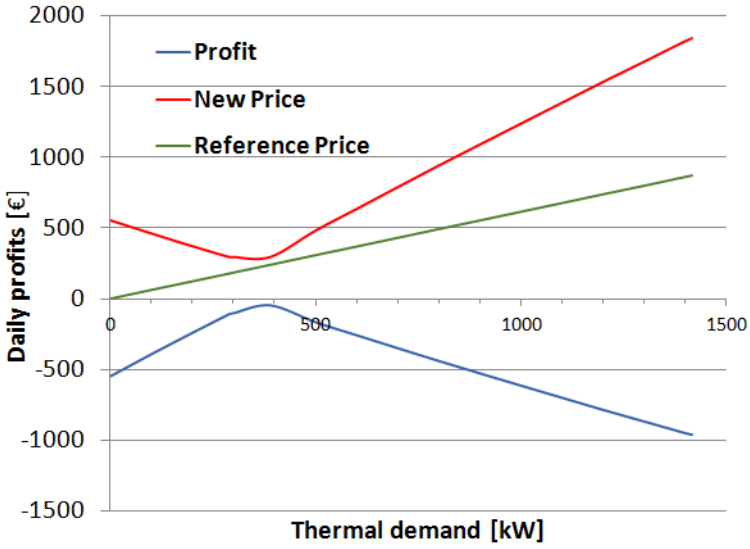

Figure 5.14: Daily profits as a function of the thermal demand. The daily profits correspond to the profits of the power plant working 24 hours at the specific thermal demand.

The parametric study starts with an optimisation of the set point temperatures T_{sp} and finishes with a parametric study of the cost of the natural gas, wood pellets and electricity. This optimisation is made for 4 different cases corresponding to three of the different working schemes (explained in Chapter 3):

No thermal demand From Table 5.4 and Figure 5.14, using the ORC during the summer seems not interesting (financial losses of more than 500€/day). However, this system might be profitable if the condensation (respectively evaporation) temperature decreases (respectively increases) and if the biomass is cheaper.

Medium thermal demand This case corresponds to a heating demand which is equal to the thermal power extracted from the ORC condenser. It seems to be the best case as the power plant is almost profitable (financial losses of only 51€/day).

Nominal thermal demand This case corresponds to a thermal demand equal or higher than $1418\ kW$. When the heating demand from the building is higher, the biomass is working at 100% of its capacity. Its power delivered to the oil is delivered to the evaporator and the oil-water heat exchanger and it also compensates the thermal losses of the oil and water loops.

Low thermal power demand During some period the year, the ORC will be used in cogeneration mode to fulfil the thermal demand alone (a thermal demand lower than $\dot{Q}_{orc,cd}$).

The last of the four cases studied is considered to show that the set point temperature of the dry cooler is important and because the slope of the profits changes around $300kW$. The

parameters that can be modified are the set point temperatures $T_{sp,eva}$, $T_{sp,cd}$, $T_{sp,DC}$, $T_{SP,VSP6}$ and $T_{SP,V3V2}$ and the parameters that can not be modified are $\dot{m}_{VSP1}$ (30kg/s), $T_{SP,2}$ (260°C), $\dot{m}_{VSP3}$ and $\dot{m}_{VSP5}$ (respectively 13 m^3/h and 37 m^3/h).

5.4.3.1 No thermal demand

This configuration corresponds to a production of electricity self-consumed and unusable heat that has to be dissipated. Considering the heat exchanger of Table 4.3, a small study was made to determine the optimal set point temperature of the controlled sensor T_{22} and T_{17} (respectively for the dry cooler and the condensation temperature of the ORC).

The daily quantity of biomass burned and the daily net electricity generated are illustrated in Figure 5.15 and the daily profits are illustrated in Figure 5.16 for different combinations of set point temperatures for the dry cooler and the condenser. Figure 5.15 shows that the power plant produces more electricity despite an increase of biomass fuel consumption. Indeed, while decreasing the condensation temperature, the set point temperature of the dry cooler has to decrease and this leads to an increase of the total electrical consumption of the dry cooler. However as the extra consumption of the dry cooler is still lower than the extra electricity generated with the ORC, the net electricity increases with a decrease of the temperature.

The optimal set point temperatures are functions of the buying prices of the biomass and electricity and a trade-off is thus necessary to find the most profitable system. A cheap biomass drives the owner to use the system with low set point temperatures to produce more electricity while a more expensive biomass makes the system not profitable.

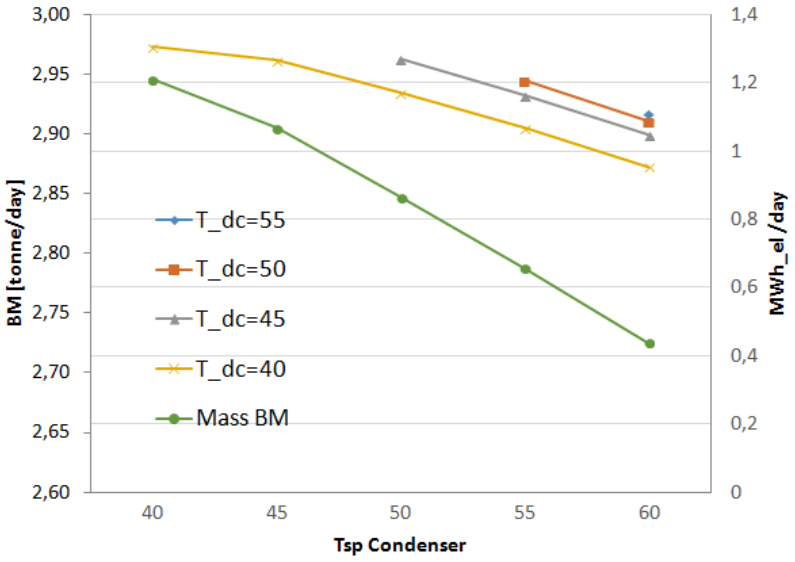

Figure 5.15: Daily quantity of biomass burned and produced net electricity using the generation mode of the ORC.

Concerning Figure 5.16, it demonstrates that the dry cooler's set point temperature should be chosen close to the set point temperature of the condenser in order to have a power plant more cost-effective. As briefly explained previously, the optimal set point temperature depends on the characteristic of the heat exchanger between the distribution and dissipation loop. Indeed, to dissipate a constant power $\dot{Q}$ in the HEX Glycol-water, a higher heating area decreases the pinch point temperature which increases the glycol HEX outlet temperature. That leads to

lower the air flow rate necessary to dissipate this specific power $\dot{Q}$ (and then lower the electrical power consumption). Figure 5.16 shows that the power should be turned off during the summer as the generation mode of the ORC is not profitable seeing that the running cost of the installation is higher than the selling price of the net electricity. Figure 5.16 also shows that the lowest condensation temperature reachable is 40°C (the lowest temperature can be under 40°C with a bigger dry cooler).

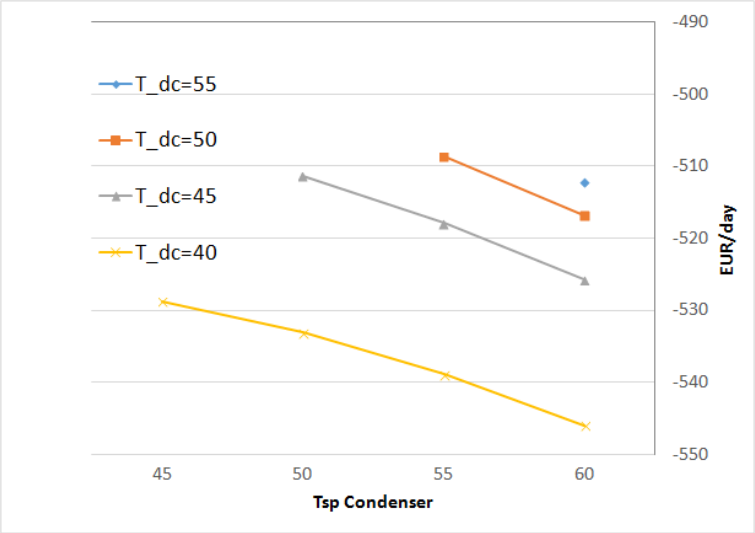

Figure 5.16: Daily profits using the Biomass only to produce electricity.

In conclusion, using the biomass boiler, the ORC and the dry cooler to produce a part of the electricity consumed and dissipating the heat is not economically a good idea.

5.4.3.2 Low thermal power demand

A low thermal demand corresponds to a thermal demand that can be completely fulfilled with the power from the condenser of the ORC. In this case, the ORC is using in cogeneration mode producing electricity and useful heat for the building. Considering a thermal demand lower than $\dot{Q}_{cd}$ (e.g varying sinuously from 0 to 380kW), the dry cooler is activated and limits the lower bond of the condensation temperature as in the previous case study. The lowest condensation temperature is still 40°C (lowest temperature possible to dissipate $\dot{Q}_{cd}$ for $T_{cd} = 40$°C, see Figure 4.20) and the corresponding distribution temperature is equal to 49.874 °C. Figure 5.17 shows the variation of the distribution temperature with the condensation temperature. It shows that the temperature in the inlet of the building varies from 49°C to 69°C depending of the condensation temperature of the ORC.

Figure 5.18 shows the biomass consumption and the daily net electricity generated as a function of the condensation temperature and the set point temperature of the dry cooler. From this figure, it's possible to determine the optimal temperature depending of the buying price of the biomass and electricity. Considering only the power plant (i.e. without the power distribution network of the building), the profits are computed with the equation (5.8).

With the predicted prices of the biomass, electricity and the selling price of the green certificates, the daily profits can be estimated and they are illustrated in Figure 5.17. This figure shows the power plant is still no profitable even with a variation of the temperature. With this figure, the optimal case can be estimated and it seems to be the lowest temperature reachable

(lower thermal losses and higher generation of electricity). However, a lower temperature also means a lower distribution temperature and this implies a higher mass flow rate inside the power distribution network (and so higher electrical consumption). Considering both the power plant and the distribution network (building), the optimal temperature might not be the lowest temperature reachable. Indeed, the electrical consumption of the distribution pumps $\dot{W}_{distri,pumps}$ increases while decreasing the temperature.

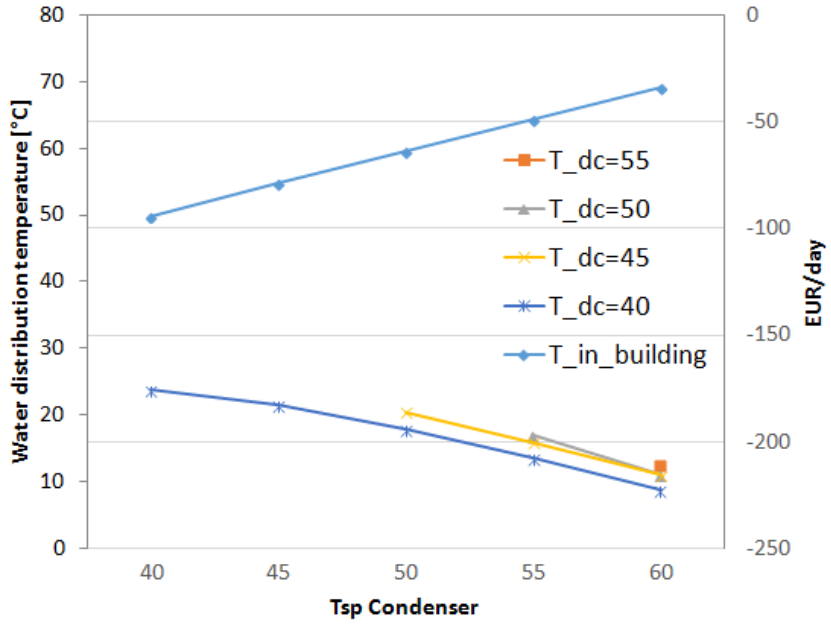

Figure 5.17: Variation of the water distribution temperature with the temperature of condensation and variation of the daily profits with different set point temperatures.

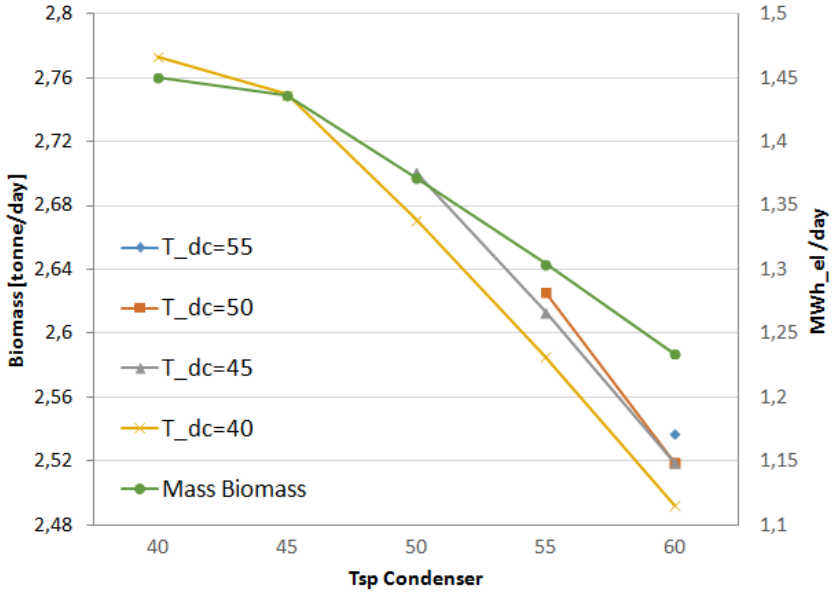

Figure 5.18: Daily net electricity generated and biomass consumption (respectively the right and left axis).

The overall profit is given by an equation similar to Equation (5.8):

$$Profit = \frac{\dot{Q}_b}{0.98} * 25.223 - \left(M_{BM} * 275.6 - GC * 65 - (EL_{net} - W_{distri,pumps}) * 215\right) \quad (5.11)$$

Where $W_{distri,pumps}$ is integral of the consumption of the pumps in the distribution network.

A trade-off is thus necessary to have the optimal overall profit (equation 5.11) instead of considering only the power plant efficiency/profit (equation 5.8). Modelling those pumps were out of the scope of this study as the whole building is not modelled in this study. A further work would be considering this supplementary electrical consumption.

For a specific thermal demand varying from 0 to 380kW (mean value of 190kW), the computation of the green certificates *GCs* showed that the quantity of CO_2 emission saved isn't high enough to claim the upper limit of 2 GCs/MWh_{el} (this issue was already seen in Figure 5.13 for low thermal demand). To claim all the GCs and have a more efficient system, the power plant should be activated for a higher mean thermal demand. The thermal demand should stay equal or higher than 289kW for a set point temperature T_{17} of 60°C. To decrease the set point temperature T_{17} and keep the number of obtained GCs at their maximum, the minimal thermal demand has to increase due to an increase of the electricity generation (300kW atleast when T_{17} is 45°C). The power 289kW and 300kW respectively correspond to the minimal thermal demand necessary to have 3.12 and 3.78 GCs per day (1.56 and 1.88 MWh_{el} generated with the ORC working at the condensation temperature of 60 and 45°C). The equation (5.8) can be used to explain the evolution of the profits with the thermal demand (Figure 5.14). For a thermal demand lower than $\dot{Q}_{cd}$ and for fixed condensation and evaporation temperatures, the term M_{BM} of this last equation is constant and the profits are then only a function of the thermal demand, the electrical consumption of the DC P_{DC} and the number of green certificates. From 0 to 300kW of thermal demand, a higher heating demand means a higher reference price ($\dot{Q}_{building}$*25.223), a higher net electricity generation due to a lower electrical consumption from the dry cooler (Equation 5.10), more GCs and so higher benefits.

In contrary, if we fulfil a heating demand higher than 289kW (or 300kW depending on the condensation temperature), the numbers of GCs reaches its limits of 2GCs/MWh$_{el}$. This is why the slope of "*New Price*" changes in Figure 5.14 once the thermal demand overpasses this value. Once this heating demand is overpassed, the profits are only a function of the dry cooler's electrical consumption and the reference price (decreasing and increasing respectively with a increase of the thermal demand). This means that the profit of the power plant keeps increasing slowly with the heating demand even if the number of obtained *GCs* is constant for a heating demand above 289kW.

Using the set point temperature T_{17} of 45°C, the profits can be computed for all the possible heating demands and this is illustrated in Figure 5.19. The curve of the profits is really close to the one of Figure 5.14 (illustration of the benefits for a temperature of 60°C). The heating demand with the optimal profit is still Q_{cd} (400kW for those temperatures) and the corresponding profits are 25€/day. This means that the power plant is profitable with the expected prices for a small range of heating demand. Once again, the consumption of the distribution pumps isn't considered and might lead to bigger financial losses if the electrical consumption of the pumps cost more than 25€/day. The simulation of the eight typical days (OFF during the summer) gives annual deficits of 58117€. Contrary to the power plant working at $T_{cd} = 60$°C (profits of -98046€), the results are more interesting due to a higher production of electricity (and a higher electrical efficiency, equation (4.28)). The other solution to improve the efficiency of the system is using an ORC with a higher electrical efficiency or an ORC with natural gas as heating source instead of biomass.

In conclusion, the power plant is still not profitable for most of the low heating demand even if the set point temperatures can be modified. However, the power plant is more interesting that the previous case as the thermal power from the ORC condenser is partially used to heat the building.

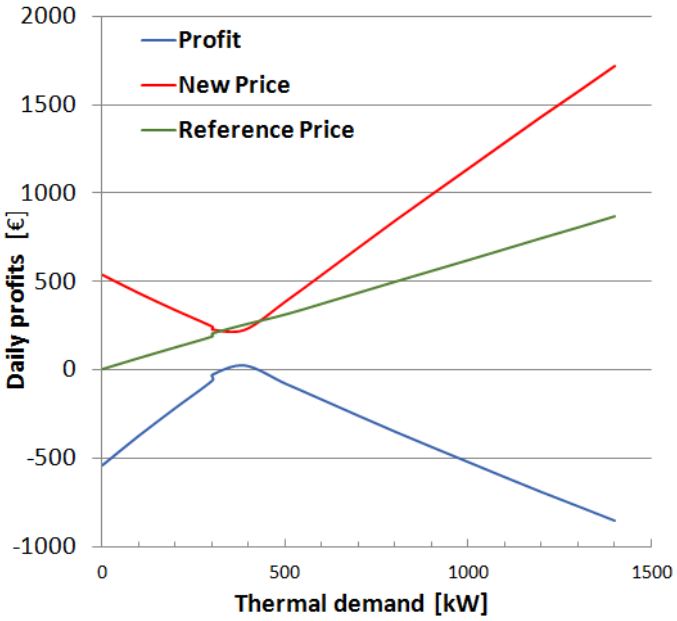

Figure 5.19: Daily profits as a function of the thermal demand. The daily profits correspond to the profits of the power plant working 24 hours at the specific thermal demand.

5.4.3.3 Medium thermal demand

This section corresponds to the specific case encountered when the thermal demand equals the power delivered in the ORC (equation 5.12). The only difference with the previous case is that we are using all the thermal power from the condenser of the ORC to heat the building (the dry cooler is unnecessary and is turned OFF). The consumption of the biomass boilers is the same as in the previous studied case and the net electrical power is higher due to dry cooler turned OFF.

$$\dot{Q}_b + \dot{Q}_{losses} = \dot{Q}_{cd} \tag{5.12}$$

$$\eta distribution = \frac{\dot{Q}_b}{\dot{Q}_{cd}} \tag{5.13}$$

In this specific case, there are only two set point temperatures that have influence on the results. The set point temperature T_4 is 225°C (evaporator side) and the set point temperature T_{17}(condenser side) is variable to see its influence on the power plant efficiency. Its influence on the profits are computed with the values of Figure 4.18, 4.19, 4.20 and the equation (5.8) and is illustrated in Figure 5.20. Figure 4.18, 4.19 and 4.20 show that a decrease of the condensation temperature increases the thermal power needed in the evaporator of the ORC, the electrical power generation and the thermal power dissipated in the condenser. Furthermore, seeing that the temperature is lower in the condenser and therefore in water loop, it also decreases the ambient thermal losses $\dot{Q}_{losses}$ from $8600W$ to $7200W$ and in consequence, it leads to a "higher" distribution efficiency (equation 5.13). All those variations with the condensation temperature increase the profits and that explains why the profits rapidly increase with a decrease of the ORC's condenser water inlet temperature (Figure 5.20).

In conclusion, Figure 5.20 shows that this case is the best financial case and that it is profitable only if the condensation temperature can be lower than 50°C (for this condensation

temperature, the distribution temperature is 59.5°C). Considering also the electrical of the pumps' distribution $\dot{W}_{distri,pumps}$ (confer equation (5.11)), the financial losses of the new power plant should be even bigger.

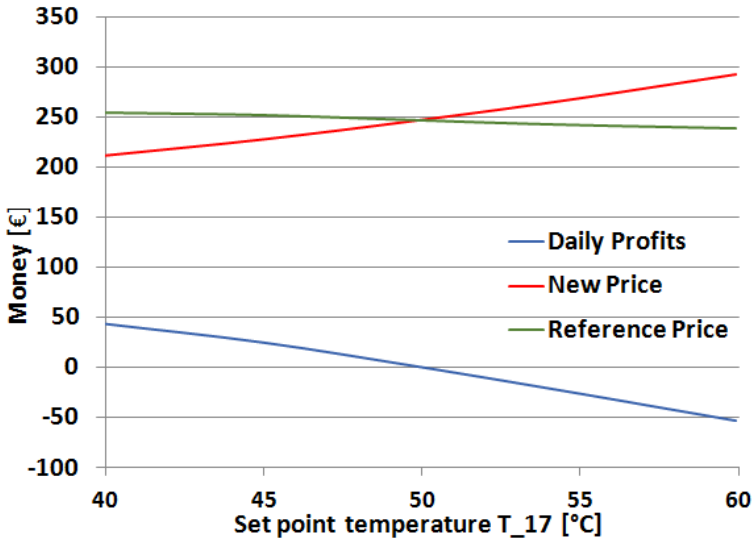

Figure 5.20: Variation of the profits with the set point temperature T_{17}. All the results are shown in €/day.

5.4.3.4 Nominal thermal demand

This study case corresponds to the biomass working at its nominal power and it is encountered every time the thermal demand from the building is higher than the nominal capacity of the biomass (966 hours during the year 2015). Indeed, as explained previously in Chapter 3, the biomass will work at 100% of its capacity during high heating demands and the natural gas boilers will generate the thermal power above the power delivered by the biomass (this is less than its nominal capacity due to the ORC and the thermal losses in the different loops, $1405kW$ and $1418kW$ respectively for $T_{cd} = 45°C$ and $60°C$). Using the equation (5.15) (similar to Equation (5.8)), the daily profits are found and illustrated in Figure 5.21 as a function of the condensation and distribution temperatures.

$$\begin{aligned} Profit &= \frac{\dot{Q}_b}{0.98} * 25.223 \\ &\quad - \left(\frac{\dot{Q}_b - Q_{1418}}{0.98} * 25.223 + M_{BM} * 275.6 - GCs * 65 - El_{net} * 215 \right) \qquad (5.14) \\ &= \frac{Q_{1418}}{0.98} * 25.223 - (M_{BM} * 275.6 - GCs * 65 - El_{net} * 215) \qquad (5.15) \end{aligned}$$

Where Q_{1418} is the integral of the useful capacity of the biomass boiler (in other words, $(1500kW - \dot{Q}_{losses}) * time = (\dot{Q}_{cd} + \dot{Q}_{HexGW}) * time = 1418kW * time$).

The figure shows that the profits of the new power plant are even worse than the previous case. Indeed, the profit of the optimal case is financial losses of 772€ per day (for a water temperature from the building of 30°C). Considering a more reasonable temperature of 40°C, the financial losses are -822€/day. This result is explained by the really high price of the biomass which is two times more expensive than the natural gas.

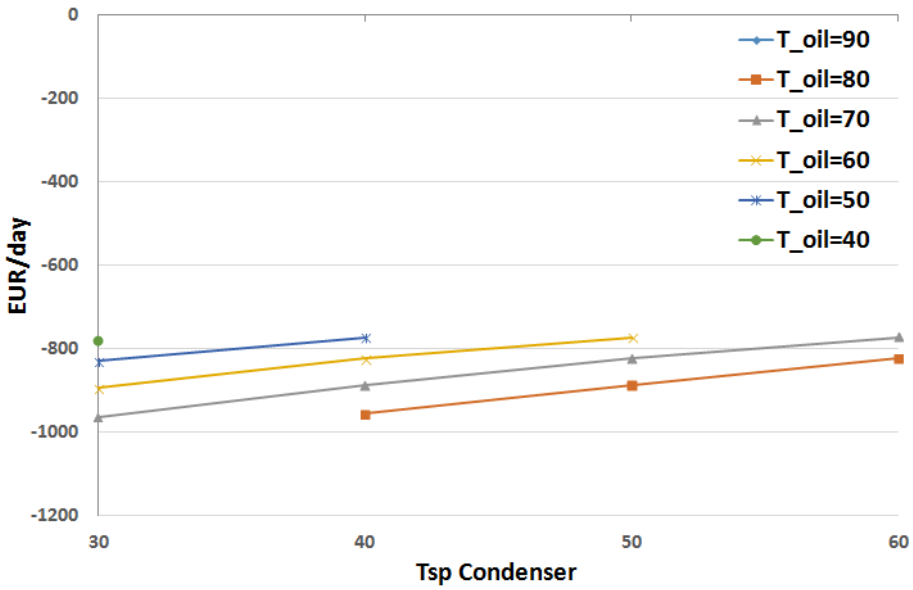

Figure 5.21: Daily net electricity generated and water distribution temperature.

When the power plant works at its nominal capacity, it reduces the CO_2 emissions by 5876 kg which is equivalent to 12.9 *GCs* per day. However, considering the upper limit of 2 GCs/MWh_{el}, only 3.78 GCs can be claimed every 24 hours (the number depends on the electricity generation and so on the working conditions of the ORC). Taking into account the price of the natural gas and biomass (respectively 25 and 57€/MWh), the efficiency of the natural gas boilers and biomass boilers (respectively 98% and 85-90%), it is not interesting to use the biomass boiler only for heating purposes. Indeed, it's more interesting to use natural gas to fulfil the extra thermal demand and so avoid using a more expensive energy.

In conclusion, using the biomass (wood pellets) only for heating purposes is not a good idea and a downsizing of the biomass boiler should be considered as the biomass is more expensive and as the biomass boilers is less efficient than one working with natural gas.

5.4.3.5 Price sensitivity

After having analysed the variation of the profits with the heating demand and the set point temperatures, it is interesting to determine the sensitivity of the profits with the buying prices of the biomass and the electricity. This study is realized for the optimal set point temperatures of each of the following cases:

No thermal demand As previously said, using the power plant to only generate electricity is not financially interesting. However, it is interesting to make a parametric study to evaluate the price of the biomass and of the electricity for which the power plant starts to be profitable. Indeed, when a power plant has a life time of 15 years, it is important to consider that the price of the electricity and the biomass might change in the next years. Furthermore, the biomass boilers are most of the time made for specific type of biomass but they can usually work with another type of similar biomass. In this case, wood chips could be used (They are almost two time less expensive [26]). The results of the study are shown in Table 5.5. This table shows that using the power plant to only generate electricity starts to be profitable for a biomass buying price of 20€$/MWh_{th}$ (which is

close to 100€/tonne of wood pellet).

Table 5.5: Parametric study of the power plant working with the ORC and DC set point temperatures equal respectively to 45°C and 40°C.

Daily Profits		Electricity[€/MWh_{el}] 235	225	215	205	195
Biomass [€/MWh_{th}]	0	297 €	285 €	272 €	259 €	247 €
	10	157 €	144 €	132 €	119 €	106 €
	20	17 €	4 €	-9 €	-21 €	-34 €
	30	-123 €	-136 €	-149 €	-161 €	-174 €
	60	-544 €	-557 €	-569 €	–582 €	-595 €

Medium thermal demand The table 5.6 regroups the results of the parametric study for a heating demand equal to $\dot{Q}_{cd}$. It shows that the power plant start to make financial losses for a biomass buying price higher than 60€/MWh_{th} ($\pm$ =290€/tonne of wood pellets) and an electrical price lower than 225€/MWh_{el}. As previously said, the daily profits are 25€ for the expected price of biomass and electricity (respectively 57€/MWh_{th} and 215€/MWh_{el}). If the biomass is cheaper, the profit increases really fast (405€/day for a biomass buying price of 30€/MWh_{th}). There are 136 days per year when the thermal demand is higher. If we use the boiler only to provide this specific thermal power, these benefits are enough to payback the power plant (685000€) in 12.43 years.

Table 5.6: Parametric study of the power plant working with the set point temperatures T_{17} and T_4 fixed at 45 and 225°C.

Daily Profits		Electricity[€/MWh_{el}] 235	225	215	205	195
Biomass [€/MWh_{th}]	0	856 €	841 €	826 €	811 €	795 €
	20	576 €	561 €	545 €	530 €	515 €
	30	436 €	420 €	405 €	390 €	375 €
	40	295 €	280 €	265 €	250 €	235 €
	50	155 €	140 €	125 €	110 €	94 €
	60	15 €	0 €	-15 €	-31 €	-46 €

Nominal thermal demand The table 5.7 shows the daily profits of the power plant working at its nominal capacity for different prices of biomass and electricity. It shows that the profits change really fast with the biomass buying price while they change in the same way as previously with a variation of the price of electricity (due to a constant production of electricity). In this case, the price of biomass for which the profits are null is $\pm$ 175€/tonne of wood pellets (36.5€/MWh). Even if this price is higher than the previous case, this specific working condition has the highest profits for an really low biomass buying price due to its high use of biomass.

Table 5.7: Parametric study of the power plant working with the set point temperatures T_{17}, T_4 and T_{16} fixed at 45, 225 and 70°C and a temperature of 58°C in the inlet of the building's heating distribution network.

Daily Profits		Electricity[€/MWh_{el}] 235	225	215	205	195
Biomass [€/MWh_{th}]	0	1459 €	1444 €	1429 €	1414 €	1399 €
	20	659.87 €	645.08 €	630.28 €	615.49 €	600.69 €
	30	260.56 €	245.76 €	230.97 €	216.17 €	201.38 €
	40	-138.76 €	-153.55 €	-168.35 €	-183.14 €	-197.94 €
	50	-538.07 €	-552.87 €	-567.66 €	-582.46 €	-597.25 €
	60	-937.39 €	-952.18 €	-966.98 €	-981.77 €	-996.57 €

In conclusion, a biomass power plant is financially interesting only if the biomass boiler only provides thermal power to the ORC evaporator and if the thermal power from its condenser is used. In the others cases (i.e. low thermal demand or big biomass providing thermal power directly to the heating distribution system), the power plant is only profitable for a cheap biomass.

5.5 Reduction of the size of the biomass boiler

The power plant needs a really low biomass buying price to have a financial interest when it is working at its nominal capacity. However, as it is demonstrated in the previous section, the power plant is economically interesting when it is working at partial load to fulfil only the thermal demand of the ORC. The optimal working condition is then a biomass boiler providing only power to the ORC. A solution to have a better financial efficiency system would be using the biomass only to provide power to the ORC. Considering the fact that the ORC evaporator required less than $500kW$, a downsizing of the biomass boiler should improve its efficiency (less thermal losses to the ambient for a smaller boiler) and reduces the electrical consumption of the pump $VSP1$ (smaller pump). For this reason, a small study is realized to see the savings of a smaller biomass boiler ($500kW$) in comparison with the real biomass boiler (1500kW producing power only for the ORC, i.e. working at partial load $497kW$ to avoid using biomass for heating purposes only).

For a thermal power higher than $\dot{Q}_{cd}$, the new system will use the biomass boiler to provide the thermal power to the ORC and the natural gas to heat the building and fulfil the extra thermal demand. This is illustrated in Figure 5.22. In conclusion, the profit of this new power plant is given by the following equation (based on the equation (5.8)) :

$$\begin{aligned} Profits &= \frac{Q_b}{0.98} * 25.223 \\ &\quad - (\frac{Q_b - Q_{cd}}{0.98} * 25.223 + M_{BM} * 275.6 - GCs * 65 - El_{net} * 215) \qquad (5.16) \\ &= \frac{Q_{cd}}{0.98} * 25.223 - (M_{BM} * 275.6 - GCs * 65 - El_{net} * 215) \qquad (5.17) \end{aligned}$$

Where the new term $Q_b - Q_{cd}$ is the integral of the $\dot{Q}_b - \dot{Q}_{cd}$ which is the power necessary

to fulfil a fraction of the heating demand with natural gas. The power plant will then work in its optimal working point during all the thermal demand higher than Q_{cd} (about 3300 hours in 2015).

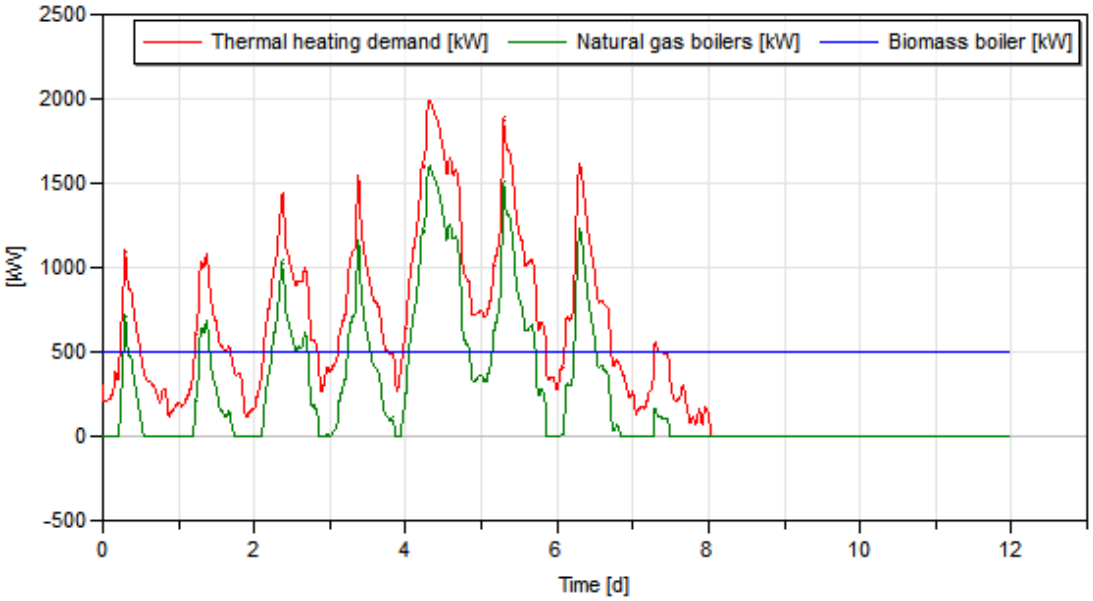

Figure 5.22: Evolution of the mix of biomass and natural gas power generation to fulfil the thermal heating demand.

The results of this small study are shown in Table 5.8. As predicted, the downsized boiler has a better financial interest. Both sizes of biomass boiler are profitable on average during the whole heating period (and both systems have financial losses if they are used during the whole year). The installed power plant $(1500kW)$ shouldn't be used during the last month of heating (8th days of the simulation) due to a decrease of the profits. In contrary, the suggested downsizing of the biomass would lead to a more profitable system considering this last month (in other words, there is an increase of the profits between the first seven and the first eight months). Even if using a smaller biomass boiler is profitable, it is impossible to payback the installation onsidering the assumptions of the buying price of the biomass and electricity(34.86 years are necessary to earn 685000€).

Table 5.8: Comparison of profits of the real and downsized power plant.

Profits	Biomass boiler	Biomass boiler
	$1500kW$	$500kW$
First two months	-130€	2702€
First seven months	10244€	19294€
First eight months	9315€	19649€
One year	-44789€	-19363€

In conclusion, the optimisation of the control logic (optimal configuration, optimal method to modulate the components, and optimisation of the set point temperatures) have improved the efficiency of the power plant and have brings a clearly non-profitable system (deficit of -101439€ per year, see Table 5.4) to a profitable system (9315€/year).

Chapter 6

Conclusion and perspectives

6.1 Conclusion

Through this work, a real biomass power plant was studied for cogenerative applications in public building and more particularly a building situated in Belgium. As the energy consumption of buildings represents an important share of the total energy consumption in Belgium, reducing the energy consumption in buildings can avoid an important emission of CO_2. At the beginning of the work, this led to the question: "Is a big biomass power plant for cogenerative applications profitable in public buildings?" To determine the usability of biomass in big buildings, a dynamic model and a study of different possible control logics were realized to analyse the energetic performance of the studied building (Building of the Higher Education Institution of the Province of Liège). Once the energetic performance of a big biomass power plant is determined, the results can be extrapolated for other buildings having different thermal demand knowing that a building with lower thermal demand should have less efficient power plant. Indeed, smaller biomass boilers are losing more heat per unit of capacity (due to a bigger surface area per unit of biomass' capacity).

The model of the whole power plant is realized in a few steps. Each component are analysed individually and the obtained results are compared with the product data to prove that each model is giving good results and that the model of the whole power plant will then give accurate results. Results show that the heat exchanger model gives really good results as the heat transfer is respectively 0.15% lower, 0.7% lower and 1.7% higher than the value of the product data for respectively the Glycol-Water, Water-Water and Oil-Water heat exchanger. The model of the dry cooler shows an error of only 2.4% with the corresponding data sheet. Concerning the models of the other components, their behaviour is verified with technical data or their expected physical behaviour.

During the modeling of the whole power plant, different configurations and different control logics are considered. This small comparison showed that the profits really depend on the control logic itself (see Table 5.4). The profits of the power plant can increase by 3393€ with the right control logic (from -101439€ to -98046€, profits for a biomass buying price of $57.09€/MWh_{th}$). The appropriate control logic can decrease the electrical consumption of the pumps and the consumption of biomass. Indeed, using variable speed pumps instead of pumps working with constant flow rate can decrease the electrical consumption (from $126.29MWh_{el}$ to $106.68MWh_{el}$) and the thermal losses in the pipes (a thermal consumption reduction of $11,093MWh_{el}$).

Then, an optimisation of the set point temperatures was made to improve the efficiency of

the power plant. Even if the modeling wasn't perfect (using Equation (5.8) instead of Equation (5.11)), the model showed that decreasing the temperature inside the heating network increases hugely the profits of the power plant (from -98046€ to -58117 €). Indeed, a decrease of the condensation temperature increases the electrical efficiency of the ORC and leads to a more economical system. Finally, some suggestions are given to improve the efficiency of the power plant like reducing the size of the biomass boiler or using it at partial load to have the power plant working at its optimal financial working point. These last suggestions respectively give a profit of 19649€ and 9315€ with an associated reduction of the CO_2 emission of 448 tonnes. This is 41% less than the case where the biomass boiler works at its nominal capacity (emission savings of 754 tonnes). A good sizing of the components and an appropriate control logic can then make a power plant financially interesting even if the buying price of the biomass is high. However, to payback the installation (685000 €), the biomass fuel should be cheaper (and/or have a higher electrical power generation with the ORC). In conclusion, the main contributions and findings of this work have been:

- the modeling of a real biomass power plant,
- the determination of the optimal control logic for the dry cooler (i.e., decreasing both the flow rate of the air and glycol-water with a faster proportional decrease of the latter),
- the comparison and implementations of different control strategies,
- and an economical study of a real power plant showing the importance of keeping a high ΔT for the ORC in order to have a higher electrical efficiency.

6.2 Further developments

To conclude this work, some perspectives are suggested about the system modeling:

- The first improvement would be a detailed implementation of the building with a model for each of the eleven water loops. Those loops connect the power plant to the eight hydraulic circuits for indoor heating (radiators) and the three circuits for ventilation units air handling units. Furthermore, a model of the building itself (with the air infiltrations, thermal losses, inertia,...) could also give more precision and give the possibility to implement a more sophisticated control logic which could improve the efficiency of the system (i.e. using the inertia, it is possible decoupling the heating demand and the thermal power production in order to have the system working most of the time at its optimal (financial) working point).
- Once some experimental data are collected, the working conditions of the ORC could be verified and tuned. In other words, when the equations (4.23),(4.24),(4.25),(4.26) and (4.27) are validated for large ranges of temperatures, a new optimisation could be carried out to see if this first work is accurate enough.
- Once some other working points of the dry cooler are known, the model of the dry cooler could be improved to reduce the error (e.g. with more than two working points, a modification of the modeling (a calibration) could decrease the error and validate the results).
- Finally, the assumption on the efficiency and the starting time of the biomass should be verified when data are available.

Bibliography

[1] Association pour la Promotion des Énergies Renouvelable. *Observatoire belge de l'énergie*. http://www.apere.org/fr/observatoire-belge-de-l-energie, last access July 2016.

[2] Therminol. *Fluid Properties of Therminol SP*. https://www.therminol.com/products/Therminol-SP, last access April 2016.

[3] Renaud GICQUEL. Cycles organiques de rankine. Technical report, Ecole des Mines de Paris.

[4] Vincent Lemort. Technologies avancées de machines et systèmes thermiques. Technical report, University of Liège, 2015-2016.

[5] Luvata. *Description of the V-shape Dry Coolers*. http://www.luvata.com/en/Products/Heat-Transfer-Solutions/Dry-coolers-Fluid-coolers/VCC/, last access April 2016.

[6] Kuppan Thulukkanam. *Heat Exchanger Design Handbook, Second Edition*. CRC Press, May 2013.

[7] Calgavin. *HEAT EXCHANGER PROBLEMS – PART 3*. http://www.calgavin.com/2014/09/heat-exchanger-problems-part-3/, last access April 2016.

[8] Sevojno. *High-finned tubes for heat exchangers - Applications*. http://spxcooling.com/products/detail/air-cooled-heat-exchangers, last access April 2016.

[9] Deltahx. *Fin Types for Finned Tube Heat Exchangers*. http://deltathx.com/uploadsdocs/fintypes.pdf, last access April 2016.

[10] Deltahx. *Fin Comparison Chart*. http://deltathx.com/uploadsDocs/FinComparisonChart.pdf, last access April 2016.

[11] SPXCOOLING. *Air Cooled Heat Exchangers - Description of the features*. http://www.femodsev.com/high_finned_tubes..en, last access April 2016.

[12] Robert Giammaruti. Performance improvement to existing air-cooled heat exchangers. *Hudson Products Corporation*, 2004.

[13] Thermopedia. *AIR COOLED HEAT EXCHANGERS*. http://thermopedia.com/content/551/, last access April 2016.

[14] Rgees. *Phase Change Energy Storage Technology - Description of the technology*. http://www.rgees.com/technology.php, last access May 2016.

[15] Roberto Ruitz and Matteo D'Antoni. *Total Renovation Strategies for Energy Reduction in Public Building Stock*, 2015.

[16] Sylvain Quoilin. Modelisation dynamique des systemes thermiques. Technical report, University of Liège, 2015-2016.

[17] Vincent Lemort. Utilisation rationnelle de l'énergie dans les bâtiments. Technical report, University of Liège, 2015-2016.

[18] Solutia. *Therminol SP - Synthetic Fluid, Optimum Cost, Performance and Heat Transfer Fluid*. Properties of Therminol SP vs Temperatures.

[19] The Engineering ToolBox. *Bulk Modulus and Fluid Elasticity*. `http://www.engineeringtoolbox.com/bulk-modulus-elasticity-d_585.html`, last access April 2016.

[20] Rosamond Jordan. Boiler efficiency heat engines and boilers. Technical report, Budapest University of Technology and Economics, 2012.

[21] Babcock wanson. *Chaudière à fluide thermique horizontale multitubulaire à haut rendement série EPC-H*.

[22] CARTIF, one partner of the Bricker project. *Curva potencia peso 3*. A study about the inertia of biomass boilers.

[23] J. Delcarte Y. Schenkel J. Good, Th. Nussbaumer. Determination of the efficiencies of automatic biomass combustion plants. Technical report, University of Zürich and Gembloux, November 2006.

[24] The Engineering ToolBox. *Boiler Efficiency*. `http://www.engineeringtoolbox.com/boiler-efficiency-d_438.html`, last access April 2016.

[25] Pedro M. Aranda F. Procedimiento de cálculo del rendimiento medio estacional de instalaciones con calderas de biomasa en el sector residencial. Technical report, University of Seville, Decembre 2010.

[26] Fredy Velez Ana I.Quijano, Cecilia Sanz. Bricker d3.14 : Two tailor made designs of the biomass combustion plants for belgian and spanish demonstrators. Technical report, Cartif, March 2015.

[27] Raymond Charlier, industrial enginerring expert. *Responsible for BRICKER within Province de Liège*.

[28] D'Alessandro Termomeccanica, boilers manufacturer. *Data sheets of their products*.

[29] DuPont. *E. I. du Pont de Nemours and Company*, Provider of the orc working fluid.

[30] Dow, Heat Transfert fluids. *DOWTHERM SR-1 Product Information*, 2013.

[31] S.A Henri Dethier Fils. *Data sheet of the product WDR 8104 STD (AERMEC)*. Adapted data sheet given to Raymond Charlier, the responsible for BRICKER within Province de Liège.

[32] AERMEC. *Technical data about the Dry coolers WTE - WTR - WDR - WTS - WTA*.

[33] I. Dressler M. Otter, K.-E. Arzén. Stategraph-a modelica library for hierarchical state machines. *4th International Modelica Conference, Hamburg*, pages 569–578, 2005.

[34] Young-Jin Kim. Variable speed heat pump (vshp) design for frequency regulation through direct load control. Presented at the 55th IEEE PES T&D Conference and Exposition, Chicago, 2014.

[35] STEVE BECKER. Variable speed drive (vsd) for irrigation pumping. Technical report, NRCS-Montana, January 2010.

[36] Afshin J.Ghajar Yunus A.Çencel. *Heat and Mass Transfer*. McGraw-Hill Higher Education, Jan 2011.

[37] Spirax Sarco. Energy consumption of tanks and vats. Computation of the heat losses of a tank.

[38] Province De Liège. Installation d'une chaudière biomasse et d'un stockage de granulés de bois, et intégration d'une cogénération orc (projet bricker). Cahier Spécial Des Charges, 2014.

[39] S. Ravelli G. Barigozzi, A. Perdichizzi. Wet and dry cooling systems optimization applied to a modern waste-to-energy cogeneration heat and power plant. *Applie Energy*, 88(4):1366–1376, 2011.

[40] Pierre Dewallef. Centrales thermiques et cogénération. Technical report, University of Liège, 2015-2016.

[41] Alessandro Guercio Andrea Duvia and Clotilde Rossi di Schio. *Technical and economic aspects of Biomass fuelled CHP plants based on ORC turbogenerators feeding existing district heating networks*. Turboden Srl, Brescia, Italy.

Appendices

Appendix A

Fluid properties

The properties of the glycol-water mix are illustrated in Figure A.1 for some temperatures between -10°C and 120°C. Concerning the properties of Therminol SP, they are shown in Figure A.2. In Dymola, the properties for all the temperatures are extrapolated from the table.

Temp. °C (°F)	Specific Heat kJ/(kg)(K) (Btu/lb°F)	Density kg/m³ (lb/ft³)	Therm. Cond. W/mK [Btu/hr ft² (°F/ft)]	Viscosity mPa·s (cps)
-10 (14)	3.562 (0.851)	1055.47 (65.89)	0.4154 (0.2400)	6.1788 (6.18)
10 (50)	3.619 (0.865)	1049.91 (65.54)	0.4420 (0.2554)	2.9482 (2.95)
40 (104)	3.704 (0.885)	1037.92 (64.80)	0.4731 (0.2733)	1.3398 (1.34)
65 (149)	3.775 (0.902)	1024.59 (63.96)	0.4909 (0.2836)	0.8246 (0.82)
90 (194)	3.846 (0.919)	1008.20 (62.94)	0.5015 (0.2897)	0.5599 (0.56)
120 (248)	3.931 (0.939)	984.53 (61.46)	0.5044 (0.2915)	0.3846 (0.38)

Figure A.1: Properties of Glycol-water mix.

THERMINOL® SP

Properties of Therminol® SP vs Temperatures

Temperature	Density	Thermal Conductivity	Heat Capacity	Viscosity		Vapour pressure (absolute)
				Dynamic	Kinematic	
°C	kg/m³	W/m.K	kJ/kg.K	mPa.s	mm²/s**	kPa*
-10	892	0.132	1.798	308.6	346	-
0	885	0.131	1.834	143.3	162	-
10	878	0.130	1.870	73.8	84	-
20	872	0.128	1.906	41.6	47.70	-
30	865	0.127	1.942	25.2	29.10	-
40	858	0.126	1.978	16.3	18.99	-
50	852	0.125	2.013	11.1	13.05	-
60	845	0.124	2.049	7.90	9.39	-
70	838	0.123	2.085	5.90	7.02	-
80	831	0.122	2.120	4.50	5.43	-
90	825	0.120	2.156	3.56	4.32	-
100	818	0.119	2.191	2.88	3.52	-
110	811	0.118	2.227	2.38	2.93	-
120	804	0.117	2.262	2.00	2.49	-
130	797	0.116	2.297	1.71	2.14	0.1
140	790	0.115	2.333	1.48	1.87	0.2
150	783	0.113	2.368	1.29	1.65	0.3
160	777	0.112	2.403	1.14	1.47	0.5
170	770	0.111	2.438	1.02	1.32	0.7
180	762	0.110	2.474	0.91	1.20	1.1
190	755	0.109	2.509	0.82	1.09	1.5
200	748	0.107	2.544	0.75	1.00	2.2
210	741	0.106	2.579	0.68	0.92	3.0
220	734	0.105	2.614	0.63	0.85	4.1
230	726	0.104	2.649	0.57	0.79	5.5
240	719	0.103	2.684	0.53	0.74	7.4
250	711	0.102	2.719	0.49	0.69	9.8
260	704	0.100	2.755	0.45	0.64	12.8
270	696	0.099	2.790	0.42	0.60	16.6
280	688	0.098	2.825	0.39	0.56	21.3
290	680	0.097	2.860	0.36	0.53	27.2
300	672	0.096	2.896	0.33	0.50	34.4
310	663	0.094	2.932	0.31	0.47	43.1
320	655	0.093	2.967	0.29	0.44	53.7
330	646	0.092	3.003	0.27	0.42	66.3
335	642	0.091	3.022	0.26	0.40	73.6

* 1 bar = 100 kPa - ** 1 mm²/s = 1 cSt

Note: Values quoted are typical values obtained in the laboratory from production samples. Other samples might exhibit slightly different data. Specifications are subject to change. Write to Solutia for current sales specifications.

Physical Property Formulae

Density (kg/m^3) = $885.597 - 0.689367 * T(°C) + 1.9228 * 10^{-4} * T^2(°C) - 8.87642 * 10^{-7} * T^3(°C)$

Heat Capacity ($kJ/kg.K$) = $1.83369 + 0.0036172 * T(°C) - 4.94238 * 10^{-7} * T^2(°C) + 7.98115 * 10^{-10} * T^3(°C)$

Thermal Conductivity ($W/m.K$) = $0.131281 - 0.000114034 * T(°C) - 1.49876 * 10^{-8} * T^2(°C) + 1.76622 * 10^{-11} * T^3(°C)$

Kinematic Viscosity (mm^2/s) = $e^{\left(\frac{798.89}{T(°C)+97.7} - 2.65773\right)}$

Vapour Pressure (kPa) = $e^{\left(\frac{-5322370}{(T(°C)+480) + (T(°C) + 480)^2} + 12.2641\right)}$

Figure A.2: Properties of Therminol SP.

Appendix B

Dymola Model

The Dymola model of the whole power plant is illustrated in Figure B.1. It regroups all the models implemented (Chapter 4).

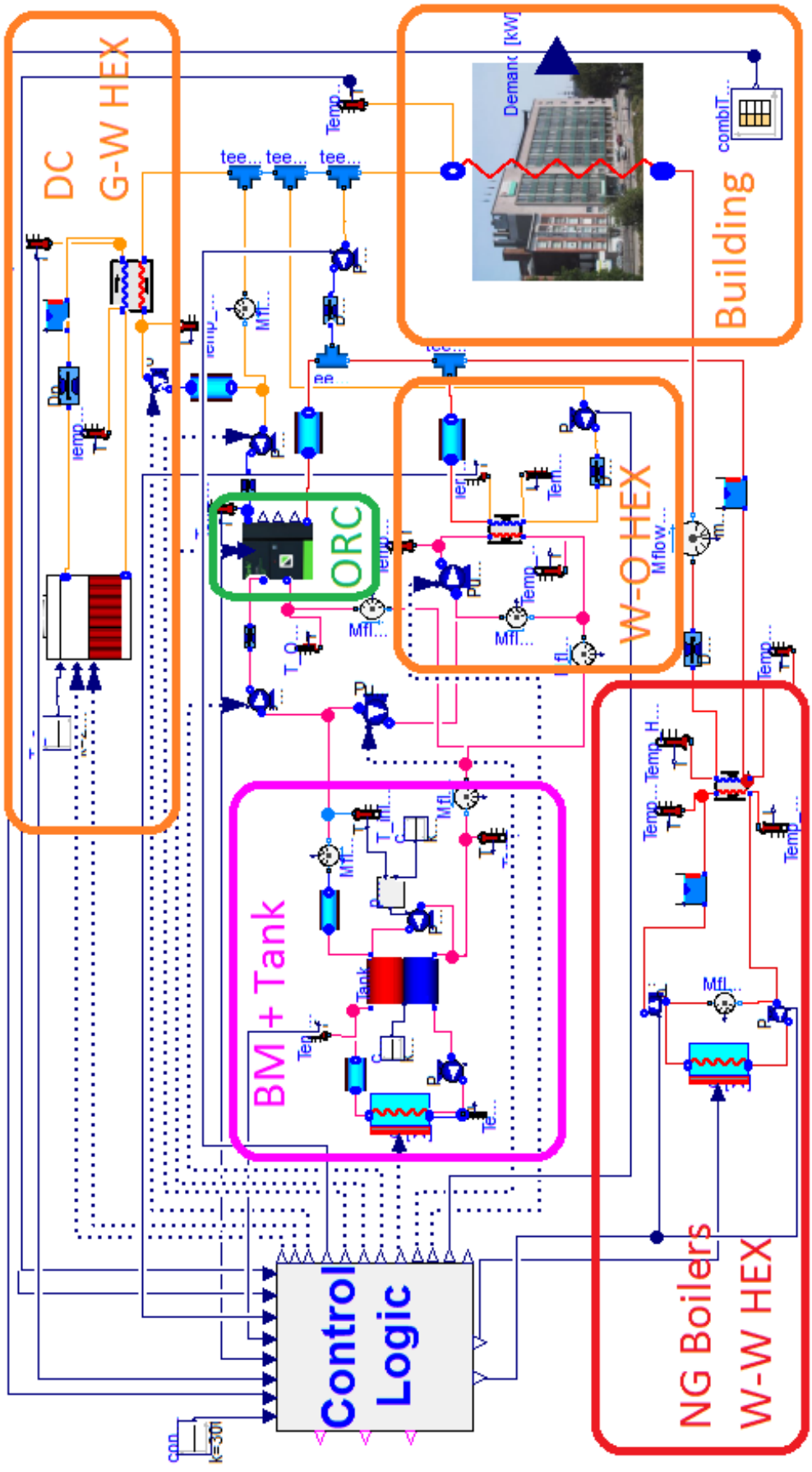

Figure B.1: Illustration of the power plant in Dymola.